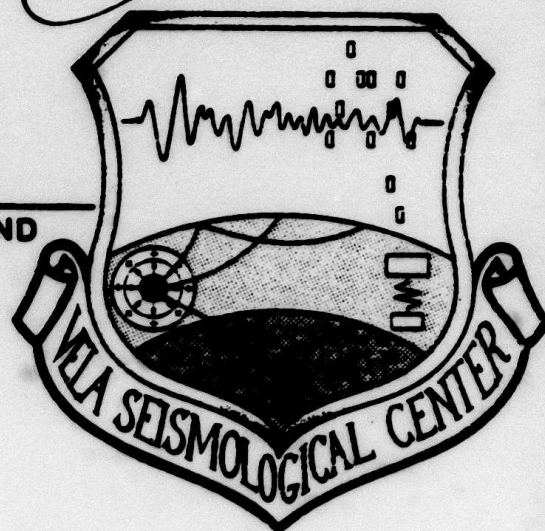


DA 126002

VSC-TR-80-3

**SEISMOLOGICAL DISCRIMINATION AND
YIELD DETERMINATION RESEARCH**



T. C. Bache
J. T. Cherry
P. L. Coleman
S. M. Day
J. R. Murphy
N. Rimer
J. M. Savino

FINAL REPORT

SYSTEMS, SCIENCE AND SOFTWARE
P. O. Box 1620
La Jolla, California 92038

February 1980

**Approved for Public Release,
Distribution Unlimited**

Monitored by:

**VELA Seismological Center
312 Montgomery Street
Alexandria, Virginia 22314**



DTIC FILE COPY

83 03 23 007

UNCLASSIFIED

SECURITY CLASSIFICATION OF THIS PAGE (When Data Entered)


REPORT DOCUMENTATION PAGE		READ INSTRUCTIONS BEFORE COMPLETING FORM
1. REPORT NUMBER VSC-TR-80-3	2. GOVT ACCESSION NO. Ab A126002	3. RECIPIENT'S CATALOG NUMBER
4. TITLE (and Subtitle) SEISMOLOGICAL DISCRIMINATION AND YIELD DETERMINATION RESEARCH		5. TYPE OF REPORT & PERIOD COVERED Final Report 11/17/78 - 9/30/79
		6. PERFORMING ORG. REPORT NUMBER SSS-R-80-4383
7. AUTHOR(s) T. C. Bache, J. T. Cherry, P. L. Coleman, S. M. Day, J. R. Murphy, N. Rimer and J. M. Savino		8. CONTRACT OR GRANT NUMBER(s) F08606-79-C-0008
9. PERFORMING ORGANIZATION NAME AND ADDRESS Systems, Science and Software P. O. Box 1620 La Jolla, California 92138		10. PROGRAM ELEMENT, PROJECT, TASK AREA & WORK UNIT NUMBERS Program Code No. 6H189 ARPA Order No. 2551
11. CONTROLLING OFFICE NAME AND ADDRESS		12. REPORT DATE February 1980
		13. NUMBER OF PAGES 124
14. MONITORING AGENCY NAME & ADDRESS (if different from Controlling Office) VELA Seismological Center 312 Montgomery Street Alexandria, Virginia 22314		15. SECURITY CLASS. (of this report) Unclassified
		15a. DECLASSIFICATION/DOWNGRADING SCHEDULE
16. DISTRIBUTION STATEMENT (of this Report) Approved for public release, distribution unlimited		
17. DISTRIBUTION STATEMENT (of the abstract entered in Block 20, if different from Report)		
18. SUPPLEMENTARY NOTES		
19. KEY WORDS (Continue on reverse side if necessary and identify by block number) Seismic Source Theory Nuclear Explosion Seismology Seismic Discrimination		
20. ABSTRACT (Continue on reverse side if necessary and identify by block number) This report summarizes research activities during Fiscal Year 1979 which were directed toward the development of improved methods for discriminating between the seismic signals from earthquakes and explosions and the development of improved methods for estimating explosion yield. Empirical, theoretical and experimental studies were completed in seven topic areas: (1) Source Calculations, (2) Discrimination, (continued)		

UNCLASSIFIED

SECURITY CLASSIFICATION OF THIS PAGE(When Data Entered)

20. ABSTRACT (continued)

9 (3) Body Wave Magnitude and Yield Determination, (4) Small-Scale Experiments, 2(5) Data Processing Analysis, 2(6) Ground Motion Analysis, and 2(7) Selected Geological Studies. The major projects in each of these topic areas are summarized. Also presented is an Appendix listing the abstracts of all reports submitted to the Vela Seismological Center since May 1975.



UNCLASSIFIED

SECURITY CLASSIFICATION OF THIS PAGE(When Data Entered)

AFTAC Project Authorization No. VT/9712/B/PMP
ARPA Order No. 2551, Program Code No. 6H189
Effective Date of Contract: November 17, 1978
Contract Expiration Date: September 30, 1979
Amount of Contract: \$847,285
Contract No. F08606-790C-0008
Principal Investigator and Phone No.

Dr. Thomas C. Bache, (714) 453-0060, Ext. 337
Project Scientist and Phone No.

Captain Michael J. Shore, (202) 325-7581

Sponsored by

Advanced Research Projects Agency
ARPA Order No. 2551

This research was supported by the Advanced Research Projects Agency of the Department of Defense and was monitored by AFTAC/VSC, Patrick Air Force Base, Florida, 32925, under Contract No. F08606-79-C-0008.

The views and conclusions contained in this document are those of the authors and should not be interpreted as necessarily representing the official policies, either expressed or implied, of the Advanced Research Projects Agency, the Air Force Technical Applications Center, or the U. S. Government.



Accession For	
NTIS GRA&I	<input checked="" type="checkbox"/>
DTIC TAB	<input type="checkbox"/>
Unannounced	<input type="checkbox"/>
Justification	
Distribution/	
Availability Codes	
Dist	Avail and/or Special
A	

TABLE OF CONTENTS

<u>Section</u>		<u>Page</u>
I.	INTRODUCTION.	1
	1.1 BACKGROUND	1
	1.2 SUMMARY OF RESEARCH.	1
	1.3 SOURCE CALCULATIONS.	2
	1.4 DISCRIMINATION	4
	1.5 BODY WAVE MAGNITUDE AND YIELD DETERMINATION.	4
	1.6 SMALL-SCALE EXPERIMENTS.	5
	1.7 DATA PROCESSING ANALYSIS	6
	1.8 GROUND MOTION ANALYSIS	6
	1.9 SELECTED GEOLOGICAL STUDIES.	7
II.	SOURCE CALCULATIONS	9
	2.1 INTRODUCTION	9
	2.2 MODEL NORMALIZATION.	9
	2.3 PARAMETER STUDY IN ONE DIMENSION	20
	2.4 SEISMIC COUPLING AT NTS.	20
	2.5 PARAMETER STUDY IN TWO DIMENSIONS.	28
	2.6 SEISMIC COUPLING IN SALT	33
	2.7 THREE-DIMENSIONAL FINITE DIFFERENCE EARTHQUAKE MODELING ON THE ILLIAC COMPUTER	36
III.	DISCRIMINATION.	43
	3.1 DATA BASE AND PROCEDURE.	43
	3.2 PROPAGATION PATH EFFECTS NEAR THE RECORDING STATIONS	44

TABLE OF CONTENTS (Continued)

<u>Section</u>	<u>Page</u>
3.3 PROPAGATION PATH EFFECTS NEAR THE SOURCE	45
3.4 CONCLUSIONS.	46
IV. BODY WAVE MAGNITUDE AND YIELD DETERMINATION .	49
4.1 \hat{m}_b	49
4.2 OBSERVATIONS OF SEISMIC WAVES FROM SPALLATION ASSOCIATED WITH UNDERGROUND NUCLEAR EVENTS	49
4.2.1 Analysis of MERLIN Data	51
4.2.2 Analysis of Teleseismic Data.	60
4.3 APPROPRIATE VALUES OF t^* FOR TELESEISMIC BODY WAVES FROM NTS EXPLOSIONS	67
V. SMALL SCALE EXPERIMENTS	77
5.1 INTRODUCTION	77
5.2 EXPERIMENT DESIGN.	77
5.3 RESULTS FOR THE SMALL SCALE EXPERIMENTS.	82
REFERENCES.	95
APPENDIX A: ABSTRACTS OF TECHNICAL REPORTS SUBMITTED TO AFTAC/VSC MAY 1975 - DECEMBER 1979.	99

LIST OF ILLUSTRATIONS

<u>Figure</u>		<u>Page</u>
1.	SKIPPER -- Analytic comparison	10
2.	SKIPPER -- Analytic comparison	11
3.	Loading and release P-V curves for partially saturated tuff	13
4.	Predicted and measured radial velocity histories at R = 11.95 feet and 12.09 feet respectively.	14
5.	Measured and calculated vertical velocities at free surface station 9007	15
6.	Comparison between velocity gauge data and one-dimensional calculation at Perret shot level station B-SL, X = 204 m, Y = 0	17
7.	Comparison between velocity gauge data and one-dimensional calculation at Perret shot level station 160SL, X = 470 m, Y = 0 . . .	18
8.	Comparison of experimental and numerically simulated source functions expressed as RVP transforms	19
9.	Effect of air-filled porosity on seismic magnitude	21
10.	Effect of maximum material strength on seismic magnitude.	22
11.	Effect of overburden pressure on seismic magnitude	23
12.	Amplitude of the b phase, corrected for instrument response, as recorded at a single seismograph station in the teleseismic field.	24
13.	Source spectra for the indicated test areas which best match the teleseismic data . . .	25
14.	Comparison of theoretical and observed relative coupling between NTS events . . .	27
15.	Measured and calculated horizontal velocities at shot level Perret station B-SL	29
16.	Measured and calculated horizontal veloci- ties at shot level Perret station 16-SL . .	30
17.	M _s versus yield for NTS granodiorite . . .	31

LIST OF ILLUSTRATIONS (continued)

<u>Figure</u>		<u>Page</u>
18.	m_b versus yield for NTS granodiorite . . .	32
19.	SALMON ground motion at 278 m.	34
20.	The P wave spectrum along a teleseismic ray path is plotted for the source inferred by Bache <u>et al.</u> for the Pocatello Valley earthquake	37
21.	(a) Relative displacement on the fault for the elastic case. (b) Slip velocity in the fault plane.	39
22.	Comparison of displacement spectra and time histories from the plastic problem with those from the elastic problem. . . .	40
23.	Vertical section through the MERLIN detonation point showing the relationship between the instrument locations and the subsurface geology at the site	52
24.	Ground motion time histories for the MERLIN event recorded at Station &6, R = 488 m . . .	53
25.	Radial displacement time histories for MERLIN	54
26.	Comparison of arrival times of low frequency, late time phase from MERLIN with hypothetical arrival times of pP and pS phases	55
27.	Free surface acceleration time histories for the MERLIN event	57
28.	Computed radial displacements at shot level generated by spall closure Model IV. . . .	59
29.	Houlton, Maine recordings of eleven Pahute Mesa explosions arranged in order of increasing source-to-surface travel time	61
30.	Construction of theoretical seismograms at HNME for three Pahute Mesa explosions . .	63
31.	Comparison of synthetic and observed seismograms.	65
32.	Comparison of theoretical and observed short period vertical seismograms for a Rainier Mesa explosion	68

LIST OF ILLUSTRATIONS (continued)

<u>Figure</u>		<u>Page</u>
33.	Comparison of synthetic and observed seismo-grams at HNME and a station in Alaska . . .	69
34.	Effect of t^* on HNME synthetics for FONTINA	71
35.	P wave velocity-depth profiles are plotted for three earth models: the average earth model C2, the western United States model HWA and the midwestern United States model HWNE	72
36.	Turning depth is plotted versus range for Model C2	73
37.	The effects of upper mantle structure are indicated by synthetics for FONTINA. . . .	74
38.	View of side 5 of grout block.	78
39.	Section view of block at height of 0.9 m . . .	79
40.	Section view of block at height of 0.6 m . . .	79
41.	Section view of gauge placement detail. . . .	81
42.	Vertical displacement in micrometers for free surface gauges V2 and V3, fully tamped charge, second grout block.	83
43.	Vertical displacement in micrometers for free surface gauges V4 and V5, fully tamped charge, second grout block.	84
44.	Horizontal displacement in micrometers for free surface gauges H3 and H5, fully tamped charge, second grout block.	85
45.	Vertical displacement in micrometers, gauge V1, cavity charge, second grout block.	87
46.	Vertical displacement in micrometers, gauges V6 and V4, cavity charge, second grout block.	88
47.	Vertical displacement in micrometers, gauges V2 and V5, cavity charge, second grout block.	89
48.	Horizontal displacement in micrometers, gauges H1 and H3, cavity charge, second grout block.	90

LIST OF ILLUSTRATIONS (continued)

<u>Figure</u>		<u>Page</u>
49.	Horizontal displacement in micrometers, gauge H5, cavity charge, second grout block.	91
50.	Comparison of vertical accelerations for fully tamped charges on second and third grout blocks	93

LIST OF TABLES

<u>Table</u>		<u>Page</u>
1	DESCRIPTION OF MODEL PARAMETERS FOR SPALL CLOSURE CALCULATIONS.	58
2	PARAMETERS FOR THE P_s PHASE IN THE SYNTHETIC SEISMOGRAM CALCULATIONS.	6
3	SUMMARY OF PEAK MOTIONS FOR ALL SHOTS	

I. INTRODUCTION

1.1 BACKGROUND

The objective of the Systems, Science and Software (S³) research program carried out during Fiscal Year 1979 under Contract No. F08606-79-C-0008 was to extend our understanding of the excitation of seismic waves by underground explosions and earthquakes. In particular, the program was directed toward the development of improved methods for discriminating between the seismic signals from earthquakes and explosions and the development of improved methods for estimating explosion yield. The research program to achieve the objectives included empirical, theoretical and experimental studies.

This report summarizes the work done by S³ during Fiscal Year 1979.

1.2 SUMMARY OF RESEARCH

The research activities carried out during Fiscal Year 1979 may be divided into seven topic areas:

1. Source Calculations.
2. Discrimination.
3. Body Wave Magnitude and Yield Determination.
4. Small Scale Experiments.
5. Data Processing Analysis.
6. Ground Motion Analysis.
7. Selected Geological Studies.

In the remainder of this section we will list the major projects in each of these topic areas. Most of the important results have been described in S³ reports and the appropriate report is listed with each project.

In later sections of this report we will summarize the most important results. Also, as a summary of all the work accomplished since the beginning of our work for AFTAC/VSC in May 1975, we have included in Appendix A the abstracts of all technical reports that have been submitted.

1.3 SOURCE CALCULATIONS

An important element of the S³ research program is the use of deterministic finite difference methods for directly computing explosion and earthquake sources. Calculations are done in one, two and three dimensions. The major source calculations done during Fiscal Year 1979 are listed below. Some summary remarks about source coupling and our approach using finite difference methods are presented in Section II.

Explosions in Salt

One- and two-dimensional calculations were done to model tamped and decoupled explosions in salt. The effect of non-hydrostatic prestress conditions were also investigated. Some of the results were reported at the Defense Advanced Research Projects Agency (DARPA) Workshop on Cavity Decoupling in February 1979, and some were reported in our May Quarterly Report (Coleman, et al., 1979).

PILEDRIIVER

A detailed two-dimensional calculation of PILEDRIIVER was carried out and the results were described in our August Quarterly Report (Rimer, et al., 1979). The constitutive models were based on analysis of results from an extensive series of one-dimensional calculations done over the past several years. Our most successful one-dimensional results were done this year and are described in the May Quarterly Report (Coleman, et al., 1979).

Explosions in Granite

Using the geology and constitutive models developed in our study of PILEDRIVER, three more two-dimensional calculations of explosions in granite were carried out near the end of the contract year. The three events include a 150 KT explosion at 1 km depth and 20 KT explosions at 1 km and 0.4 km depth. The results of these calculations have not yet been reported.

Earthquake Modeling

In Section 2.6 we give a brief summary of our earthquake work. We are using a three-dimensional finite difference model (TRES) of earthquake faulting which was made operational on the ILLIAC computer in Fiscal Year 1978. In the initial calculations done with this model the rupture velocity was prescribed and the boundary conditions on the fault surface were governed by a Coulomb friction law. The results of these calculations were described in our February Quarterly Report (Bache, et al., 1979).

The first set of calculations were useful for improving understanding of the geometric and kinematic parameters of the fault. However, they bypass consideration of many aspects of the physics of the faulting process. A new algorithm incorporating a fracture criterion in which rupture advance is governed by the constitutive properties of the material in the fault zone was developed. A partial description of this algorithm was described in the May Quarterly Report (Coleman, et al., 1979).

Analytic Continuation of Complex Source Calculations

The source calculations are carried out until the stress waves have propagated into a region where the material response is linear elastic. In order to compute theoretical seismograms

at ranges of interest which are usually much farther than this "elastic radius," it is necessary to have some analytic continuation scheme. When the source is considered to be in a wholespace, as is the case for the earthquake and one-dimensional explosion calculations, methods previously developed at S^3 are used (e.g., Bache and Harkrider, 1976). For the two-dimensional explosion calculations where a free surface is present, new methods are required.

The basic theoretical development for analytical continuation of sources in a layered halfspace was done during Fiscal Year 1978 and was reported in the April (Rodi, et al., 1978) and August (Savino, et al., 1978) Quarterly Reports. The implementation and testing of this method for surface waves was described in our August Quarterly Report (Rimer, et al., 1979). The method has also been implemented and tested for body waves, but has not yet been reported.

1.4 DISCRIMINATION

A major part of our effort during Fiscal Year 1979 was the completion of the S^3 contribution to the Vela Seismological Center (VSC) discrimination experiment. In Section III we summarize our major conclusions from that effort.

1.5 BODY WAVE MAGNITUDE AND YIELD DETERMINATION

Several research projects were carried out during Fiscal Year 1979 under this task. First, an algorithm for automatically computing body wave magnitude was developed and tested on a data set including recordings of eleven Pahute Mesa explosions at six teleseismic stations. We also modeled many of these seismograms.

An important conclusion of our modeling work is that an excellent match to the observations at a transparent station like HNME is obtained by modifying the source representation in the following way. A downward impulse source is added to represent spall impact. This impulse has amplitude and time lag (with respect to the explosion) consistent with near field estimates of these quantities. Further, to represent the loss of energy due to spallation, the upward waves from the explosion are halved. In Section IV we summarize in more detail our arguments for the importance of spall impact for explaining observed seismic waveforms.

Also presented in Section 4.3 is a brief summary of our arguments for choosing t^* near unity when synthesizing seismograms. Much smaller t^* values (at 1 Hz) require a substantial adjustment in our conventional wisdom about the structure of the upper mantle at depths below 750 km and/or in the amplitude and corner frequency of the source-time function.

1.6 SMALL-SCALE EXPERIMENTS

Small-scale explosion experiments were carried out with the objective being to measure the free surface motion due to the detonation of small high explosive charges within a uniform, well-characterized medium. These experiments were intended to be more complex versions of similar experiments carried out in 1976 and 1977 and reported by Cherry, et al. (1977). An important difference was that the explosive charges used for the earlier experiments were no longer available to us. Therefore, our initial effort was directed toward the construction of new charges and verification that the deviations from sphericity were small and that the energy output was uniform from one experiment to the next.

A discussion of the experiments is presented in Section V. The first experiments demonstrated that the fully tamped charges gave a spherically symmetric radiation field. Fairly large shear waves were recorded from the experiments conducted in 1976 and these were attributed to asymmetric tamping. This problem has apparently been solved.

The next step was to detonate the charges in cylindrical cavities to study the radiation field asymmetry. Two experiments were done and large shear waves were recorded. However, a significant experimental problem was not solved. Most of the charges did not experience a prompt high order detonation. This is attributed to a loss of contact between the explosive and bridgewire that occurs during the preparation of the grout block. This makes the experiments difficult to model theoretically.

1.7 DATA PROCESSING ANALYSIS

The major effort accomplished under this task was a design study for the hardware configuration of a Seismic Research Center (SRC). This study was reported by Berger (1979). The system discussed is to perform the tasks of the present SDAC and to meet the requirements of a data center which can record and process the data from up to 50 NSS Mod II type seismic stations.

1.8 GROUND MOTION ANALYSIS

This task was mainly carried out by John R. Murphy and his staff at the S³ offices in Reston, Virginia. A major part of that effort was a review of the available free-field data from underground nuclear explosions in alluvium, tuff, dolomite, sandstone-shale and interbedded lava flows. This review was reported by Murphy and Bennett (1979).

1.9 SELECTED GEOLOGICAL STUDIES

The objective of this task was to organize a group of consultants to review the relevant Soviet literature for understanding the geophysical environment at selected test sites. A meeting of the study group was held in December 1978 and minutes of that meeting were prepared and distributed.

II. SOURCE CALCULATIONS

2.1 INTRODUCTION

In this section we describe our approach to understanding source coupling by using a deterministic technique for predicting the seismic coupling for both body waves and surface waves. The basic element of the technique is a computer model of near field, nonlinear stress wave propagation which calculates the ground motion at arbitrary distances from the explosive source. For seismic coupling predictions the distances at which the calculation is monitored are always chosen to be outside the nonlinear region. This elastic ground motion forms the basis for estimating seismic coupling.

Within the computer model are descriptions (constitutive relations) of the response of the rock environment to stresses varying from a few megabars in pressure down to the elastic level. The most critical constitutive relations affecting seismic coupling are those involving irreversible pore collapse, tension failure and effective stress.

The next section presents the normalization of these constitutive relations by comparisons between calculated and observed ground motion from explosive sources. We then summarize the results from some calculations of seismic coupling as a function of rock type and depth of burial.

2.2 MODEL NORMALIZATION

For estimating seismic coupling, the monitored stations must be in the elastic region. Therefore, the model must eventually be able to accurately propagate an elastic wave. Figures 1 and 2 (Cherry, et al., 1973) compare the analytic and computer model solutions to an elastic disturbance generated

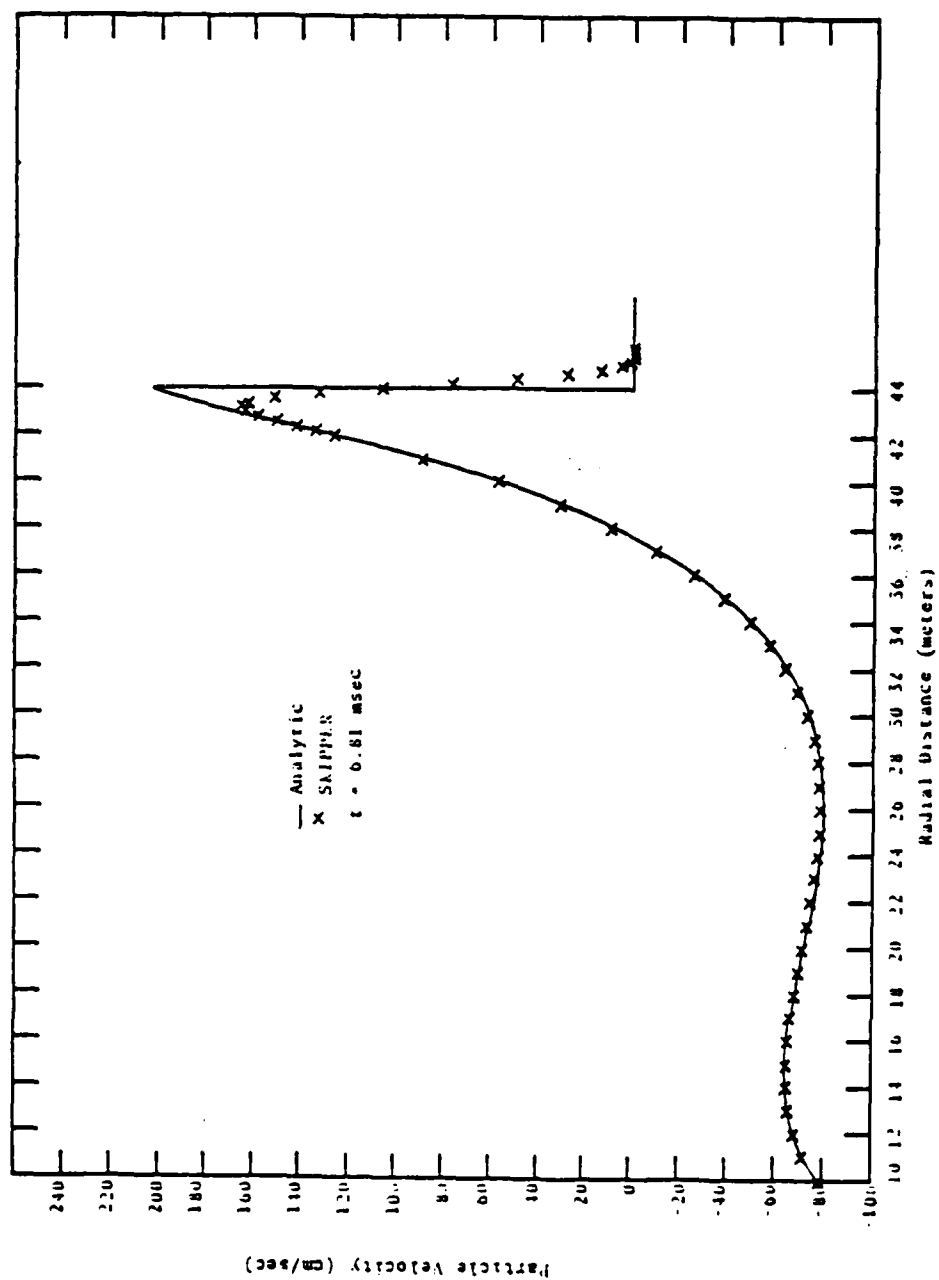


Figure 1. SKIPPER - Analytic comparison.

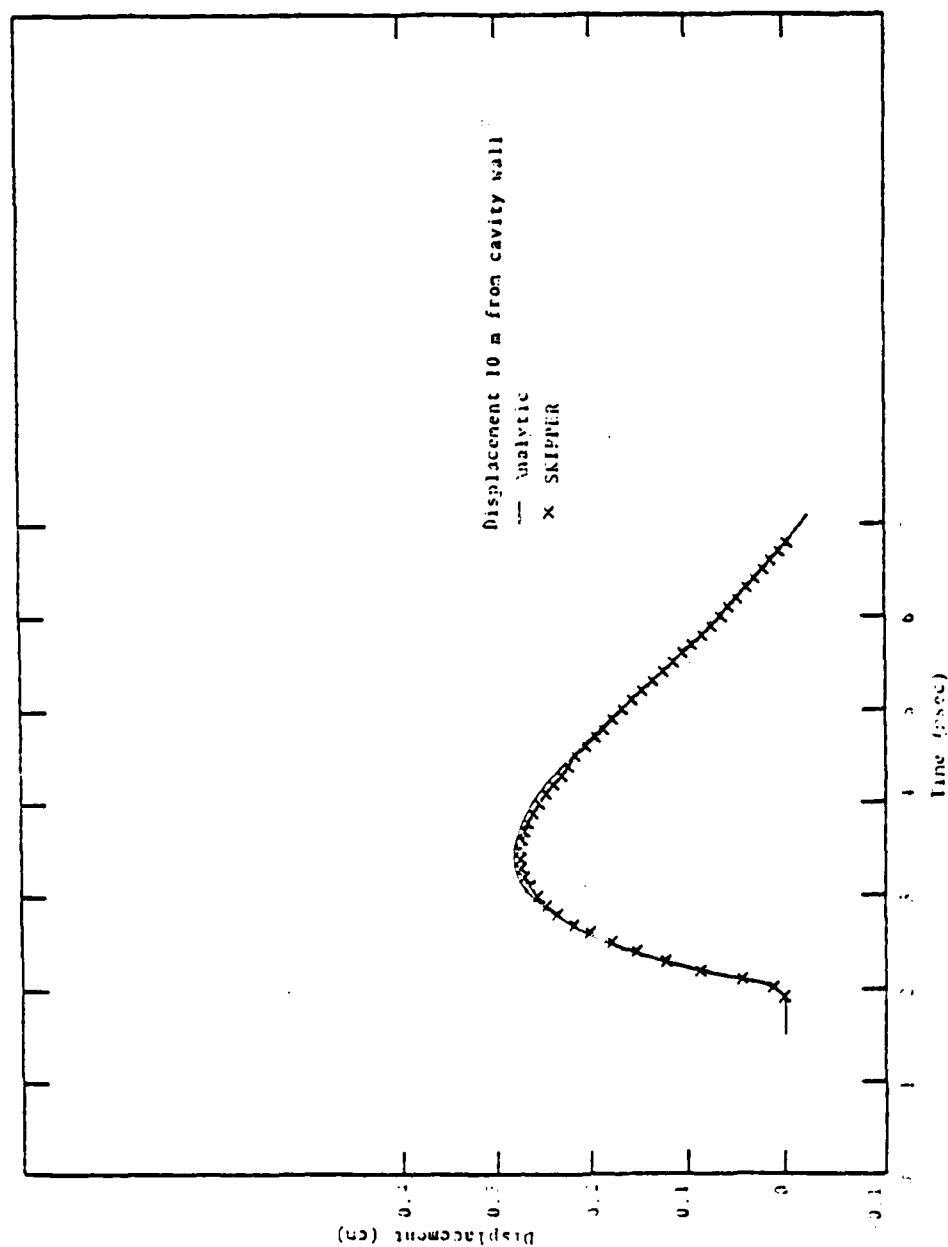


Figure 2. SKIPPER -- Analytic comparison.

by an exponentially decaying pressure load applied to the inside of a 10 m cavity. The model is capable of accurately simulating the propagation of a small displacement elastic disturbance.

A constitutive model for irreversible pore collapse was presented by Cherry, et al. (1973). The pressure loading and release states obtained from this model for a partially saturated tuff are shown in Figure 3. Riney, et al. (1973) used this model to predict the ground motion from the MINE DUST HE shot, a 1,000 pound nitromethane explosion detonated May 10, 1972 at NTS Area 16. Figure 4 shows a comparison between the computer model, run on May 8, 1972, and the particle velocity recorded from the shot. The agreement shown in this figure is typical of comparisons at other distances. These results provided us with a great deal of confidence that realistic ground motion predictions can be made in weak rocks where the dominant mechanism for stress wave attenuation is the removal of air filled porosity.

The basic features of the tension failure model were presented by Cherry, et al. (1975) and used by Rimer, et al. (1979) to match the surface spall and slap down phases from the PILEDRIIVER event. Figure 5 compares calculated and observed particle velocities 368 m from SGZ for this event. This comparison indicates that the tension failure model contains the physics necessary to model spall effects from a nuclear event. As a result we proceed with a two-dimensional parameter study to determine the effects of yield and depth of burial on body waves and surface waves in NTS grandiorite. Preliminary results from this study will be presented later in this summary.

Two features are included in the material strength portions of the constitutive model that are not usually present in calculations performed by other investigators. These include the dependence of material strength on both the

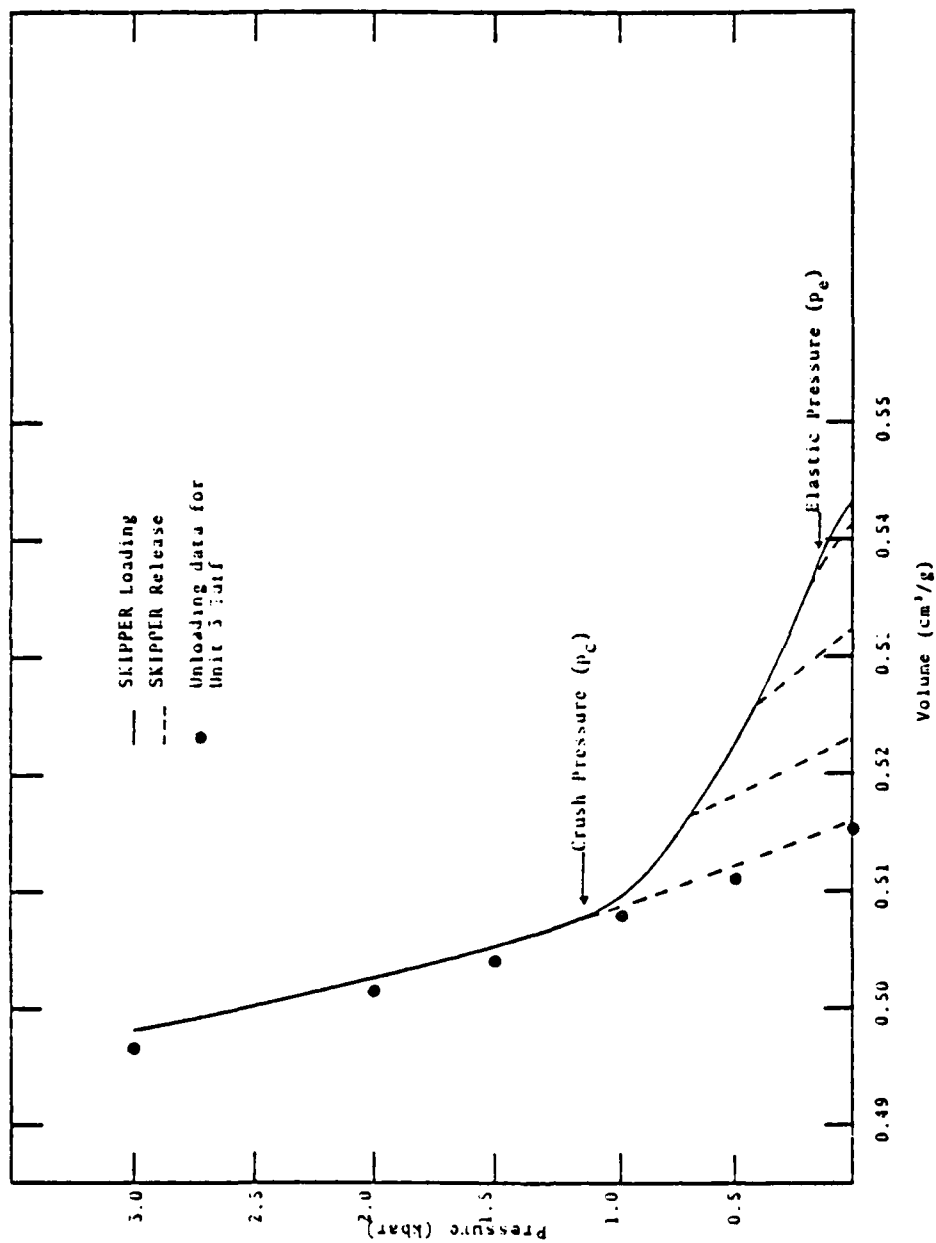


Figure 3. Loading and release P-V curves for partially saturated tuff ($f = 0.17$, $\phi_0 = 0.05$).

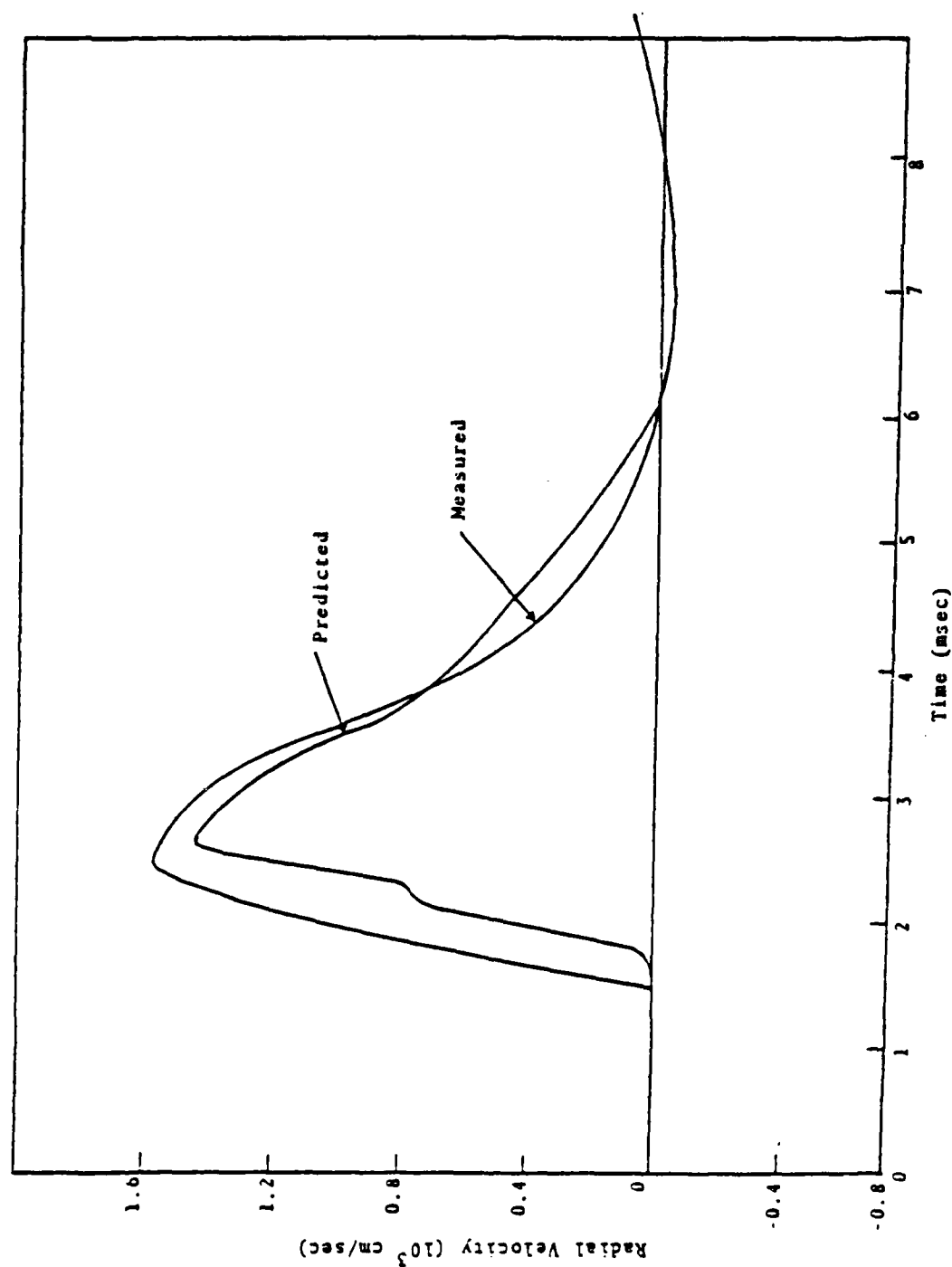


Figure 4. Predicted (May 8 Run) and measured (ATI) radial velocity histories at $R = 11.95$ feet and 12.09 feet respectively.

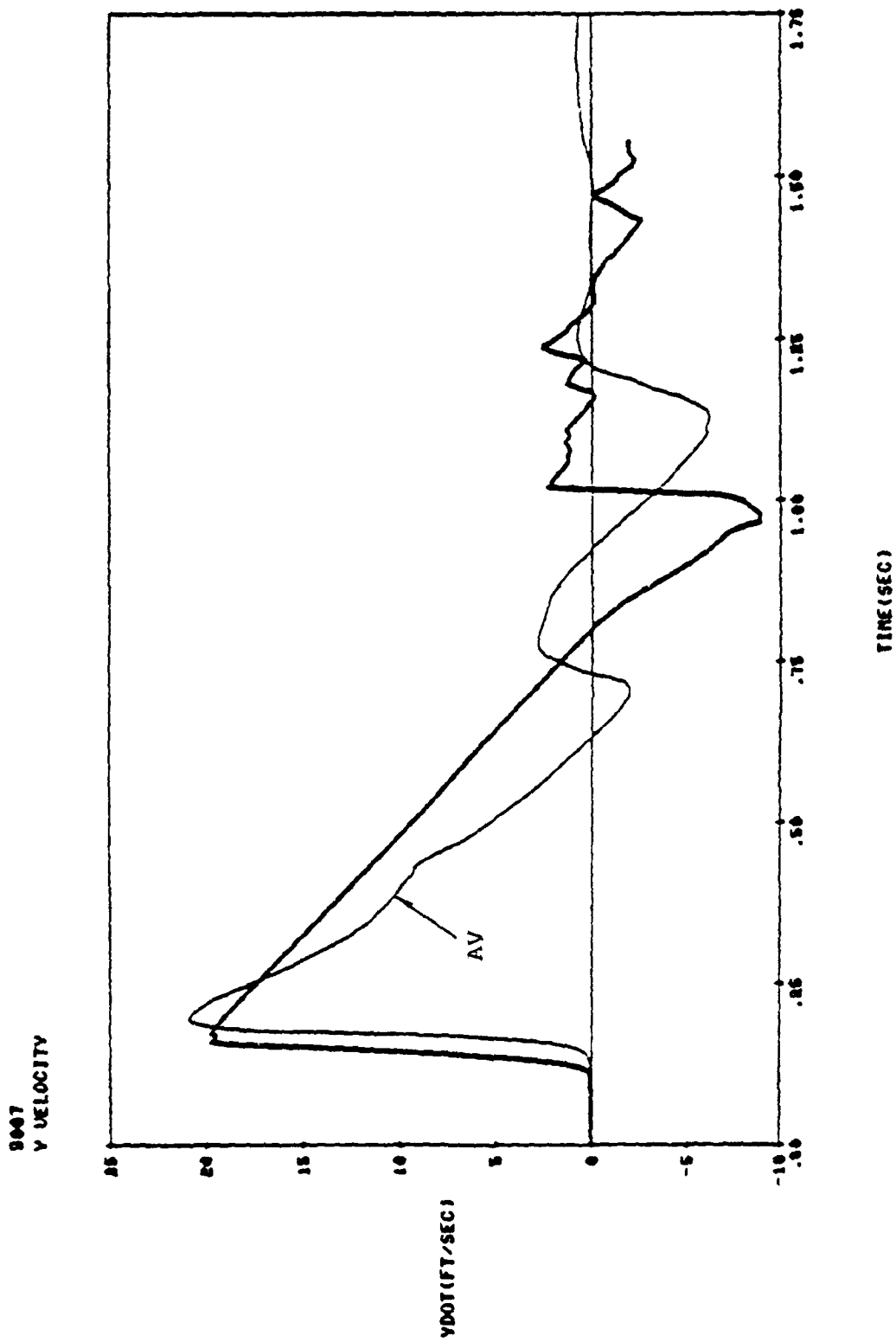


Figure 5. Measured and calculated vertical velocities at free surface station 9007 (horizontal range = 368 m).

third deviatoric stress invariant (Cherry and Petersen, 1970) and pore fluid pressure (Cherry, et al., 1975; Rimer, et al., 1979). These features have allowed the model to accurately calculate ground motion in saturated and partially saturated rocks having large values of material strength when tested dry in the laboratory. Figures 6 and 7 compare the observed and calculated ground motion from the PILEDRIIVER event at shot level. This type of agreement is only possible if the rock environment is assumed partially saturated and the effect of pore fluid pressure is included in the material strength portion of the model.

Near field ground motion measurements are sparse and often inadequately address the low frequency content of the ground motion responsible for body wave and surface wave coupling at teleseismic distances. Therefore, as an additional aid for model normalization, we conducted laboratory experiments to obtain high quality measurements of rock motion from an explosive source (Cherry, et al., 1977). The measurements were taken on the surface of specially prepared concrete cylinders and the source was 0.25 gm of PETN. Figure 8 compares the experimental data with two calculations, with and without tension failure. A characteristic of tension failure is a peaked RVP spectrum, caused by a discontinuity in tangential stress at the linear-nonlinear boundary. The calculation with tension failure in the material model is in better agreement with the data.

Finally, a definition of what we mean by "elastic behavior" is now appropriate. We define elastic behavior as the absence of irreversible pore collapse, tension failure and yielding. In addition, the stress-strain relation is obtained from single values of bulk modulus and shear modulus. We have not found it necessary to include rate dependent effects in the model. However, near field ground motion data in salt suggest that salt's material strength may be dependent on inelastic strain energy.

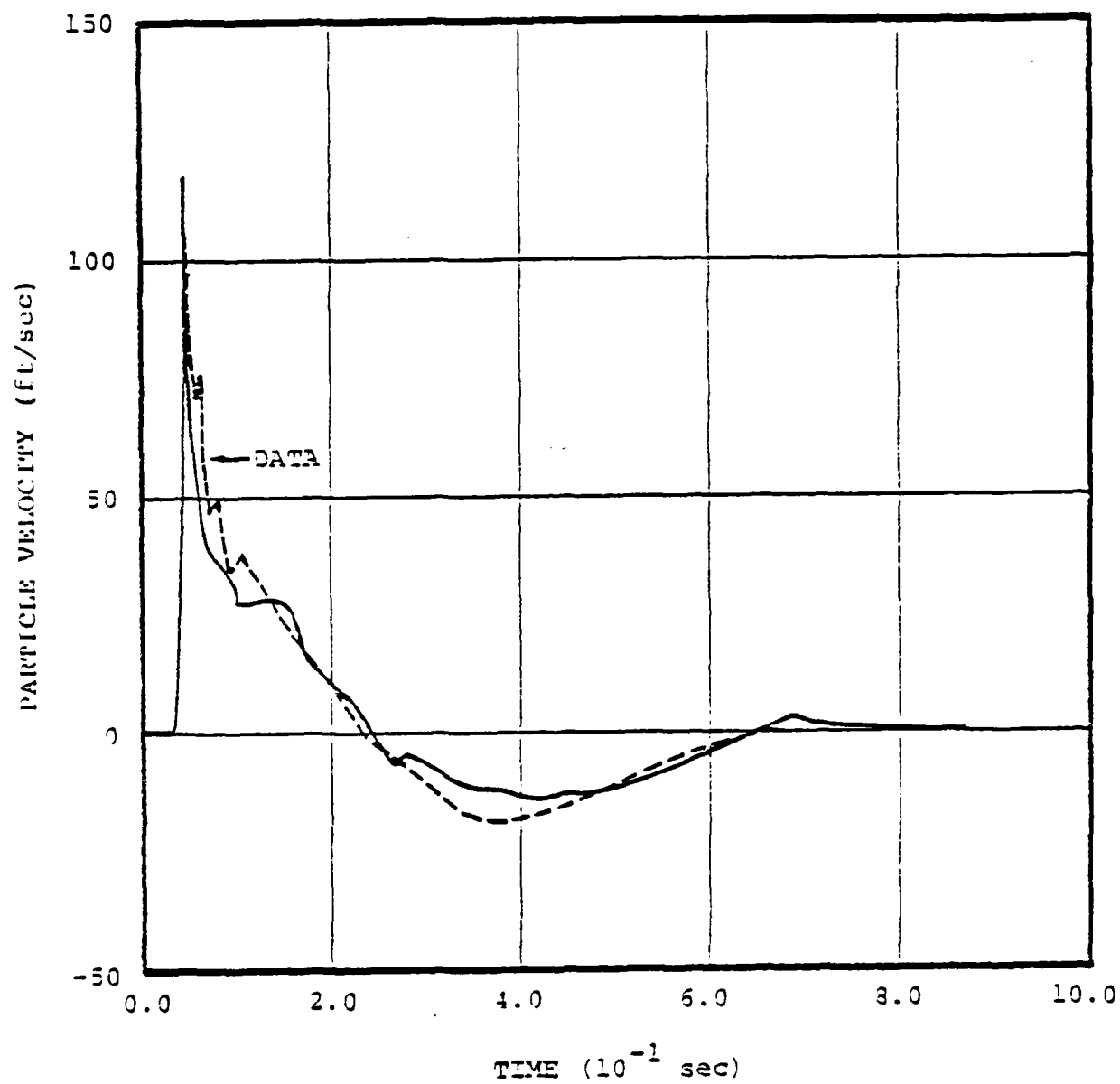


Figure 6. Comparison between velocity gauge data and one-dimensional calculation at Perret shot level station B-SL, X = 204 m, Y = 0.

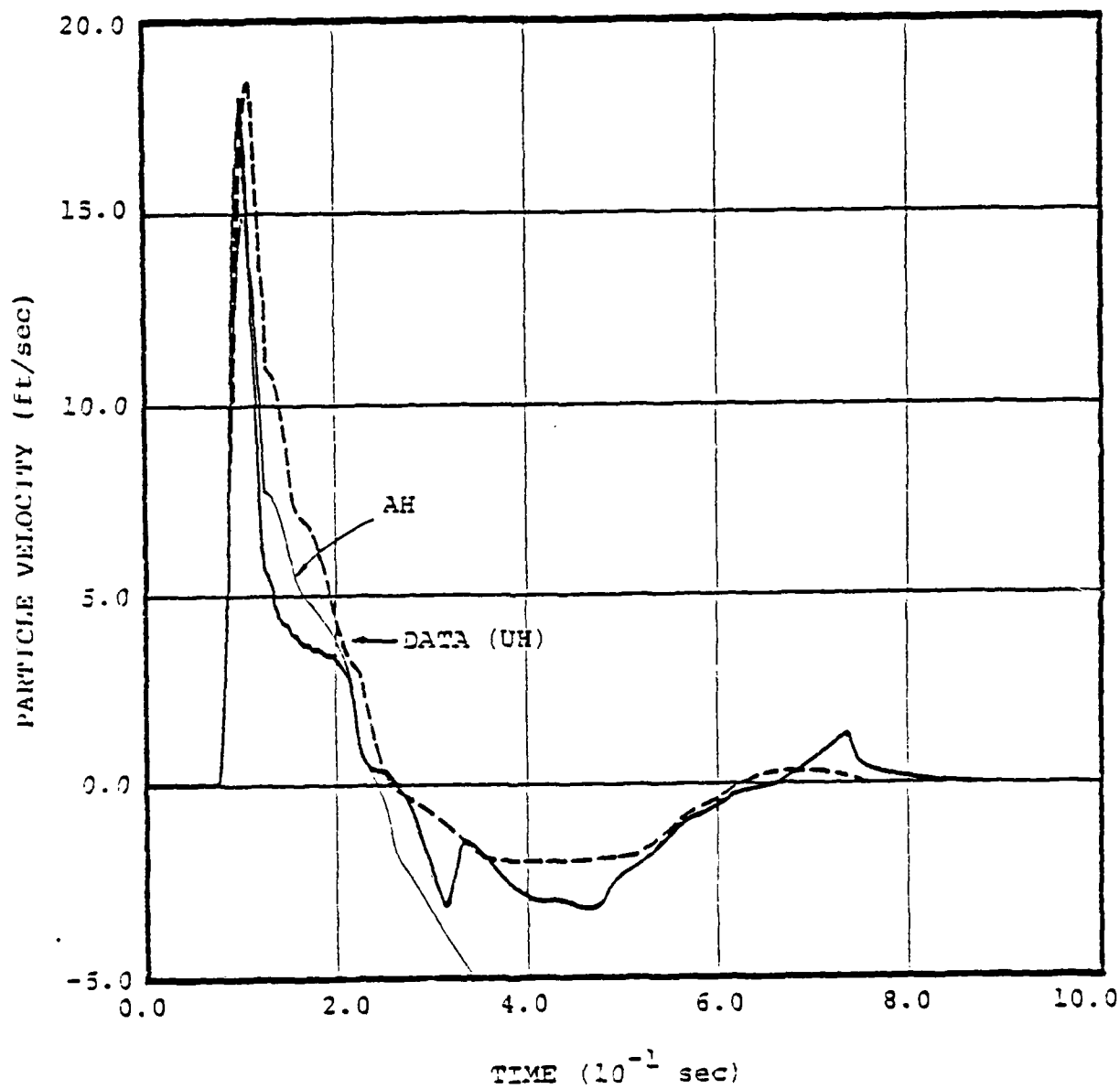


Figure 7. Comparison between velocity gauge data and one-dimensional calculation at Perret shot level station 16-SL, X = 470 m, Y = 0.

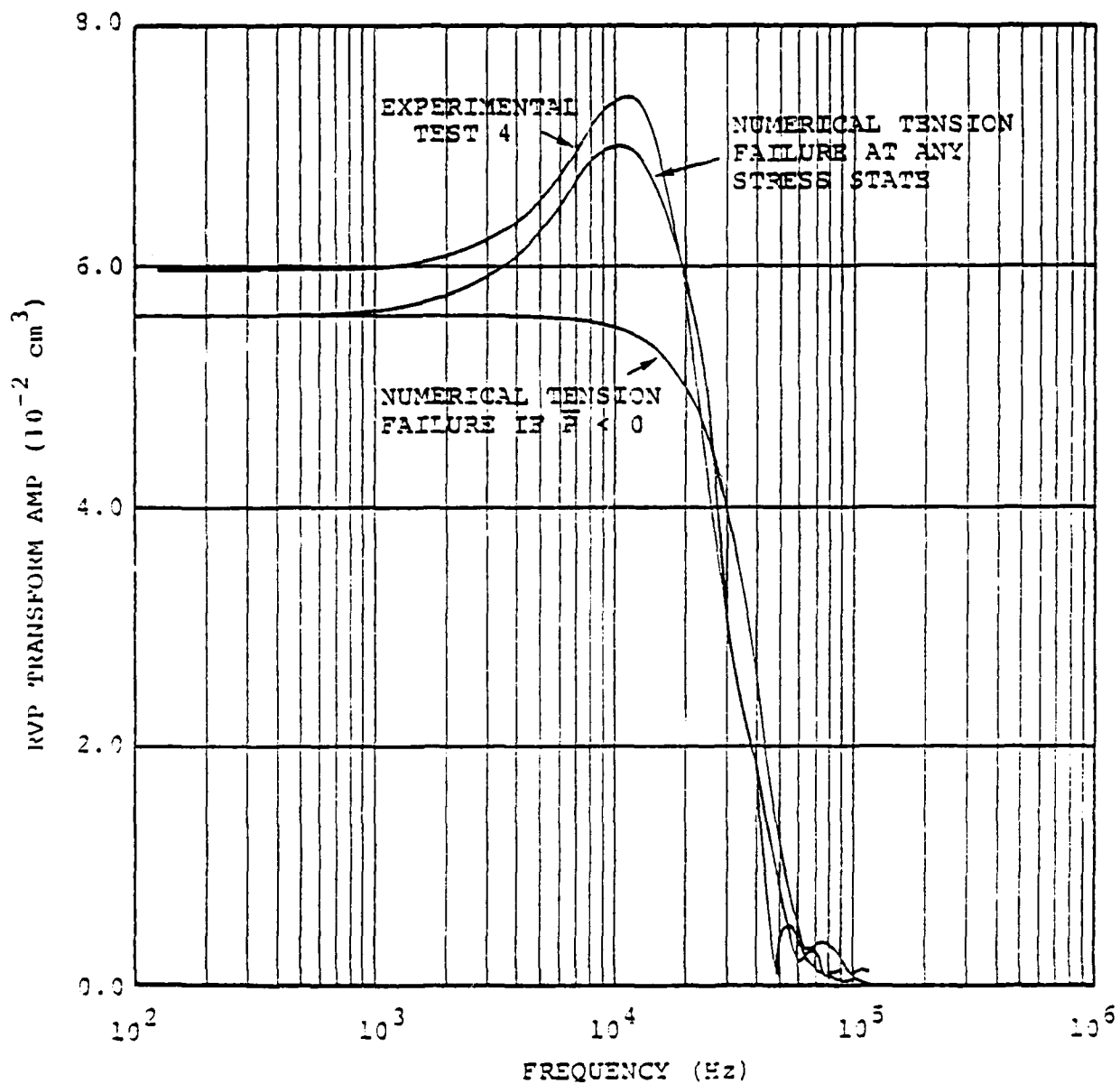


Figure 8. Comparison of experimental and numerically simulated source functions expressed as RVP transforms.

2.3 PARAMETER STUDY IN ONE DIMENSION

Cherry, et al. (1975) conducted a one-dimensional parameter study to determine the dependence of teleseismic magnitudes on the nonlinear behavior of the near source rock environment. They calculated $\psi(\infty)$ for systematic changes in material properties and computed the corresponding change in magnitude (Δm), where

$$\Delta m = m^i - m^k = \log \left[\frac{\alpha_i \psi_i(\infty)}{\alpha_k \psi_k(\infty)} \right] .$$

Figures 9, 10 and 11 show the effect of air filled porosity, maximum material strength and overburden pressure on Δm . These were shown to be the most sensitive parameters in the model.

2.4 SEISMIC COUPLING AT NTS

Bache, et al. (1975) used this computer model to explain the relative differences in body wave coupling between various testing areas at NTS. The observed teleseismic data is shown in Figure 12.

Material properties used for the equivalent elastic source calculations were obtained from both laboratory tests on appropriate rock samples and CEP reports. The RVP spectra computed for each testing area is shown in Figure 13. The reasons for the differences in these sources are as follows:

1. The ratio of the spectral peak to the zero frequency limit ($\psi(\infty)$) increases with increasing material strength. Therefore, both Piledriver and Pahute Mesa rhyolite, having the largest values of material strength, show highly peaked spectra compared to the other three areas.

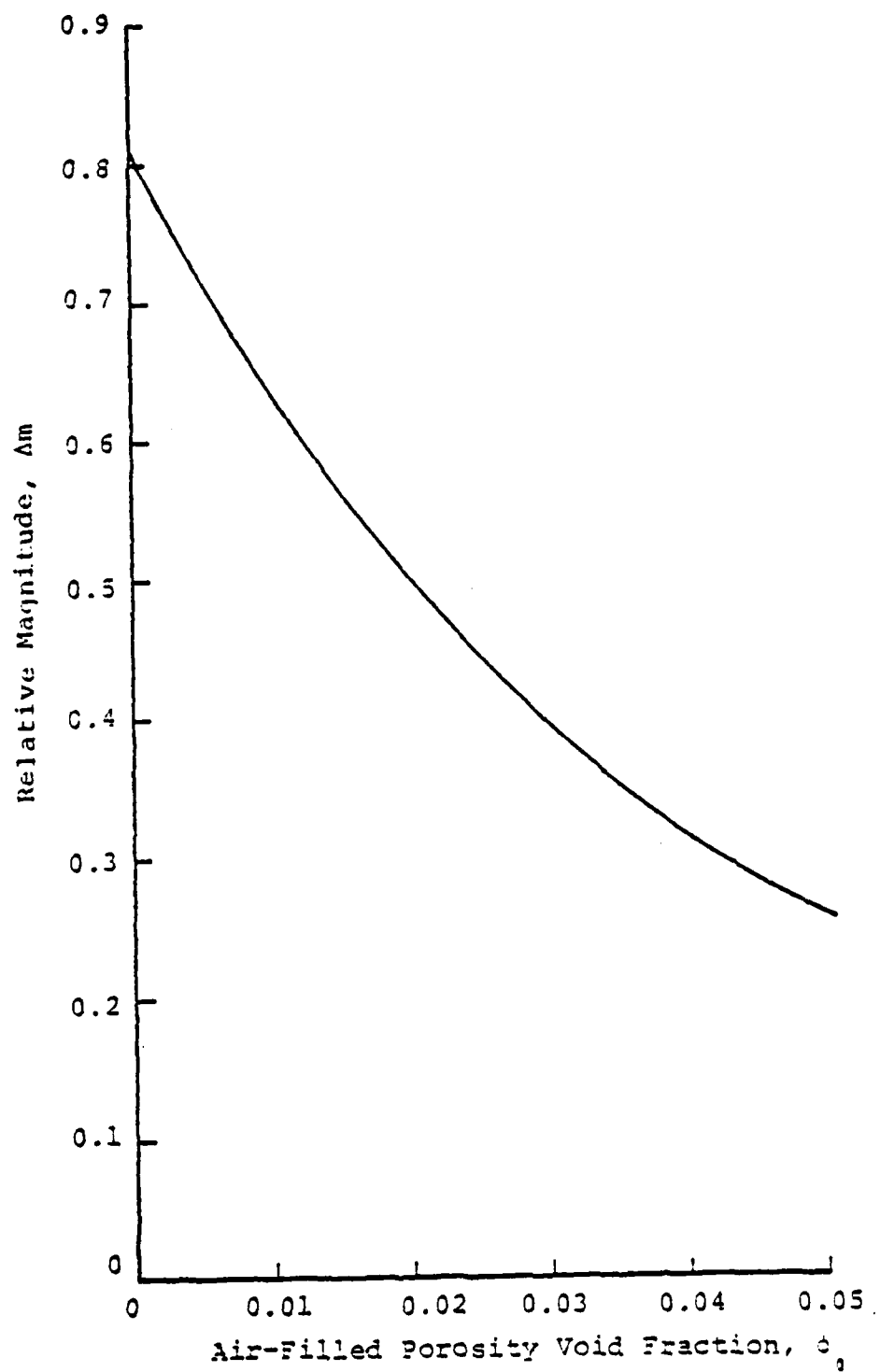


Figure 9. Effect of air-filled porosity on seismic magnitude.

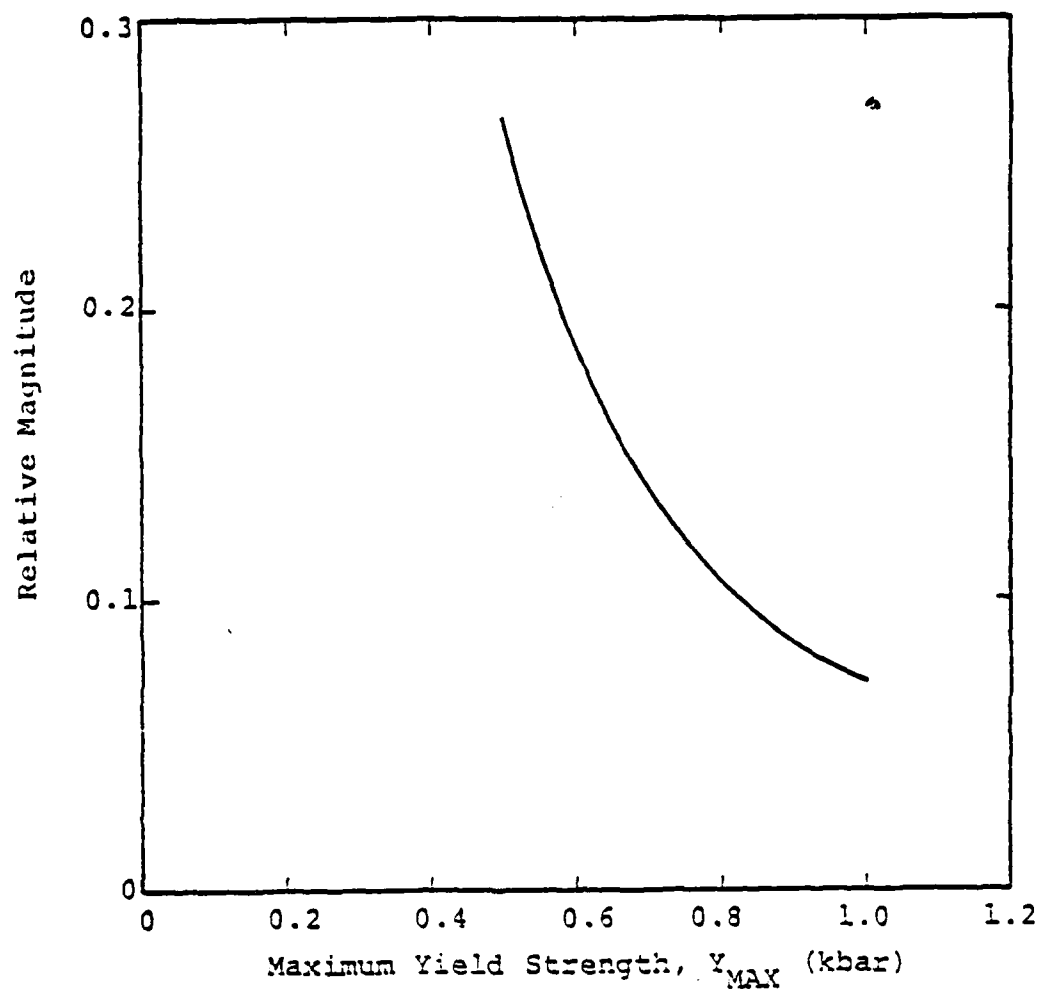


Figure 10. Effect of maximum material strength on seismic magnitude.

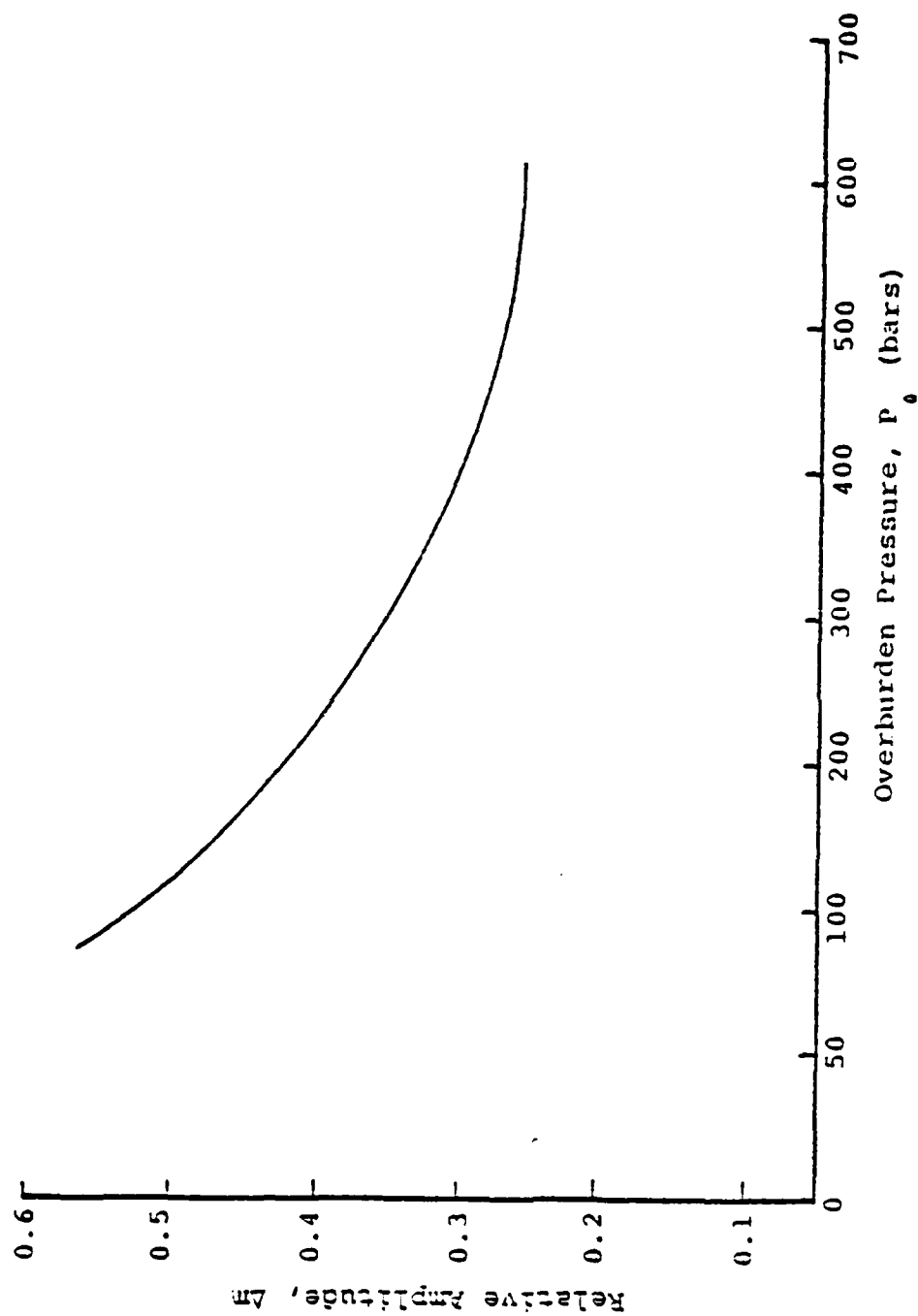


Figure 11. Effect of overburden pressure on seismic magnitude.

Amplitude, b/l (millimicrons)

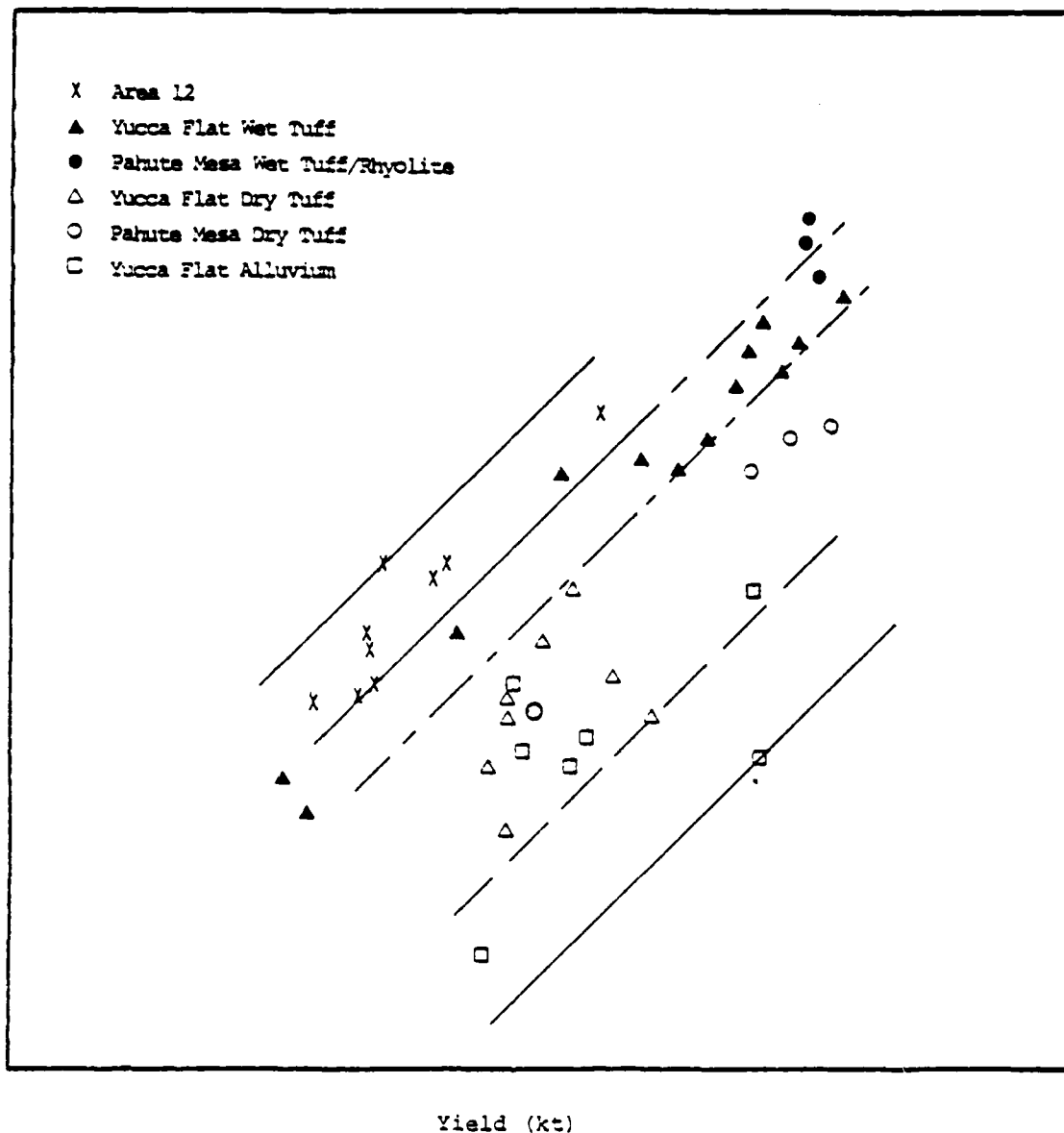


Figure 12. Amplitude of the b phase, corrected for instrument response, as recorded at a single seismograph station in the teleseismic field. The plot is log-log with three cycles on each axis. The re-recorded events are separated into groups of superficially common source material characteristics as indicated in the legend. The lines are of unit slope.

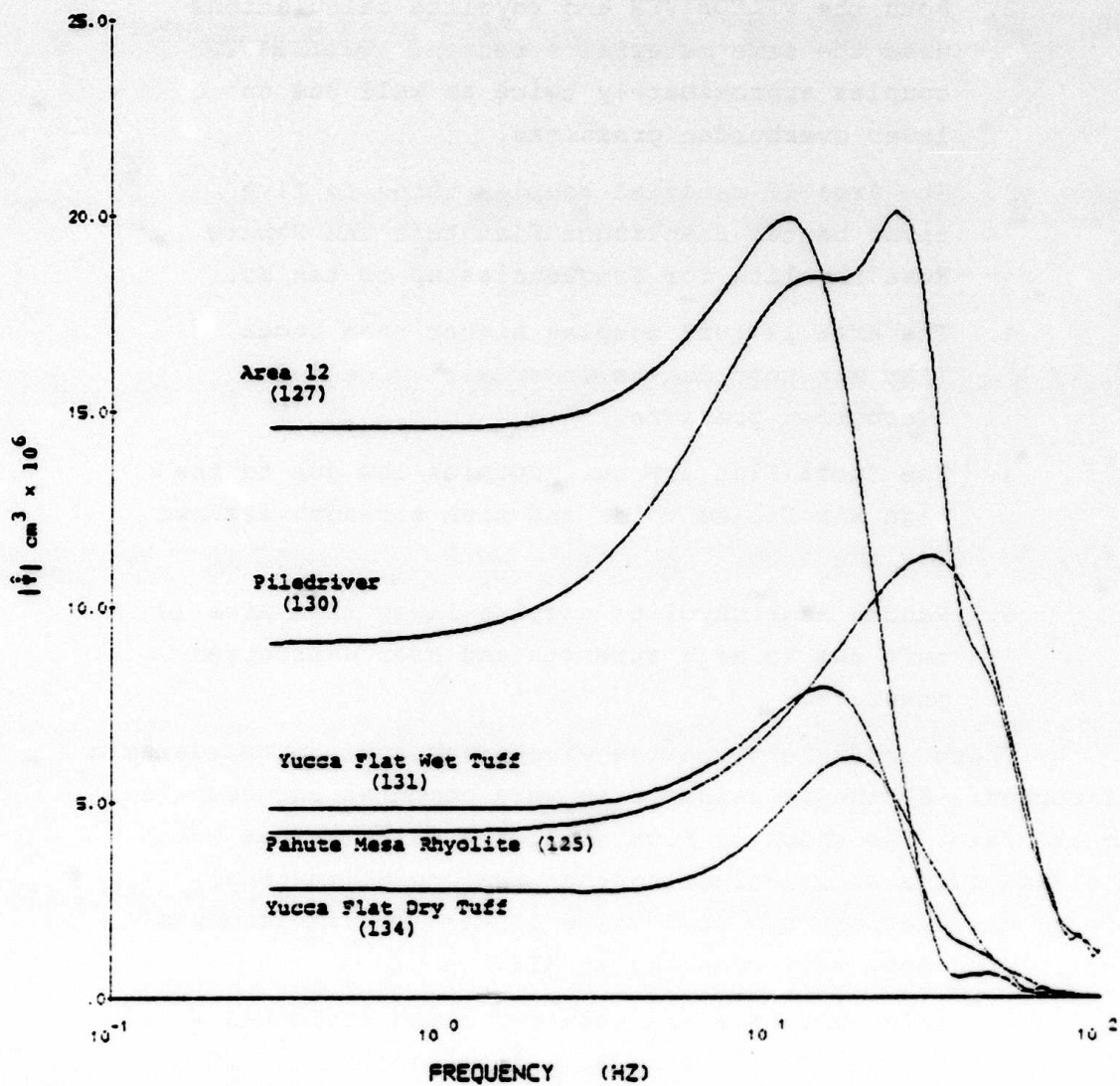


Figure 13. Source spectra for the indicated test areas which best match the teleseismic data. The device yield for each calculation was 0.02 KT.

2. Both the PILEDRIVER and rhyolite calculations used the same material strength. PILEDRIVER couples approximately twice as well due to lower overburden pressures.
3. The Area 12 material couples three to five times better than Yucca Flat tuff and Pahute Mesa rhyolite for frequencies up to ten Hz.
4. The Area 12 tuff couples higher than Yucca Flat wet tuff due to lower air voids and overburden pressure.
5. The Yucca Flat dry tuff couples low due to the high air filled voids and high strength assumed for the site.
6. Pahute Mesa rhyolite couples lower than Area 12 tuff due to high strength and high overburden pressure.

These equivalent sources were propagated to teleseismic distances. Synthetic seismograms were computed and compared to the data. As shown in Figure 14, the calculations match the data quite well indicating that the one-dimensional source calculations are accounting for the robust features controlling body wave coupling at NTS.

A similar analysis has been performed by Bache, et al. (1978) for surface waves using data from stations at Tucson and Albuquerque. They concluded that the $\psi(\infty)$ values obtained from the source calculations are within acceptable limits to those inferred from the data.

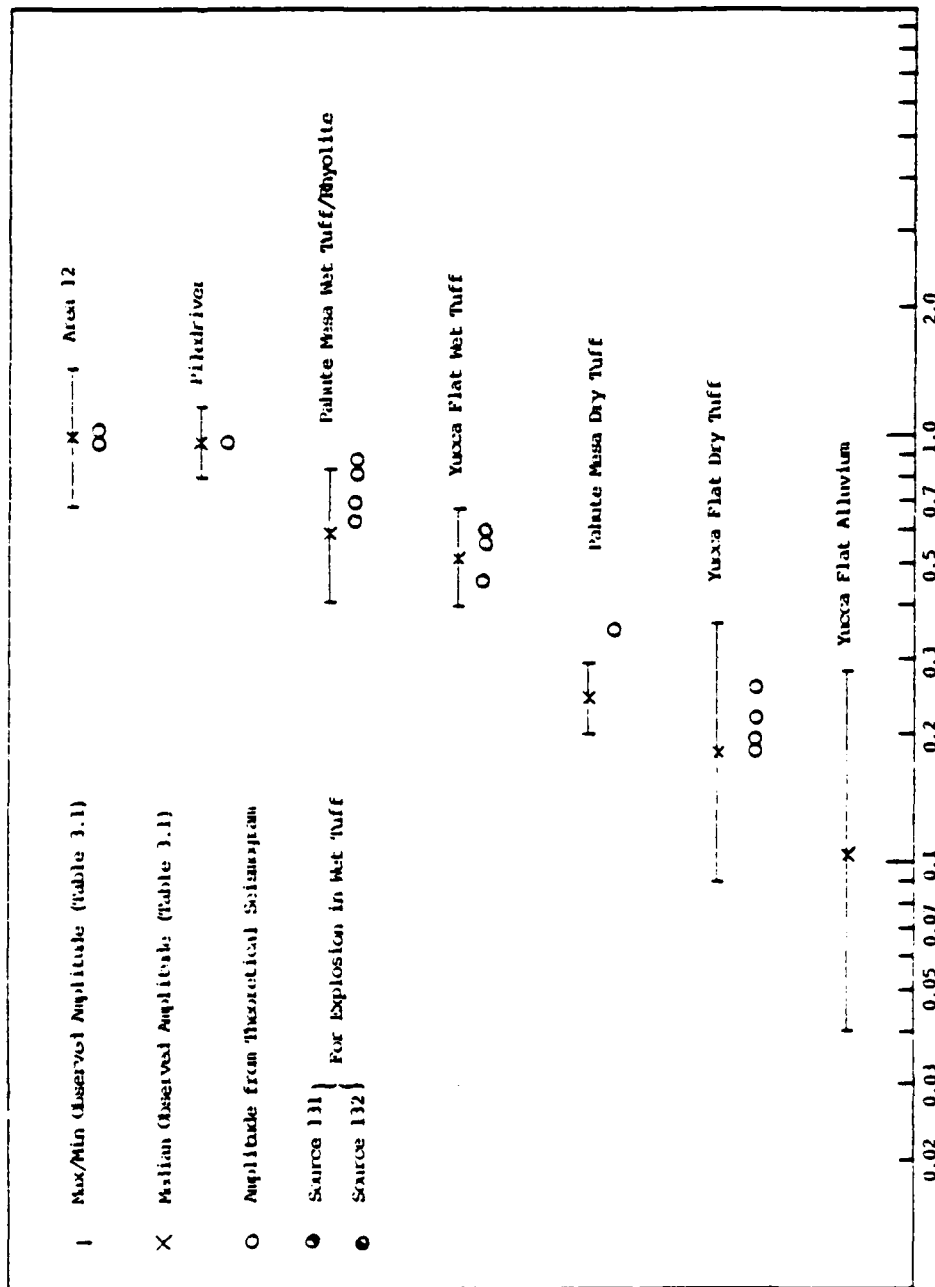


Figure 14. Comparison of theoretical and observed relative coupling between NPS events. The observed data is directly from Table 2.1. The theoretical amplitudes, $|A_p|$, have been normalized to the median for the theoretical Area 12 events.

2.5 PARAMETER STUDY IN TWO DIMENSIONS

Rimer, et al. (1979) conducted a two-dimensional parameter study to determine the effect of yield and depth of burial on surface wave and body wave magnitudes. The rock environment was NTS fractured granodiorite. Near field data from the PILEDRIVER event (61 KT, 460 m) was compared to the results of the PILEDRIVER calculation (Figures 5, 15 and 16). The conclusion was that the agreement was good enough to warrant a systematic investigation of the degradation of pP by spall and the resulting effect on seismic coupling. The yields (W) and depth of burial (DoB) comprising the study are given in the following table.

W (KT)	DoB (m)	Scaled DoB (m(KT) ^{1/3})
20	400	147
20	1000	368
61	460	117
150	1000	188

Each calculation was monitored on a cylindrical surface in the elastic regime. These results were then analytically continued to the far field in order to obtain estimates of m_b and M_s .

The surface wave calculations (Figure 17) show 0.3 magnitude units difference between the one- and two-dimensional PILEDRIVER calculations and 0.6 magnitude units difference between the shallow and deep two-dimensional calculations of the 20 KT sources. Agreement between the one- and two-dimensional calculations is good for the two deep shots.

The body wave magnitudes are shown in Figure 18. the variation of these magnitudes with yield and depth of burial is much reduced from that found for surface waves. It appears

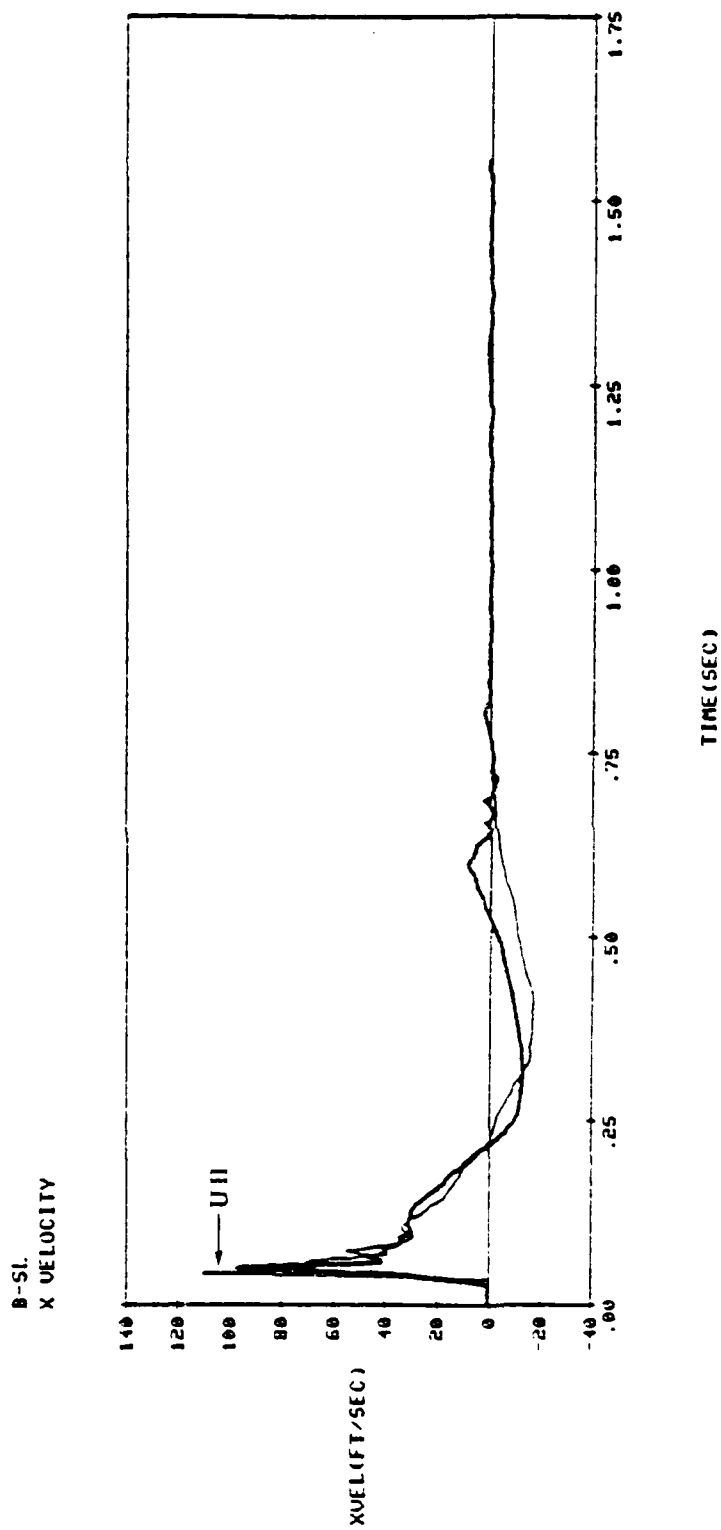


Figure 15. Measured and calculated horizontal velocities at shot level Perret station B-SL (range = 204 m).

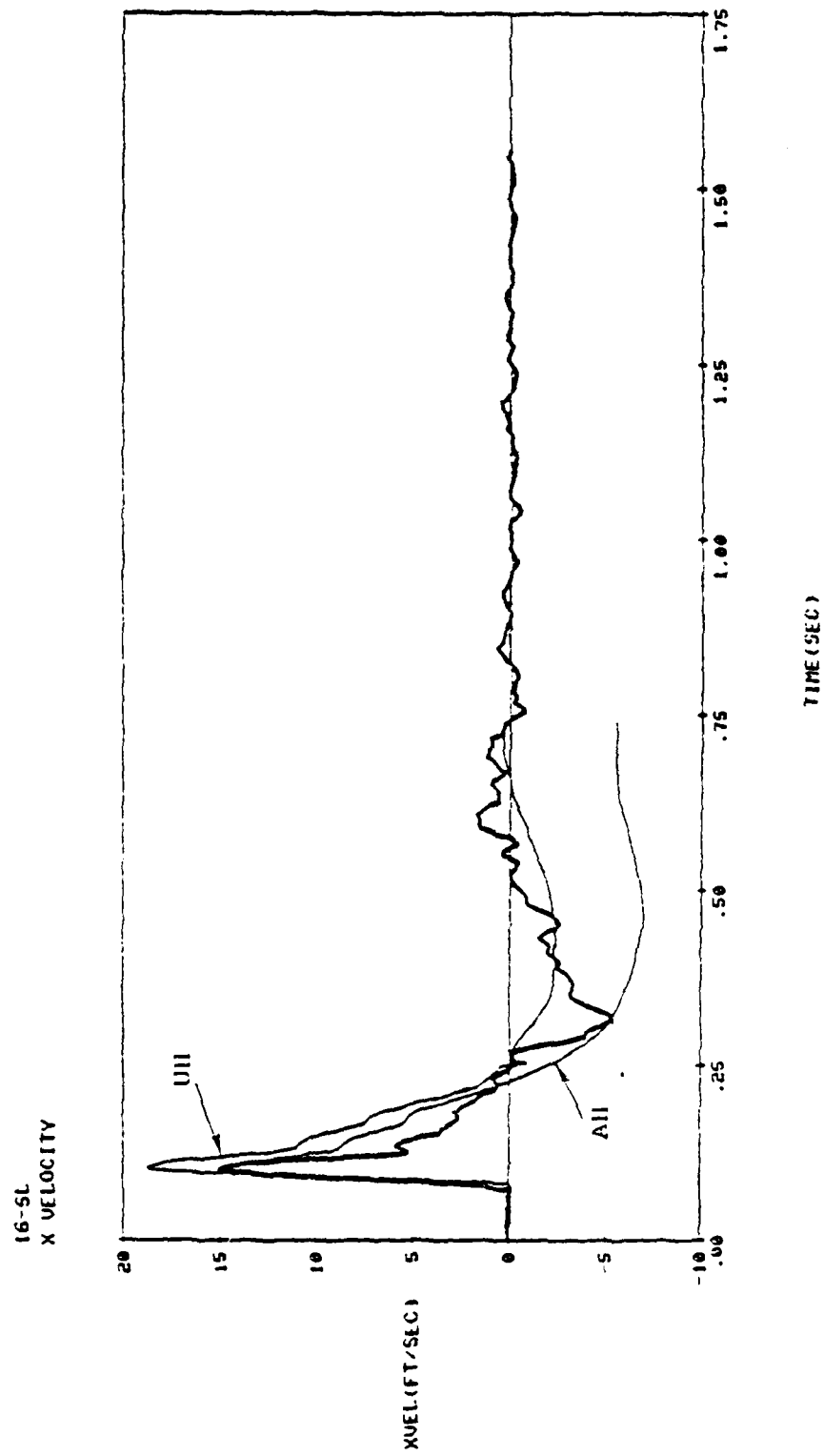


Figure 16. Measured and calculated horizontal velocities at shot level perret station 16-SL (range = 470 m).

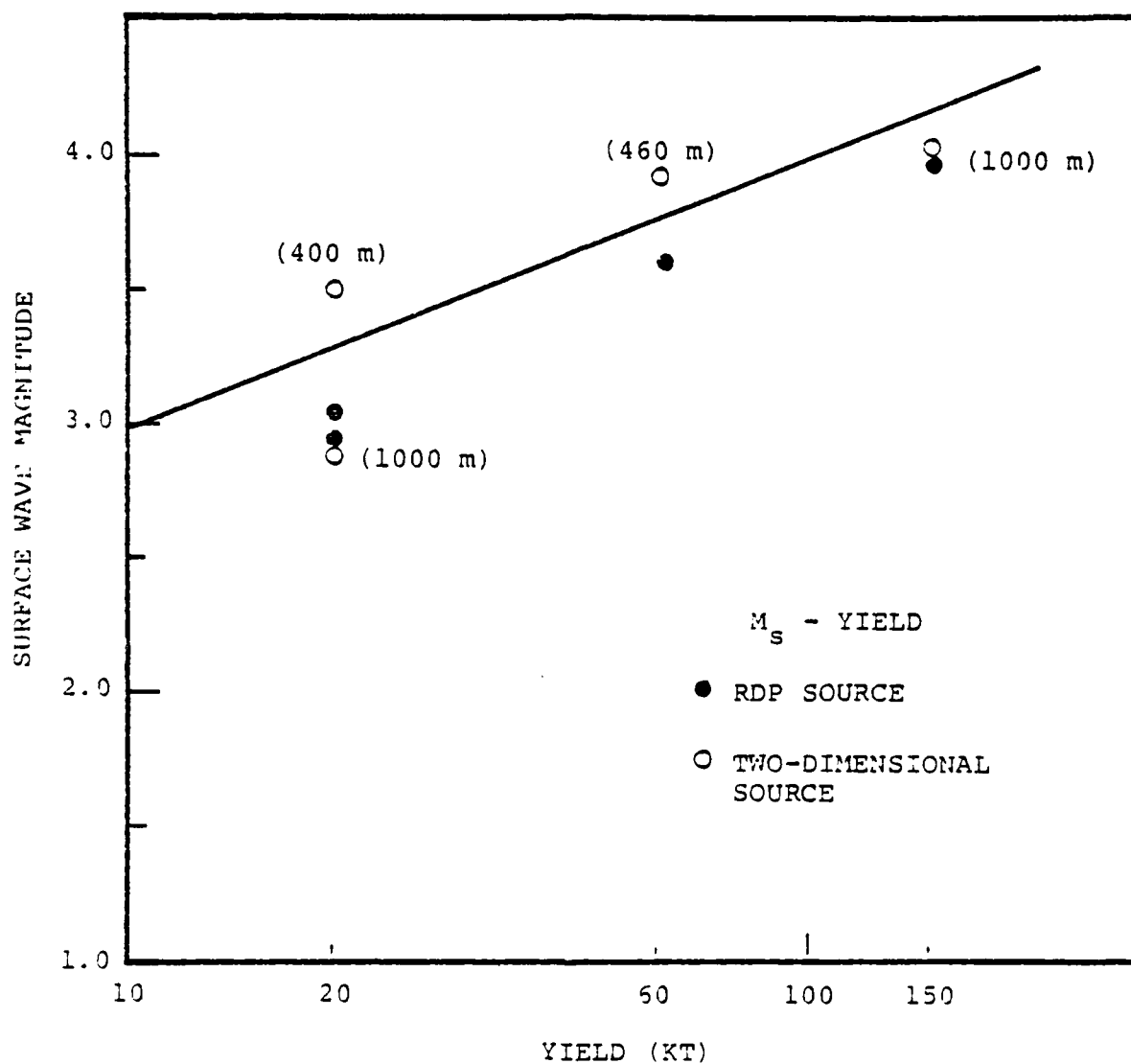


Figure 17. M_s versus yield for NTS granodiorite.

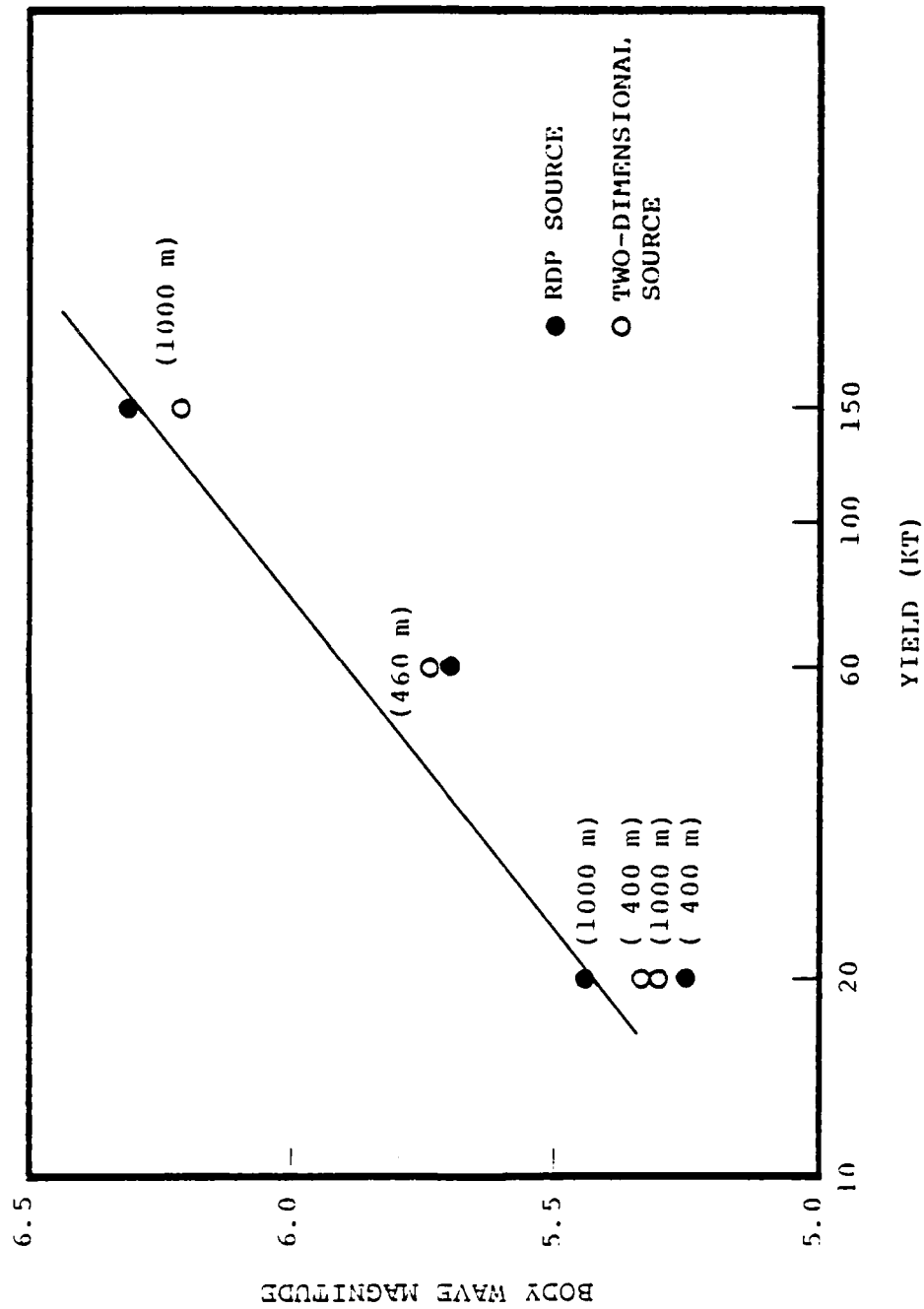


Figure 18. m_b versus yield for NTS granodiorite.

that the "b" phase is adequately modeled by a one-dimension simulation for the depths and yields considered here.

These results are preliminary in that the analytic continuation procedures are still being tested and the physical basis for the variations shown here has not been fully addressed. However, it does appear that two-dimensional simulations can improve our understanding of the effect of "spall" on seismic coupling and hopefully permit a more detailed match of the short period seismogram.

2.6 SEISMIC COUPLING IN SALT

Realistic decoupling scenarios in salt can be developed only after appropriate free field ground motion data in this rock are understood. The SALMON event (Perret, 1968) provided a large subset of this data. These data exhibit a number of puzzling features, the most important being a small amplitude "elastic" precursor which is not consistent with laboratory strength measurements or the overburden pressure at shot depth.

Here we present a possible explanation of this precursor which depends on the SALMON shot environment being "saturated." If we assume saturation, then the precursor emerges. Its amplitude depends on the assumed "saturated" strength.

Figure 19 shows a comparison between the calculated and observed radial ground motion at a distance of 278 m from the SALMON event. The peaks have been aligned by shifting the time axis. In the calculation we assumed that the salt was totally saturated.

In the data the "elastic" precursor has a peak velocity of approximately 0.4 m/sec while the precursor in the calculation peaks at 1.2 m/sec. Therefore, the assumed saturated strength for salt was too high by about a factor of three. We should note that there are no strength data for saturated salt.

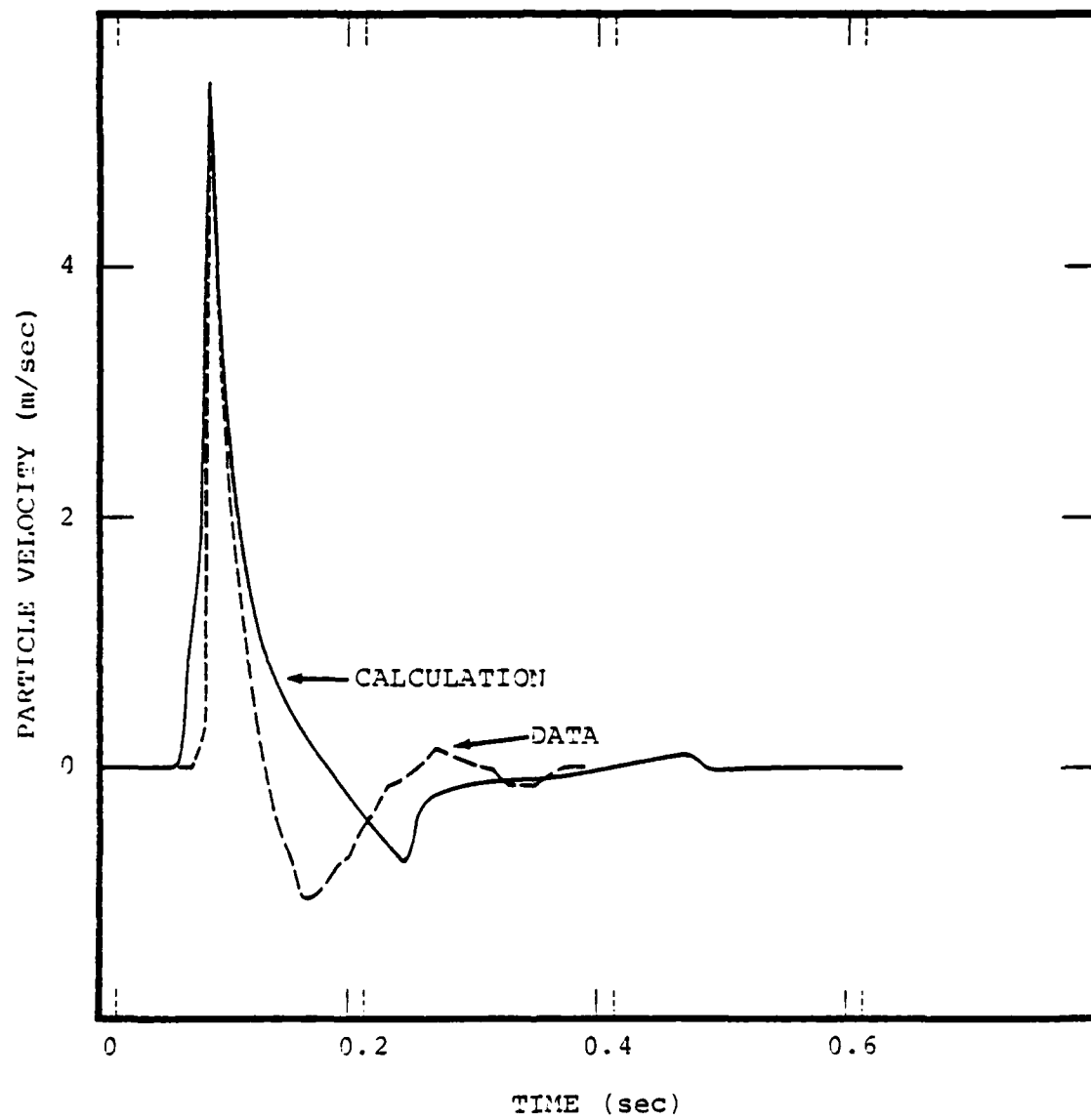


Figure 19. SALMON ground motion at 273 m.

Our assumed strength was 77 bars, obtained from an extrapolation of triaxial compression data to zero mean stress. There is no reason to expect this extrapolation to accurately represent the strength of salt at low stress states.

In addition, the width of the calculated velocity pulse is about a factor of two broader than the data. Therefore, the assumed saturated strength was low by at least a factor of two during that portion of the velocity pulse which follows the precursor.

This conflict between the material strengths associated with the precursor and that following the precursor can be resolved if salt is assumed to work harden after the saturated strength is attained. The physical explanation for the work hardening may be an increase in the effective stress, and, conversely, a decrease in pore fluid pressure, caused by dilatancy.

It is interesting that salt apparently requires a constitutive model different from those used for the rocks at NTS. They all have one feature in common however, namely that seismic coupling is controlled by low strength states, i.e., those that are between the tensile strength and the unconfined compressive strength. This reduction in strength has been attributed to pore fluid pressure and effective stress. Therefore, the degree of saturation at shot depth and the location of the water table are critical seismic coupling site properties. In addition, it is important that laboratory strength data be obtained for critical rock types at stress states below unconfined compression.

Some words of explanation are in order concerning the use of the term "saturated" to describe the SALMON rock environment. This term was used to identify a physical process which permitted a reduction in material strength caused by pore fluid pressure. That is, the ground motion data from SALMON required a material strength that was consistent with the assumption that the salt

was "saturated." However, ground motion data only provides an indirect measure of the intrinsic properties of the rock environment that are consistent with a specific model (i.e., we measure ground motion, choose a model, and, by using this model to match the ground motion, invert for the material properties required by the model). Is the salt really "saturated"? We can't answer that. However, within the constraints imposed by our constitutive model, the answer is affirmative.

2.7 THREE-DIMENSIONAL FINITE DIFFERENCE EARTHQUAKE MODELING ON THE ILLIAC COMPUTER

An improved understanding of the physics of both earthquake and explosion sources is important for providing a satisfactory theoretical basis for proposed discrimination techniques. A great increase in research directed toward understanding earthquake source theory has occurred in the last few years, though nearly all of that work is focused on the strong motion characteristics of the source.

In our earthquake modeling research at Systems, Science and Software our objective is to construct realistic models of earthquake faulting that are consistent with modern concepts of earthquake physics, with particular attention to those aspects controlling the far-field seismic waves important for discrimination. Careful studies of the broad-band character of earthquake signatures indicate that the relative excitation of long and short period waves is inconsistent with predictions from simple models (Bache and Barker, 1978; Bache, Lambert and Barker, 1979; Hartzell and Brune, 1979). For example, the far-field body wave spectrum deduced by Bache, et al. (1979) for the 1975 Pocatello Valley, Idaho earthquake is shown in Figure 20. As noted by these authors simple source models are incapable of simultaneous accounting for both the long- and short-period teleseismic signal. More complex rupture physics is required to explain these differences which are, of course, precisely those exploited by most discriminants.

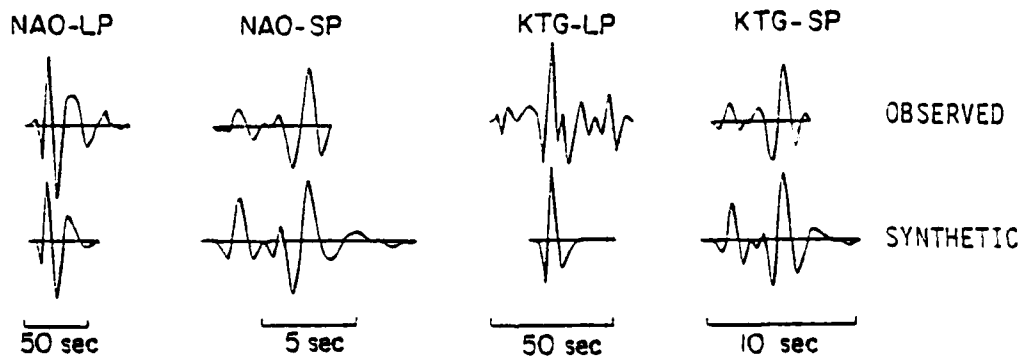
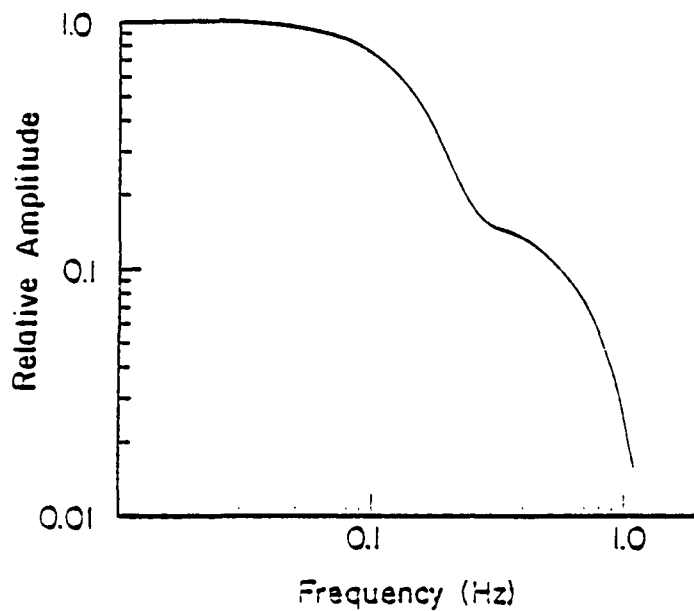


Figure 20. The P wave spectrum along a teleseismic ray path is plotted for the source inferred by Bache, et al. (1979) for the Pocatello Valley earthquake. Also shown is a comparison of the observed and synthetic teleseismic P wave. The source was obtained by summing two independent constant-stress-drop earthquake source models.

The essential analytic tool for our earthquake modeling program is the TRES code, a three-dimensional, explicit finite difference code operating on the ILLIAC IV. Three classes of earthquake models have been considered thus far: (1) elastic material behavior, with stress-relaxation propagating at constant rupture velocity, (2) elastic-perfectly plastic material behavior, with stress-relaxation propagating at constant rupture velocity, and (3) elastic material behavior, with spontaneous rupture propagation governed by a slip-weakening law. The calculations have been directed towards verifying the numerical methods, obtaining an understanding of the underlying physics controlling simple earthquake models, and developing a model of spontaneous rupture growth and arrest for simulating realistic faulting.

Figure 21a shows the slip time-functions obtained along the fault diagonal of a constant stress drop, square fault which grows circularly from a point at constant rupture velocity (solid curves), and compares this finite difference solution to the analytic solution for an expanding circular crack which does not stop growing (dashed curves). The good agreement at early times verifies that the finite difference treatment gives accurate results for dynamic crack problems. Figure 21b shows the slip velocities for points along the fault diagonal. Peak slip velocity grows as the square root of distance from the point of first rupture, also in accord with theory. Figure 22 shows far-field spectra and time functions at several locations on the focal sphere. P and S wave corner frequencies are found to be azimuth dependent, and are controlled by the travel time difference between stopping phases from the near and far edge of the fault. The effect of permitting plastic yielding is essentially that of extending the effective fault area.

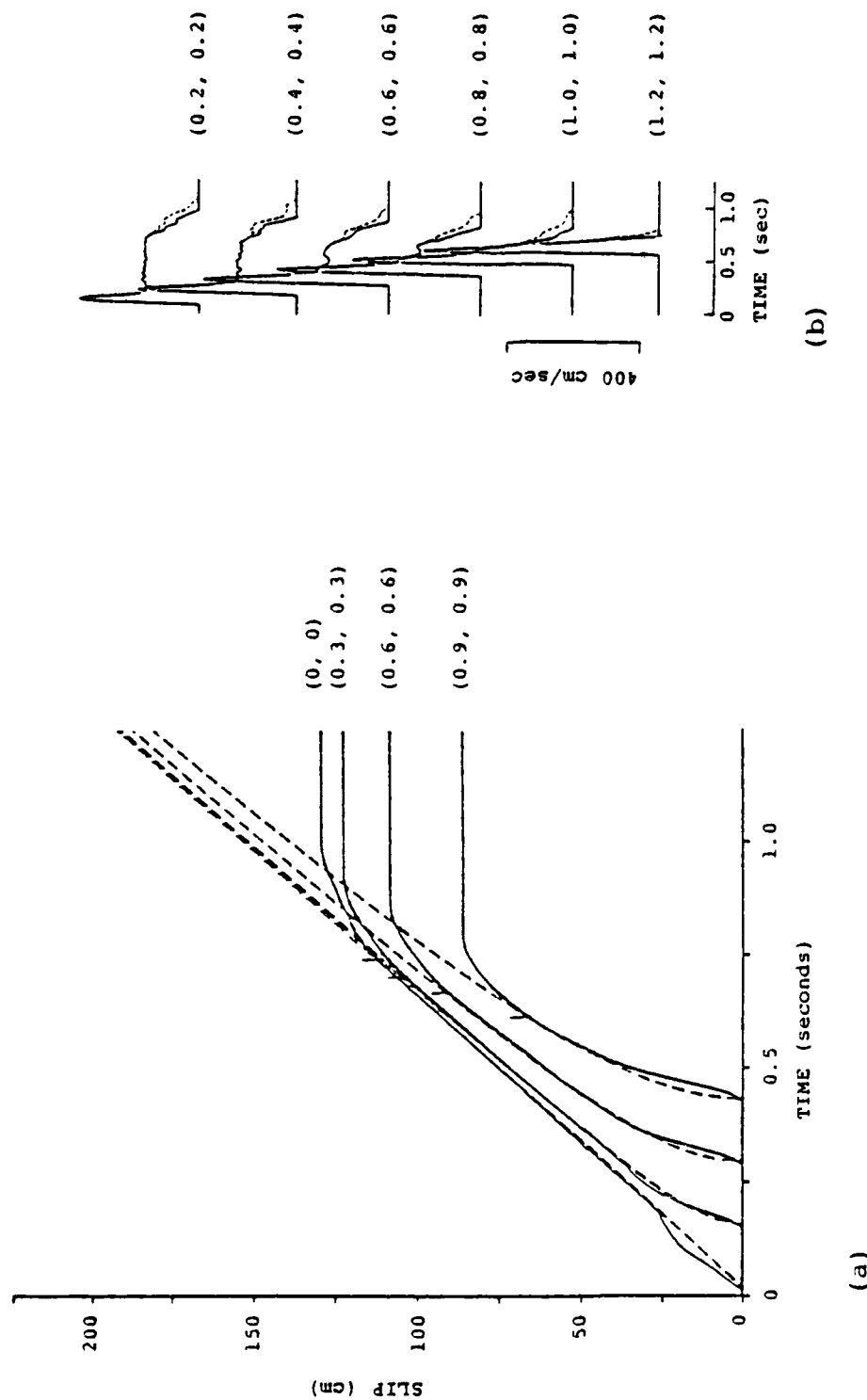


Figure 21. (a) Relative displacement on the fault for the elastic case. The dashed curves are Kostrov's analytic solution; the solid curves are the finite difference results. x, y coordinates in kilometers are given in parenthesis. Vertical lines indicate the arrival times of edge effects due to fault finiteness. (b) Slip velocity in the fault plane. Solid lines are the elastic case, dashed lines the elastoplastic case. x, y coordinates in kilometers are shown in parenthesis.

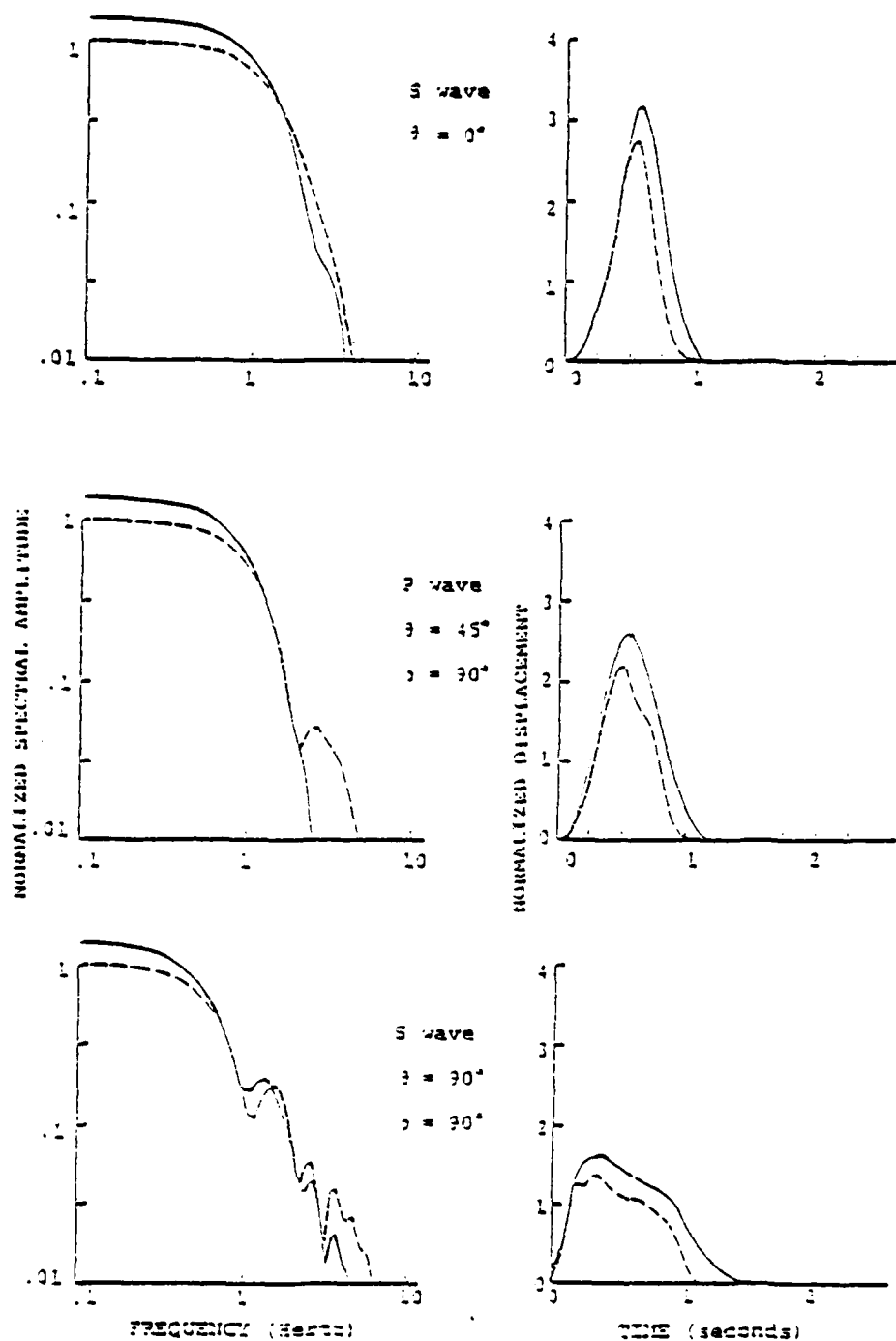


Figure 22. Comparison of displacement spectra and time histories from the plastic problem (solid curves) with those from the elastic problem (dashed curves).

The slip-weakening model of failure, in which shear strength of the fault zone is a decreasing function of its deformation, results in energy dissipation and bounded stress at the crack tip. Since nonlinearities are confined to the plane of the fault, only the computed displacement discontinuity on the fault plane is then required in order to construct far-field spectra and seismograms for the earthquake simulation. Initial numerical experiments, under conditions of uniform stress drop, give rapid growth in the prestress direction, and less rapid growth in the direction perpendicular to the prestress, forming an initially elliptical rupture front. The next step will be to perform more detailed calculations with uniform stress drop, and then investigate the influence of inhomogeneous stress drop on the teleseismic signal.

III. DISCRIMINATION

3.1 DATA BASE AND PROCEDURE

The discrimination experiment was completed during Fiscal Year 1979 and the final results of the variable frequency magnitude (VFM) discrimination procedure were presented at the review meeting held in Alexandria, Virginia, on July 25, 1979. A total of 133 Eurasian events, 106 earthquakes and 27 presumed explosions, were analyzed. The analysis was performed on short-period vertical component recordings of P waves from one or more globally distributed seismograph stations.

The central feature of the VFM technique is the application of a set, or "comb," of Gaussian shaped narrow band filters to decompose a digital time series, consisting of signal plus noise, into a set of quasi-harmonic modulated signals. For each filter a time domain envelope function is constructed from the filtered and quadrature signals. The filtered signal is corrected for instrument transfer function. The time of the maximum of a particular envelope function is the group or energy arrival time, t_g , of "signal" with a frequency near the filter center frequency. The amplitude of the envelope function at time, t_g , is the spectral amplitude, $A_g(f)$, of the signal energy arrival.

For identification of a signal as to the originating event type, the procedure is simply to compute the magnitude $m_b(f) \propto \log A_g(f)$ and construct $m_b(f)$ planes wherein event $m_b(f)$ values at a high frequency (i.e., > 2.0 Hz) are plotted versus $m_b(f)$ values at a lower frequency (i.e., 0.5 Hz). Observed signals can then be characterized by the location of their $m_b(f)$ values in these planes. Particular combinations of high and low frequencies are selected for optimal discrimination at a given station from an examination of many $m_b(f)$ plots.

3.2 PROPAGATION PATH EFFECTS NEAR THE RECORDING STATIONS

The $m_b(f)$ results obtained from this experiment indicated that the VFM approach may be able to discriminate between Eurasian earthquakes and explosions recorded at both teleseismic and regional distances. Individual station performance, however, is influenced by the attenuation properties of the upper mantle beneath a particular station. For instance, a station overlying high Q upper mantle (as evidenced either by the siting of the station in a shield region and/or a region characterized by large negative P wave travel-time residuals) provides much greater separation of earthquakes and explosions in the $m_b(f)$ plane representation than a station located over a low Q upper mantle. A low Q upper mantle acts as a low-pass filter applied to incoming teleseismic P waves which, in turn, forces us to use a lower $m_b(f_{HIGH})$ than we would prefer for optimal discrimination. As examples, we cite results from two stations for which a variety of regional geophysical information pertaining to the structure of the upper mantle is available. The two stations are Red Lake, Ontario (RKON) and Albuquerque, New Mexico (ANMO).

VFM discrimination results for RKON are representative of results from that subset of the stations analyzed which provided the best discrimination of the Eurasian event data set. The other stations that fall in this category are: Kabul, Afghanistan (KAAO); Charters Towers, Australia (CTAO); and the NORSAR array. A plot of $m_b(f_{LOW})$ versus $m_b(f_{HIGH})$ estimates for events recorded at RKON exhibits separation of the earthquake and explosion populations on the order of one m_b unit when we compare the earthquake and explosion high frequency m_b levels for a fixed low frequency m_b level. As for the attenuation properties of the upper mantle beneath this station, we note that RKON is located within the Canadian Shield in a region characterized by relatively low heat flow and large negative travel-time residuals (Masso, et al., 1978). These

geophysical data sets, together with the results from several other studies (e.g., Brune and Dorman, (1963), suggest that the upper mantle in this region is relatively high Q (low attenuation).

In striking contrast to an RKON-type station, we have the VFM discrimination results for ANMO. This station is located in the Basin and Range Province of the western United States and is in a region characterized by large positive travel-time residuals and high heat flow (Masso, et al., 1978). Numerous geophysical studies performed in this region (Thompson and Burke, 1974) indicate the existence of an extensive low Q-low velocity zone in the upper mantle. In terms of discrimination, an $m_b(f)$ plot obtained for the Eurasian events recorded at ANMO can best be described as a shotgun pattern over most of the event magnitude range, with significant overlap of earthquakes of all focal depths and explosions. Other stations which behave like ANMO, and in some cases are known to be situated in regions characterized by large positive travel-time residuals, are the following: Mashhad, Iran (MAIO); Chiang Mai, Thailand (CHTO); Taipei, Taiwan (TATO); Guam, Marianas Island (GUMO); and Zongo Valley, Bolivia (ZOBO).

3.3 PROPAGATION PATH EFFECTS NEAR THE SOURCE

In terms of VFM, or any other short-period P-wave discrimination procedure, one of the most interesting source regions included in this experiment is the Lake Baikal Rift zone in eastern Siberia. The Baikal Rift is located in a region of high heat flow and active normal faulting. In addition, Vinnik and Godzikovskaya (1972) found anomalously high P-wave attenuation, compared to an average for the USSR, in the upper mantle beneath this region.

The importance of this source region for discrimination purposes became evident once the multistation VFM results were

obtained for two presumed explosions occurring in the immediate vicinity of Lake Baikal. One of these explosions originated to the north of Lake Baikal - the other explosion to the south. Discrimination of these two events was found to depend quite strongly on the take-off azimuth of the P-waves relative to the Rift zone. In those few cases where both events were recorded at the same station one explosion appears earthquake-like while the other appears explosion-like. Examination of the seismograms clearly indicated that if the event P-wave traveled through the mantle beneath the Rift zone then the high frequency energy was heavily filtered as compared to the event P-wave that skirts the Rift. As a result, when these two events are plotted in the $m_b(f)$ planes, the high frequency m_b estimates literally slide across (a fixed low frequency m_b level) the plot: in one case landing in the earthquake-like population and in the other case falling in with the explosion-like events. In terms of the applicability of short-period body wave discriminants, it is extremely important to identify other possibly similar source regions.

3.4 CONCLUSIONS

The principal conclusions resulting from the discrimination experiment are the following:

1. VFM discrimination based on both regional and teleseismic stations is approximately 95 percent effective for all the events in this experiment.
2. A few deep earthquakes (ten percent of the total) were misidentified by the VFM technique and require depth estimates for correct identification.

3. About five percent of all the events considered in this study were classed as "unidentified." This is probably typical of results to be expected from (largely) teleseismic data sets. Discrimination of these "unidentified" events will require additional VFM results from regional stations and/or that other discriminants (e.g., focal depth) be used jointly.
4. Stations can be classified as to VFM discrimination effectiveness/reliability using P-wave travel-time residual data and other information pertaining to the attenuation properties of the upper mantle beneath a site.
5. The VFM technique is an effective discriminant principally because of the enriched high frequency source spectra of explosions relative to comparable earthquakes.

IV. BODY WAVE MAGNITUDE AND YIELD DETERMINATION

4.1 \hat{m}_b

In Section II we discussed the results of our participation in the discrimination experiment conducted by VSC. Our discrimination was done with the MARS program which automatically detects a signal and computes variable frequency magnitude, $\bar{m}_b(f)$, at two frequencies, one high and one low. These two $\bar{m}_b(f)$ values are not directly comparable to conventional m_b values, which are usually computed from the time signal which is dominated by frequencies near 1 Hz, a value between the high and low frequencies for the $\bar{m}_b(f)$ calculations.

An automated magnitude measure called \hat{m}_b was described in reports by Bache (1979) and Bache, *et al.* (1979). This magnitude is based on the spectral amplitude in a narrow window in both time and amplitude. The algorithm for computing \hat{m}_b is closely related to that used to compute the $\bar{m}_b(f)$ values used for discrimination.

The \hat{m}_b was applied to a data set including recordings of eleven Pahute Mesa explosions at six teleseismic stations. The \hat{m}_b was found to be at least as good a magnitude measure as the most carefully determined time domain m_b . This conclusion is based on a comparison of m_b and \hat{m}_b in terms of the scatter in network magnitude estimates and in the magnitude-log yield relationship.

4.2 OBSERVATIONS OF SEISMIC WAVES FROM SPALLATION ASSOCIATED WITH UNDERGROUND NUCLEAR EVENTS

During the contract period we did two independent studies addressing the effect of spallation on the seismic waves from underground explosions. One of these was an analysis of the near-field recordings of MERLIN and was described by Murphy and

Bennett (1979). The second was a synthetic seismogram study of three Pahute Mesa explosions described by Bache, et al. (1979). In this section we give a unified presentation of those results.

The existence and general character of the spallation associated with contained underground nuclear explosions is well documented by studies of ground motion recordings in the vicinity of the explosions. Spall closure or slapdown is a source of seismic waves which are commonly observed on accelerometer recordings. These slapdown phases are quite high frequency and would generally not be expected to propagate to large distances due to the attenuating character of the earth.

From an entirely different perspective, several seismologists have advanced the hypothesis that certain secondary arrivals on teleseismic (> 3000 km) recordings of nuclear explosions are due to spall closure. These arrivals are much lower frequency (about 1 Hz) than the slapdown pulses usually identified on near field recordings.

In this section we have two points to make. First, we will show one particular example, MERLIN, in which a low frequency pulse which appears to be due to spall closure is identified on shot-level ground motion recordings. While we cannot be certain that this is typical for underground explosions, we point out that MERLIN is nearly unique in having shot level gauges at large scaled ranges that have been integrated to highlight the long period energy.

The second point is that a secondary arrival observed on teleseismic recordings of Pahute Mesa explosions has arrival time and amplitude that is entirely consistent with independent estimates for these events. This gives additional credibility to these estimates for the dimensions of the spall plate as a function of explosion yield.

4.2.1 Analysis of MERLIN Data

MERLIN was a 10 KT (Springer and Kinnaman, 1971) nuclear explosion which was denoted at a depth of about 300 m in Yucca Flat alluvium. Figure 23 shows an approximate sub-surface geophysical profile together with the locations of the shot depth recording stations which will be considered here. Figure 24 shows the radial component acceleration, velocity and displacement data recorded at Station U6 at a range of 488 m. The late time, low frequency phase which is of interest is identified by the dashed line. Notice that due to its low frequency character, the signal is barely evident on the acceleration trace, but becomes increasingly important with each successive integration. This may explain why such phases have not been identified in previous studies which have concentrated on acceleration data. Figure 25 shows the radial displacement time histories recorded at the four different observation ranges. The most diagnostic characteristics of this pulse appear to be: (a) late arrival time (~ 1.5 seconds), (b) relatively low frequency (~ 1 Hz), (c) moderate horizontal phase velocity ($\sim 1,800$ m/sec), and (d) nearly constant amplitude over the range of observation. We have considered three possible sources for this arrival: (1) free surface reflected phases (i.e., pP or pS), (2) reflections from a deep interface, and (3) signals generated by spall closure. Figure 26 shows that the observed arrival times are not consistent with what would be expected for pP or pS. This, together with inconsistencies between the observed and expected amplitude behavior, allows us to exclude surface reflected phases as the source of the observation. Similarly, if the pulse represents a reflection from a deep interface, the late arrival time constrains the interface to be at a depth of 1 km or more, and the apparent velocity across the shot depth stations from a reflection at

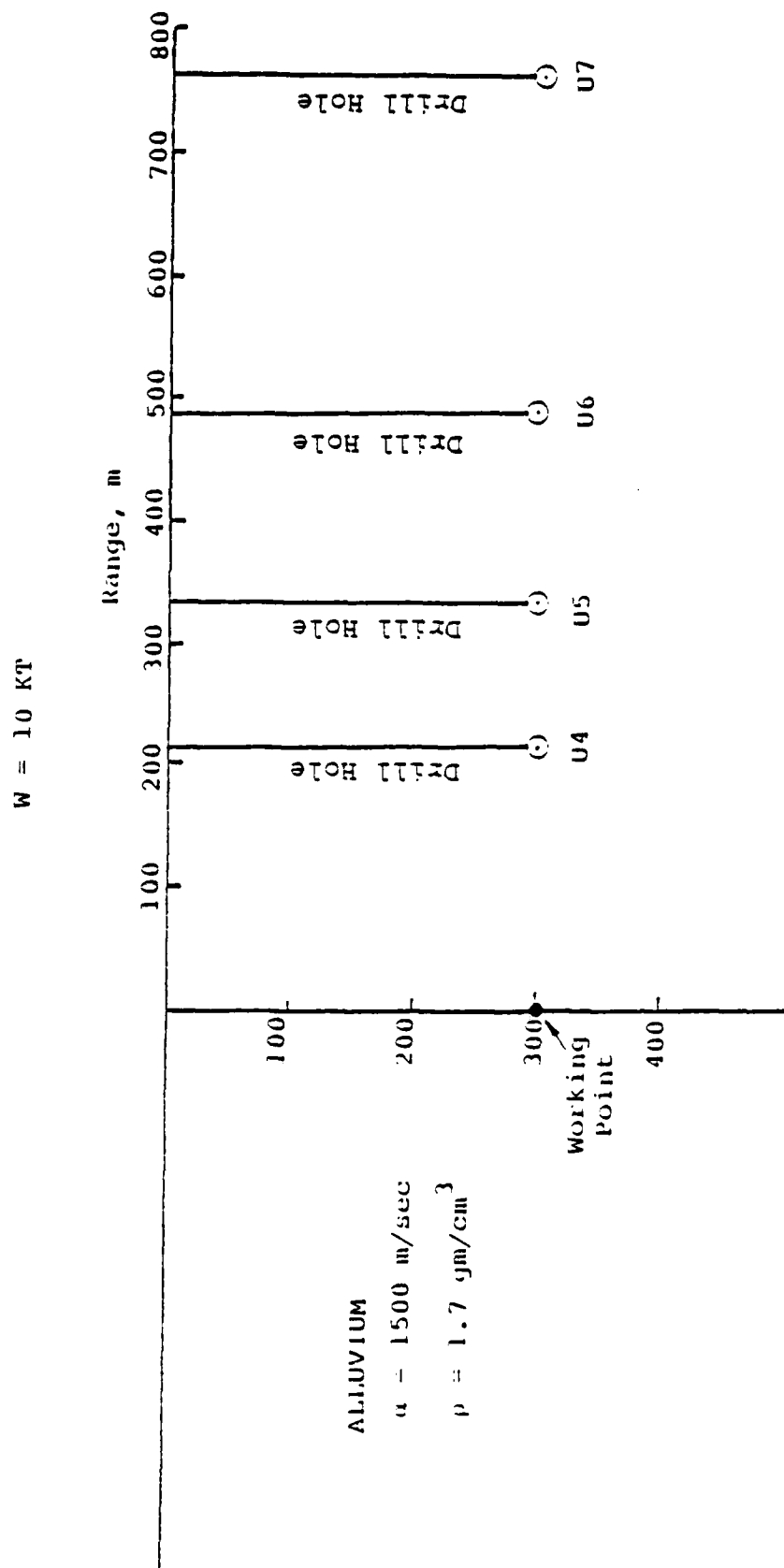


Figure 23. Vertical section through the MERLIN detonation point showing the relationship between the instrument locations and the subsurface geology at the site.

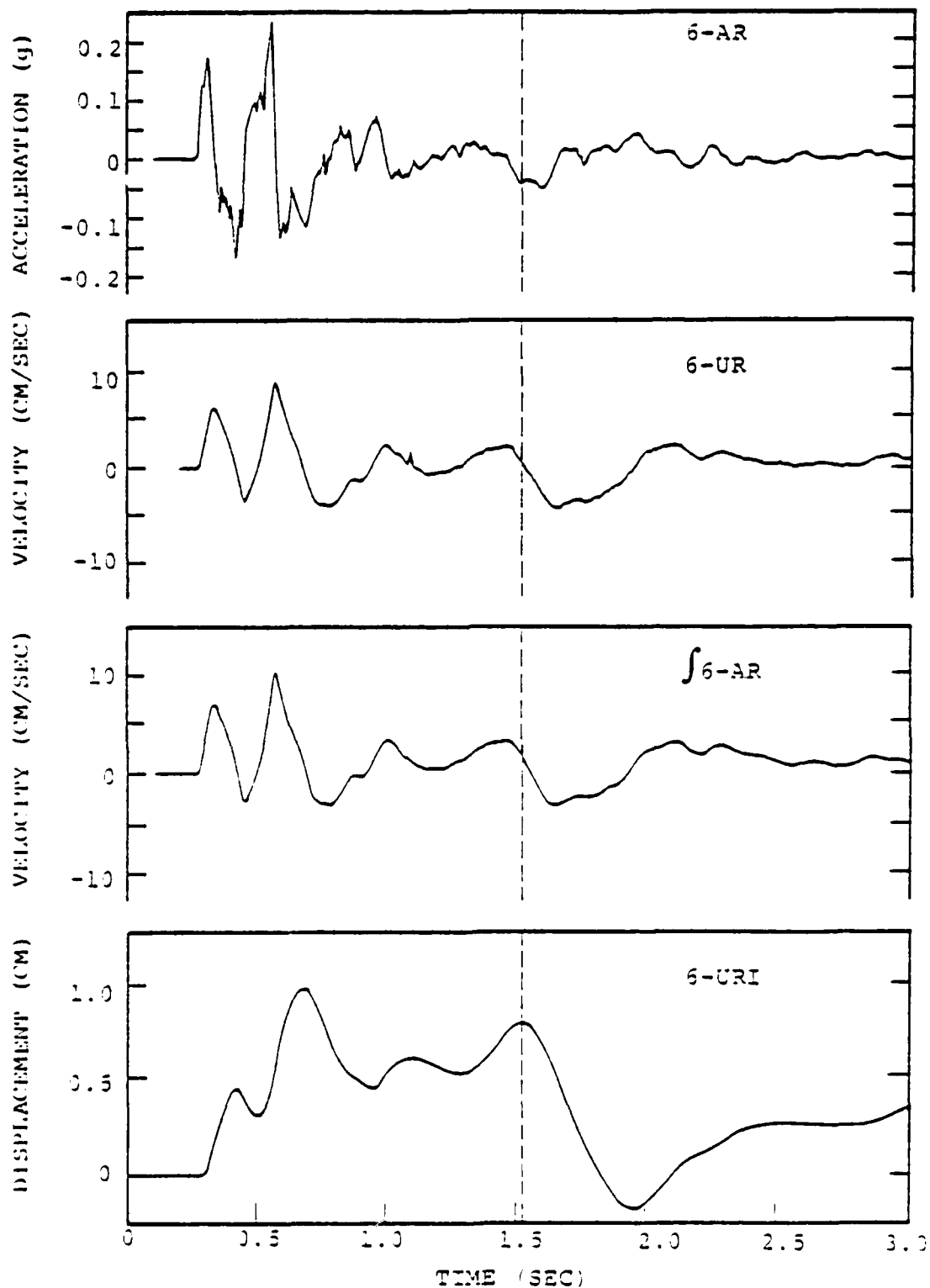


Figure 24. Ground motion time histories for the MERLIN event recorded at Station U6, R = 488 m; positive represents outward radial motion.

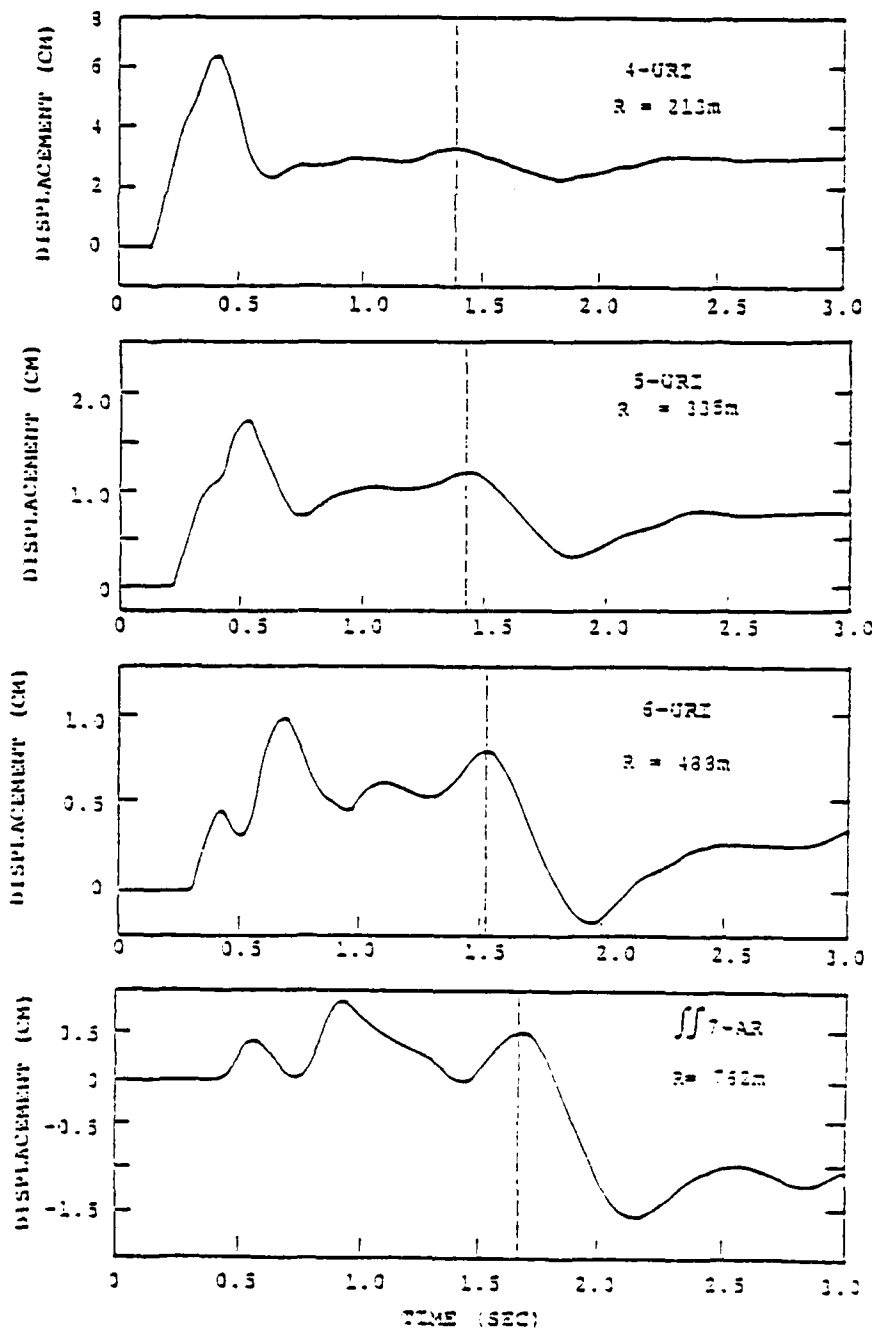


Figure 25. Radial displacement time histories for MERLIN (dashed lines denote arrival time of arrival of interest).

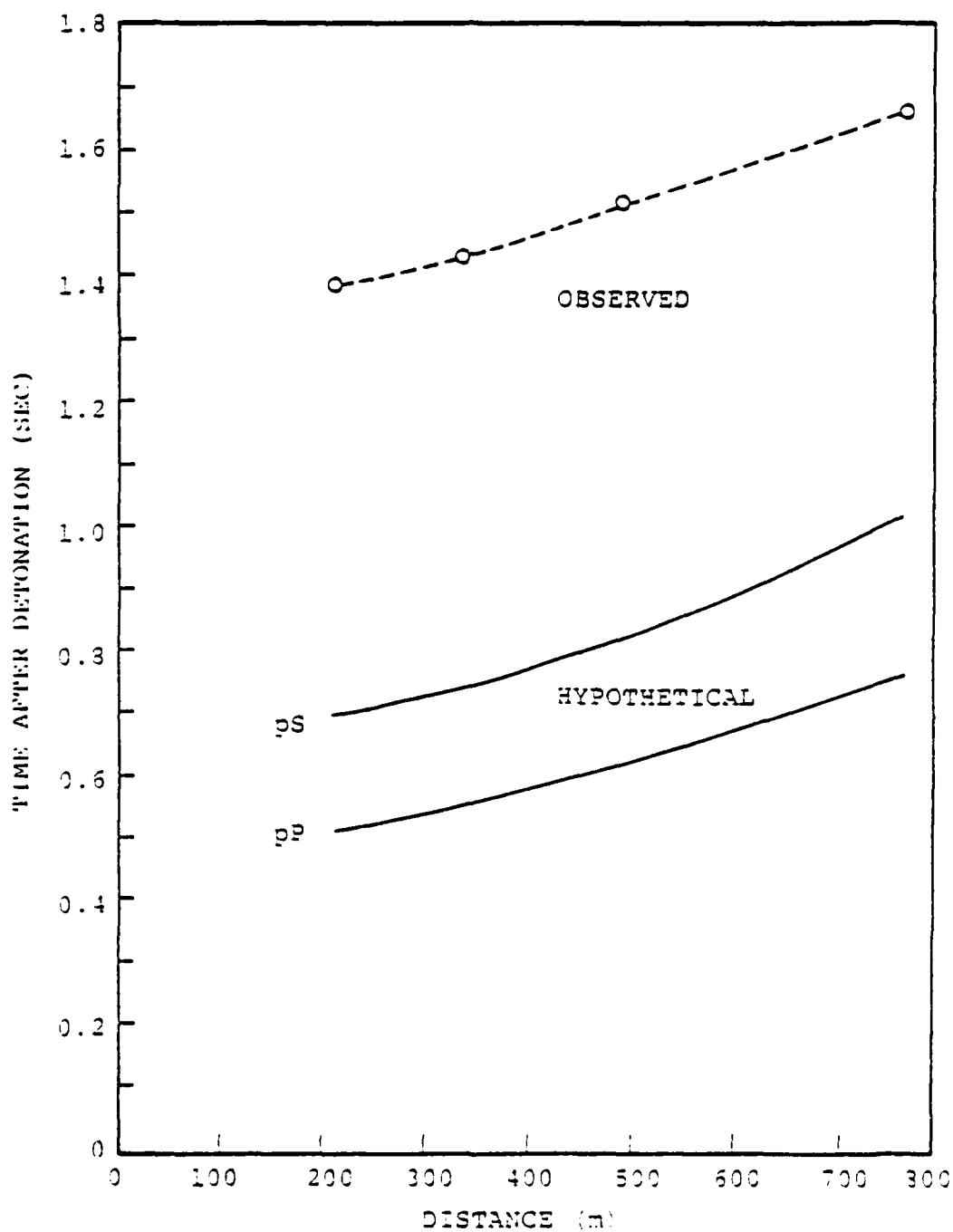


Figure 26. Comparison of arrival times of low frequency, late time phase from MERLIN with hypothetical arrival times of pP and pS phases.

this depth would be expected to be much greater than the observed apparent velocity of 1,800 m/sec.

Having eliminated surface reflections and deep reflections as explanations of the observations, we are left with the spall closure mechanism. Figure 27 shows the MERLIN vertical acceleration time histories recorded on the surface at distances from 30 to 152 m from ground zero. A simple calculation reveals that a P wave originating from this region at the time of the last significant closure pulse (~ 1.15 sec) indicated by dashed lines on this figure, would be expected to arrive at the shot level stations very close to the observed arrival times of the phase under investigation. This observation prompted a more detailed analysis of the near field displacements to be expected from spall closure.

A series of simple elastodynamic finite element simulations of spall were carried out in which a cylindrical region of radius r_0 and thickness h_0 was simply assigned an initial, radially dependent, vertical velocity V . The parameters for the series of calculations which have been performed are summarized in Table I where they are compared with those predicted by the scaling laws deduced by Viecelli (1973) from a study of the near source data from six NTS explosions. The quantities V_0 and V_1 in these simulations were selected to give absolute displacement amplitudes which match the observed amplitude of the late time pulse at the 335 m range station. Figure 28 shows the radial displacement time histories computed using Model IV. This model appears to be physically plausible in that the spall dimensions are within the limits delineated by the surface observations, the initial spall momentum is conically distributed with respect to radius and the total spall momentum is within about a factor of two of Viecelli's

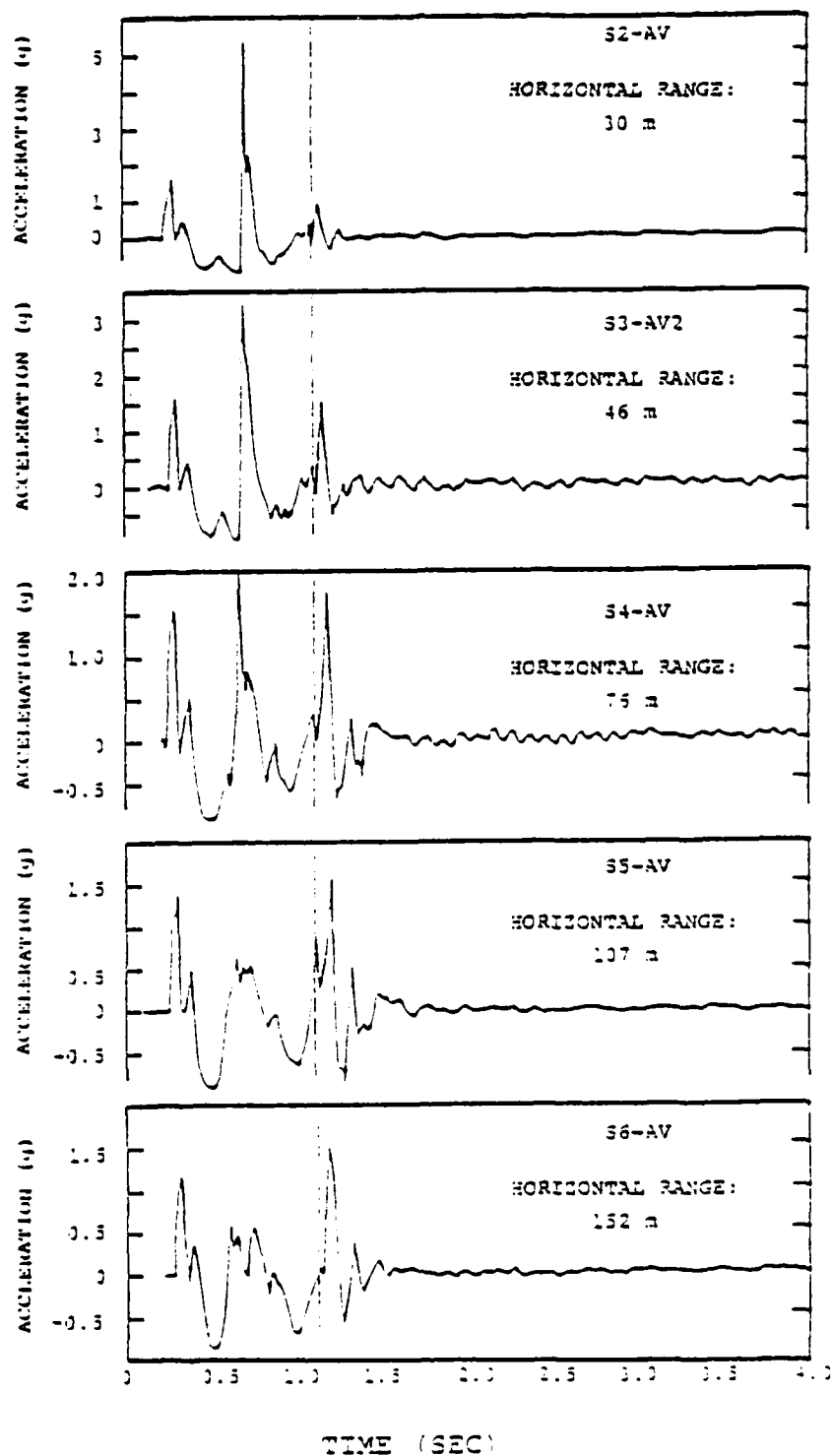


Figure 27. Free surface acceleration time histories for the MERLIN event. The dashed line indicates the assumed time of spill closure.

TABLE 1
DESCRIPTION OF MODEL PARAMETERS FOR SPALL CLOSURE
CALCULATIONS

<u>Model</u>	<u>Spall Radius (m)</u>	<u>Spall Thickness (m)</u>	<u>v₀[*] (m/sec)</u>	<u>v₁[*] (m/sec)</u>	<u>Total Impulse (Nt-sec)</u>
Model I	150	60	1.28	0.0	0.98×10^{10}
Model II	150	60	0.0	3.07	0.78×10^{10}
Model III	300	60	0.54	0.0	1.65×10^{10}
Model IV	300	60	0.0	1.28	1.30×10^{10}
Viecelli (1973)	230	50	0.0	5.6	2.79×10^{10}

$$*v = \left[v_0 + v_1 \left(1 - \frac{r}{r_0} \right) \right] H (r_0 - r).$$

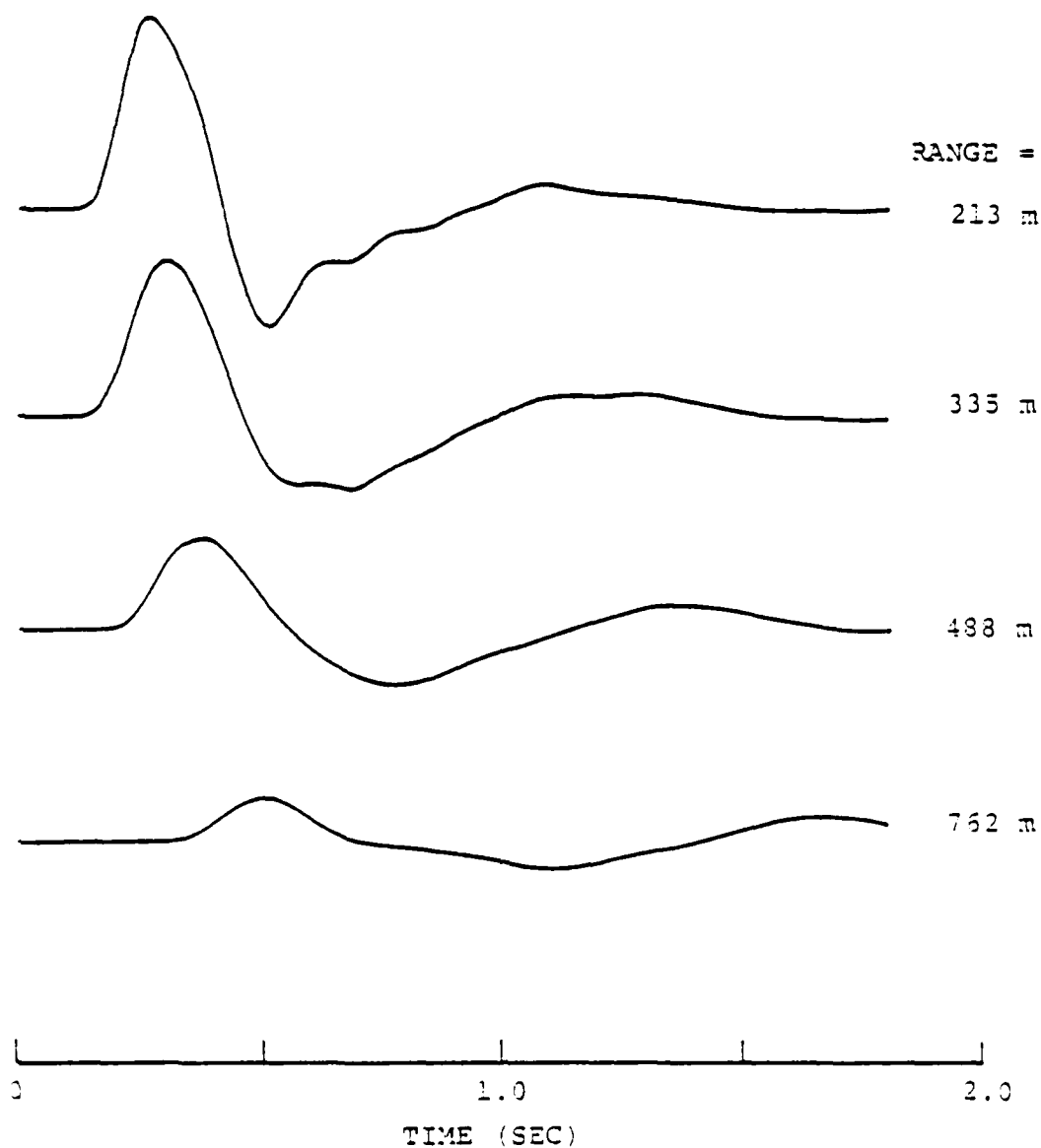


Figure 28. Computed radial displacements at shot level generated by spall closure Model IV. Spall closure is assumed to occur at time equal 0.

empirical estimate. Comparing with Figure 25 it can be seen that this simulation successfully matches the MERLIN observations to the extent that the first arrival times are correct, the amplitudes at the near stations are reasonable and the pulse shapes roughly resemble the observed pulses in that they consist of an outward motion followed by a rather slowly decaying inward motion of about the right period. However, some discrepancies are also evident. In particular, the predicted amplitude of the positive phase is too large relative to that of the negative phase and the amplitude of the computed pulse decays much more rapidly with range than that of the observed. These are probably indications that our elastodynamic spall closure approximation is too simple to provide a detailed, quantitative fit to the observations. However, the qualitative agreement is good enough for us to conclude that the observed MERLIN pulse is probably induced by spall closure and, consequently, that spall closure can be a source of low frequency motion which can be expected to propagate to teleseismic distances.

4.2.2 Analysis of Teleseismic Data

In Figure 29 we show recordings of the P wave from 11 Pahute Mesa explosions. These seismograms were recorded at Houlton, Maine, at a distance of about 4,050 km and are arranged in order of increasing source-to-surface travel time (determined from a ground zero gauge). This is roughly in order of increasing depth and, therefore, yield.

There is a distinct secondary arrival, marked P_s , on each seismogram. This arrival has amplitude proportional to yield; that is, it stays the same size with respect to the P wave which arrives first. Its arrival time is roughly proportional to Δt ; that is, it arrives later when the source-to-surface travel time increases. These features are generally

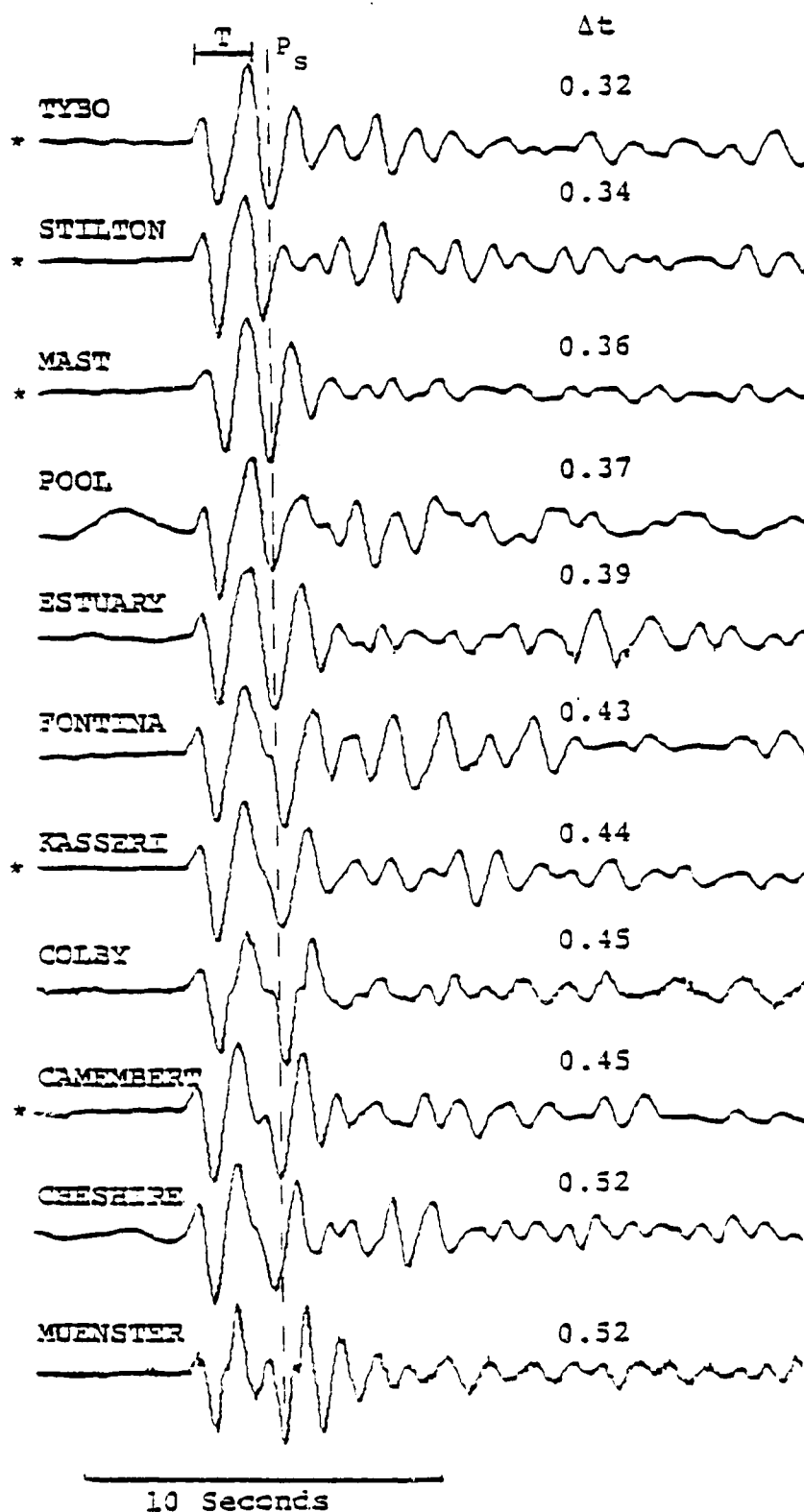


Figure 29. Houlton, Maine recordings of eleven Pahute Mesa explosions arranged in order of increasing source-to-surface travel time (Δt).

consistent with what might be expected for a phase due to spall closure. Other stations show much the same thing.

For Pahute Mesa explosions we have a fairly good estimate for the explosion source function as well as the other parameters needed to compute a synthetic seismogram at Houlton, Maine. The next step in this analysis is to compute synthetics for these explosions. These synthetics will be dominated by the direct P and free surface reflected pP from the explosion. Having computed the synthetics for the explosion, we add a surface impulse force to represent spall closure. This impulse is characterized by two parameters: its amplitude, $\langle I \rangle$, and lag time, T_L , with respect to the explosion.

Studies of the near field gauge records by Viacellulari (1973) and Sobel (1978) provide independent estimates of $\langle I \rangle$ and T_L in terms of scaling laws with respect to explosion yield and depth. These estimates are not very precise and are not for these specific events. Therefore, our approach was to (1) adjust $\langle I \rangle$ and T_L to obtain good agreement with the observations, and (2) compare the inferred $\langle I \rangle$ and T_L with the estimates of Viacellulari and Sobel. We point out that the $\langle I \rangle$ and T_L estimates obtained in (1) should be as accurate as our knowledge of the explosion source function. We compare to the Viacellulari and Sobel estimates to demonstrate the consistency of the results from two entirely independent methods.

The construction of the synthetic seismograms for three of the events is shown in Figure 30. We show the seismograms for P and for P + pP for each event. The small oscillations later in the records are due to reverberations in the layering used to model the earth. The P_s phase has the same shape for all three events since the source is an impulse force. If a large mass of material is spalled, we would expect a

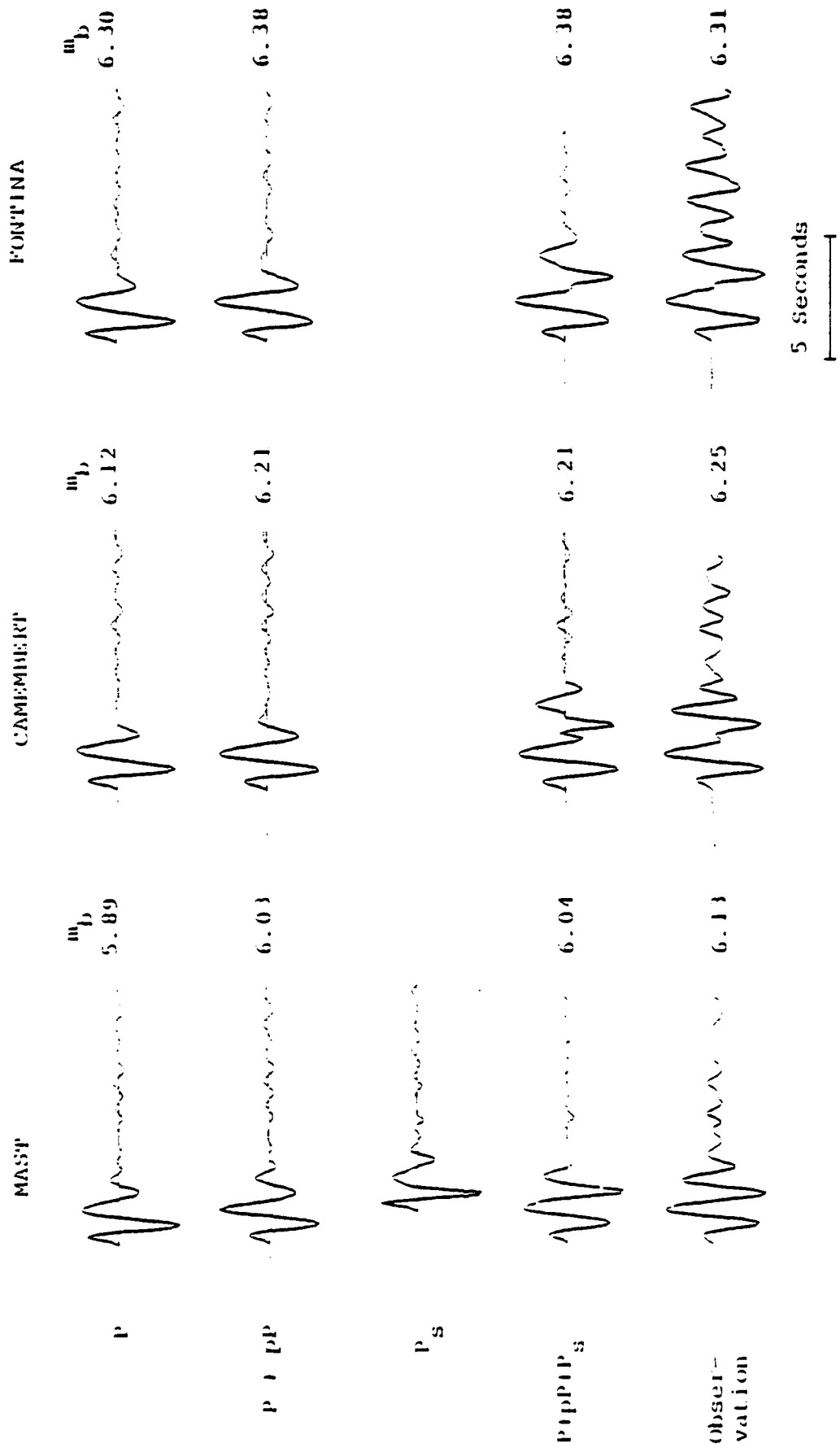


Figure 30. Construction of theoretical seismograms at INME for three Pahute Mesa explosions.

substantial degradation of the energy in the pP pulse. To account for this, we simply cut the pP phase in half. A reduction of pP by such a factor does perceptibly improve the agreement with the observations.

The final composite seismograms are compared at the bottom of Figure 30 and in Figure 31 where they are overlain. The m_b is a logarithmic quantity, the magnitude, which indicates the amplitude of each record.

The agreement of synthetic and observed seismograms is quite good. Recall that these records were recorded more than 4,000 km from NTS. The parameters for the P_s that give this agreement are listed in Table 2. We see that the $\langle I \rangle$ and t_L inferred from the teleseismic records are in good agreement with the estimates of Viecelli and Sobel. That is, they are well within the scatter of the estimates from the near field data.

In summary, Viecelli and Sobel estimated the spall plate dimensions from high frequency pulses recorded on near source accelerometers. These dimensions, in turn, can be used to estimate the spall closure impulse. From our study we conclude that:

1. A low frequency pulse consistent with the Viecelli and Sobel estimates can be seen on the shot level gauges from at least one explosion, MERLIN.
2. Teleseismic body wave recordings of Pahute Mesa explosions have a secondary arrival which is also consistent with the Viecelli/Sobel estimates and, therefore, with the low frequency pulse observed on the MERLIN gauges.

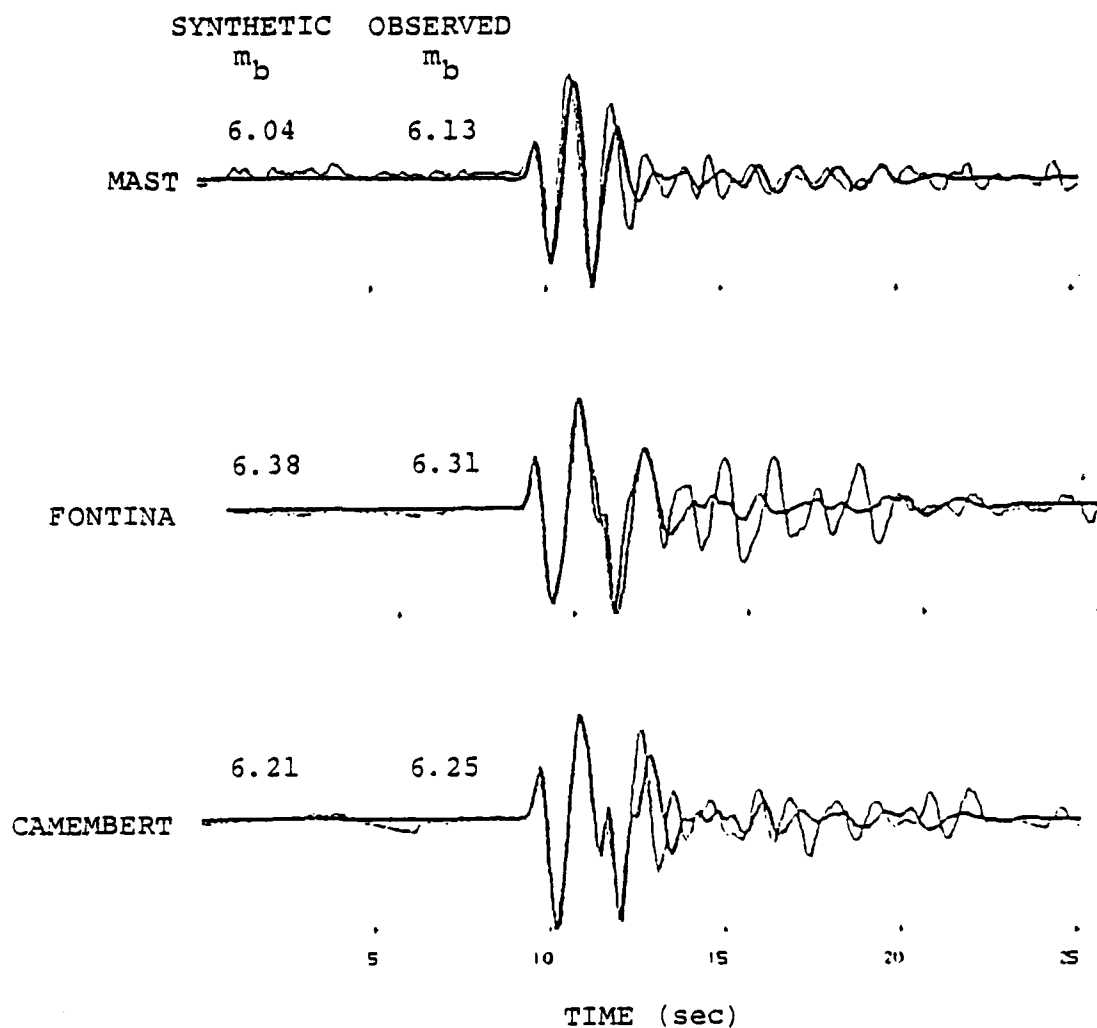


Figure 31. Comparison of synthetic (heavy line) and observed seismograms.

TABLE 2
PARAMETERS FOR THE P_s PHASE IN THE SYNTHETIC SEISMOGRAM
CALCULATIONS

	<u>MAST</u>	<u>CAMEMBERT</u>	<u>FONTINA</u>
Spall Impulse (dyne-sec/kt), $\langle I \rangle$	$10 \times 10^{14} W$	$14 \times 10^{14} W$	$9 \times 10^{14} W$
P-P _s Lag Time (sec), t_L	1.43	2.10	2.04

Estimates of $\langle I \rangle$ From Near Field Data

Viecelli (1973): $4.6 \times 10^{14} W$

Sobel (1978): $21-25 \times 10^{14} W$

4.3 APPROPRIATE VALUES OF t^* FOR TELESEISMIC BODY WAVES FROM NTS EXPLOSIONS

A convenient way to account for anelastic attenuation in synthesizing teleseismic body waves is via a causal Q operator with amplitude $\exp [-\pi f t^*]$, where f is frequency and t^* is the ratio of travel time and effective path Q . In this formulation Q is assumed to be frequency independent, which is a reasonable assumption as long as the operator is applied over a narrow frequency band. However, in selecting an appropriate t^* , one must consider that Q values deduced from data in another frequency band may not be valid for the frequency window of interest.

At S^3 the study of teleseismic body waves from NTS explosions has emphasized the analysis of source differences and most of our computations are for stations in Alaska and HNME. The t^* values used in our computations, about 1.05 for Alaska and 0.8 for HNME, were selected to achieve the best fit to the observations in both amplitude and frequency content. There are, of course, tradeoffs with the earth models used to compute the elastic attenuation, the crustal models for the local source and receiver regions, and the source function.

In Figures 32 and 33 we show comparisons of synthetic and observed seismograms for stations in Alaska and HNME. Figure 32 is from Bache, et al. (1975). The source functions for that study were computed with finite difference techniques. For the seismograms of Figure 33 the semi-empirical source due to Mueller and Murphy (1971) was used. These seismograms (from Bache, et al., 1979) also include a contribution from a secondary phase assumed to be spall closure.

The finite difference computed and Mueller/Murphy source functions lead to essentially the same conclusions about the best value for t^* . The effect of choosing a different value

"b" AMPLITUDES

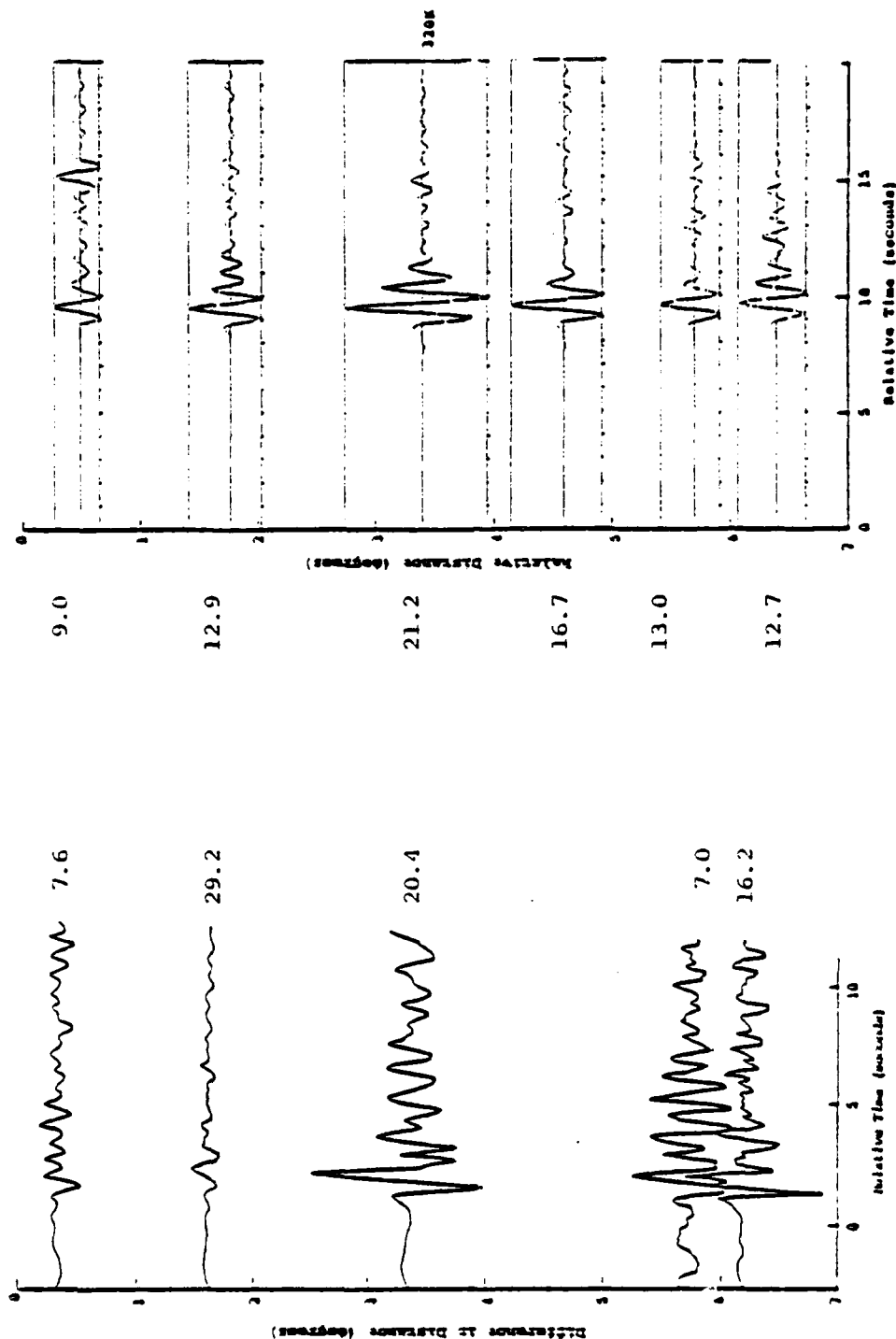


Figure 32. Comparison of theoretical and observed short period vertical seismograms for a Rainier Mesa explosion. The records are from stations in Alaska and are arranged vertically with distance and the gain at 1 Hz is indicated. The b amplitude, corrected for instrument response, is given for each record.

HNME

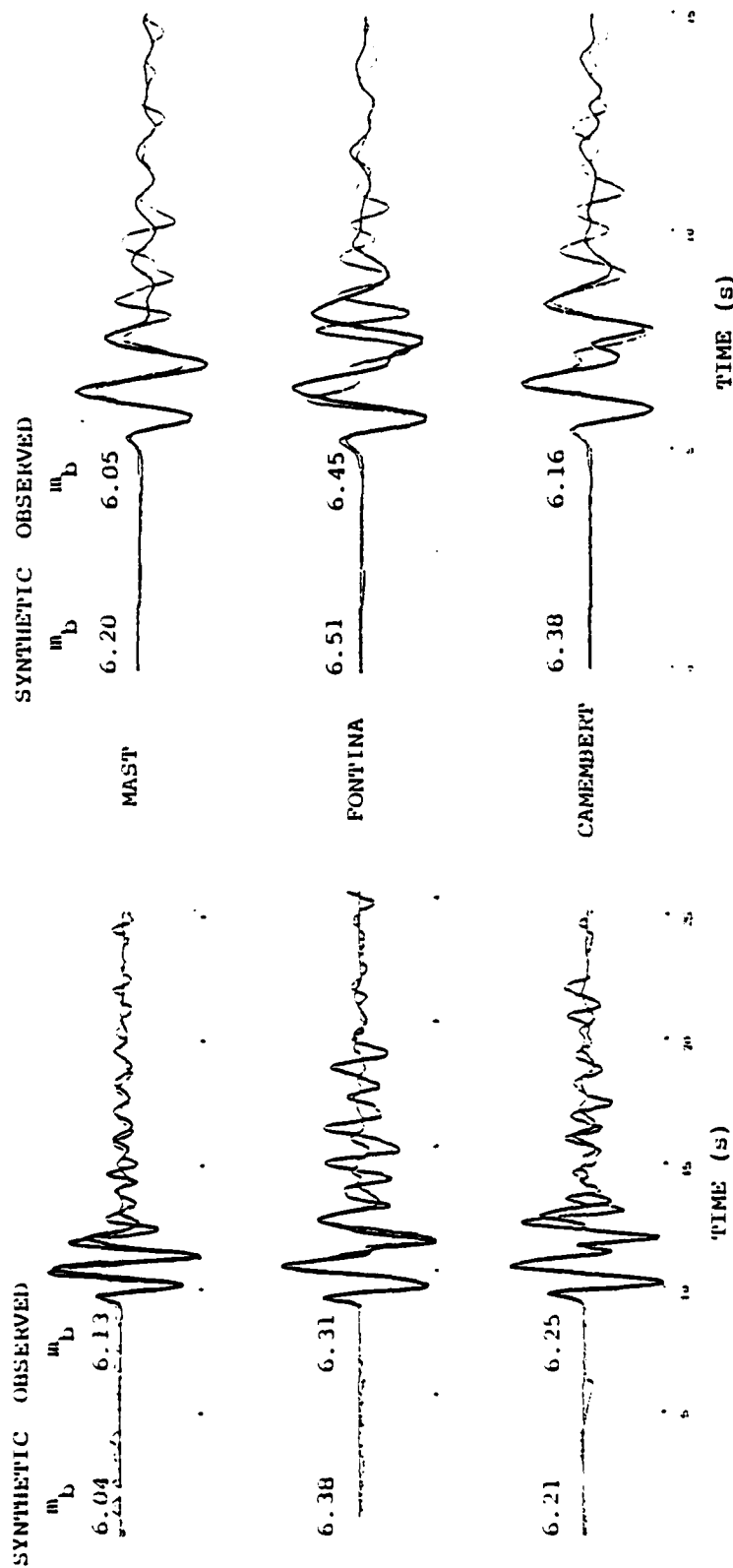


Figure 33. Comparison of synthetic (heavy lines) and observed seismograms at HNME and a station in Alaska.

for t^* is indicated by the example in Figure 34. Values of t^* much different than 0.8 would require a substantial adjustment in our ideas of the corner frequency and amplitude of the source spectrum and/or the earth structure controlling elastic attenuation.

How could the analysis we have just outlined be wrong? There are basically two places for the error to arise:

1. The elastic attenuation (geometric spreading) might be much larger than we assume at those stations that control our t^* estimate.
2. The source RDP might be much smaller and have lower corner frequency than we assume. The implicit assumption is that all path effects are frequency-independent except for those represented by the t^* . This is a reasonable assumption and is consistent with the frequency-domain method for estimating t^* .

The second category is a more complex and likely source for errors. Effects unaccounted for in estimating the source RDP may be much more important than we think. However, to match the data with a $t^* = 0.4$, the "real" RDP must have an amplitude smaller by about a factor of three and a corner frequency smaller by about a factor of two than our conventional estimates.

To give some idea of the conventional view of geometric attenuation, we plot in Figure 35 the P wave velocity profile for three conventional upper mantle models. The turning depth for P waves is plotted versus range in Figure 36. For teleseismic ranges, the models have little character and the spreading is close to R^{-1} . In Figure 37 we show the FONTINA synthetics at HNME for several earth models. The changes are quite small.

One interesting feature of this comparison is that the C2 synthetic is much more like the data in the amount of energy

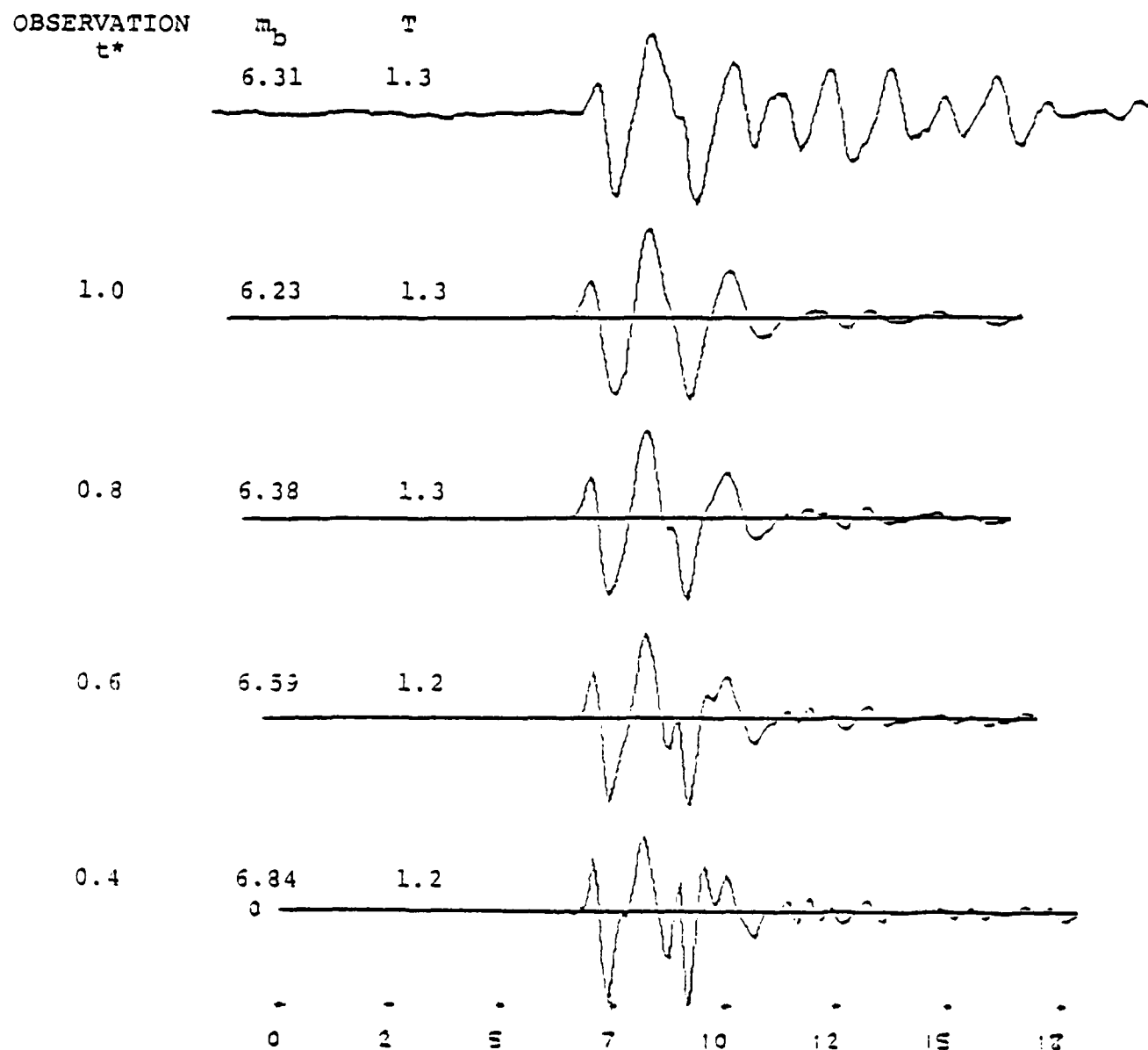


Figure 34. Effect of t^* on HNME synthetics for FONTINA.

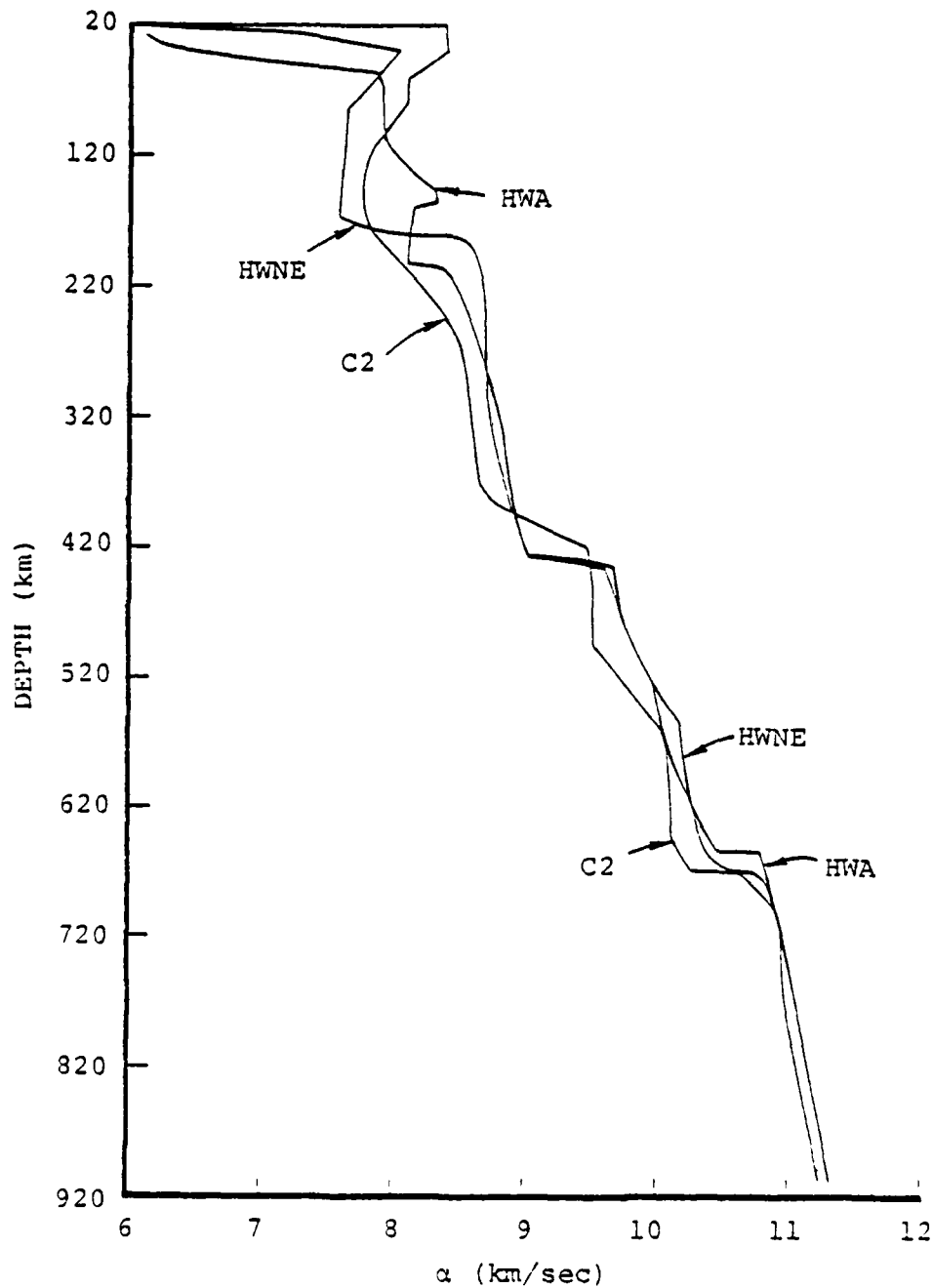


Figure 35. P wave velocity-depth profiles are plotted for three earth models: the average earth model C2 (Anderson and Hart, 1976), the western United States model HWA (Wiggins and Helmlberger, 1973) and the midwestern United States model HWNE (Helmlberger and Wiggins, 1971).

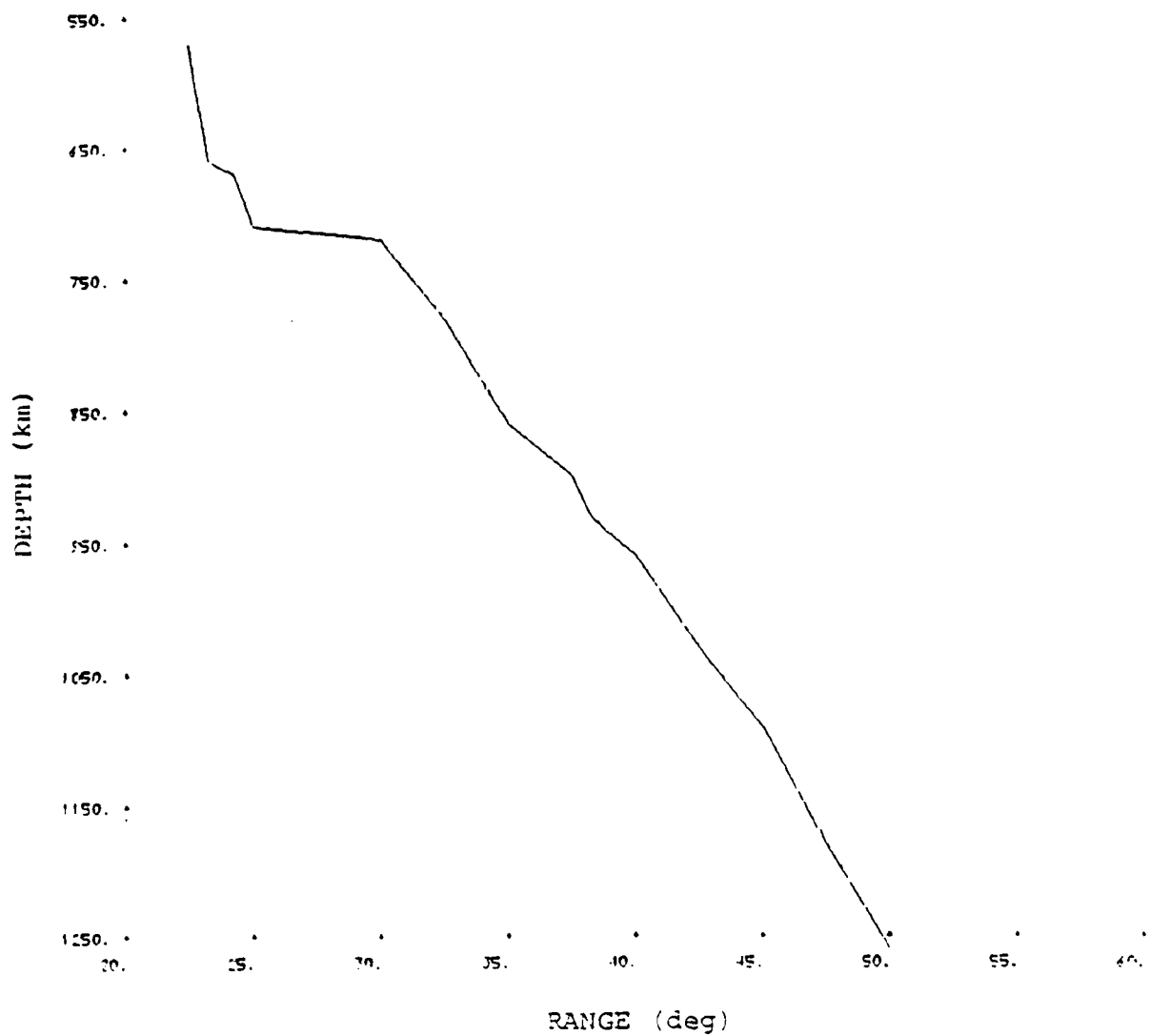


Figure 36. Turning depth is plotted versus range for Model C2.

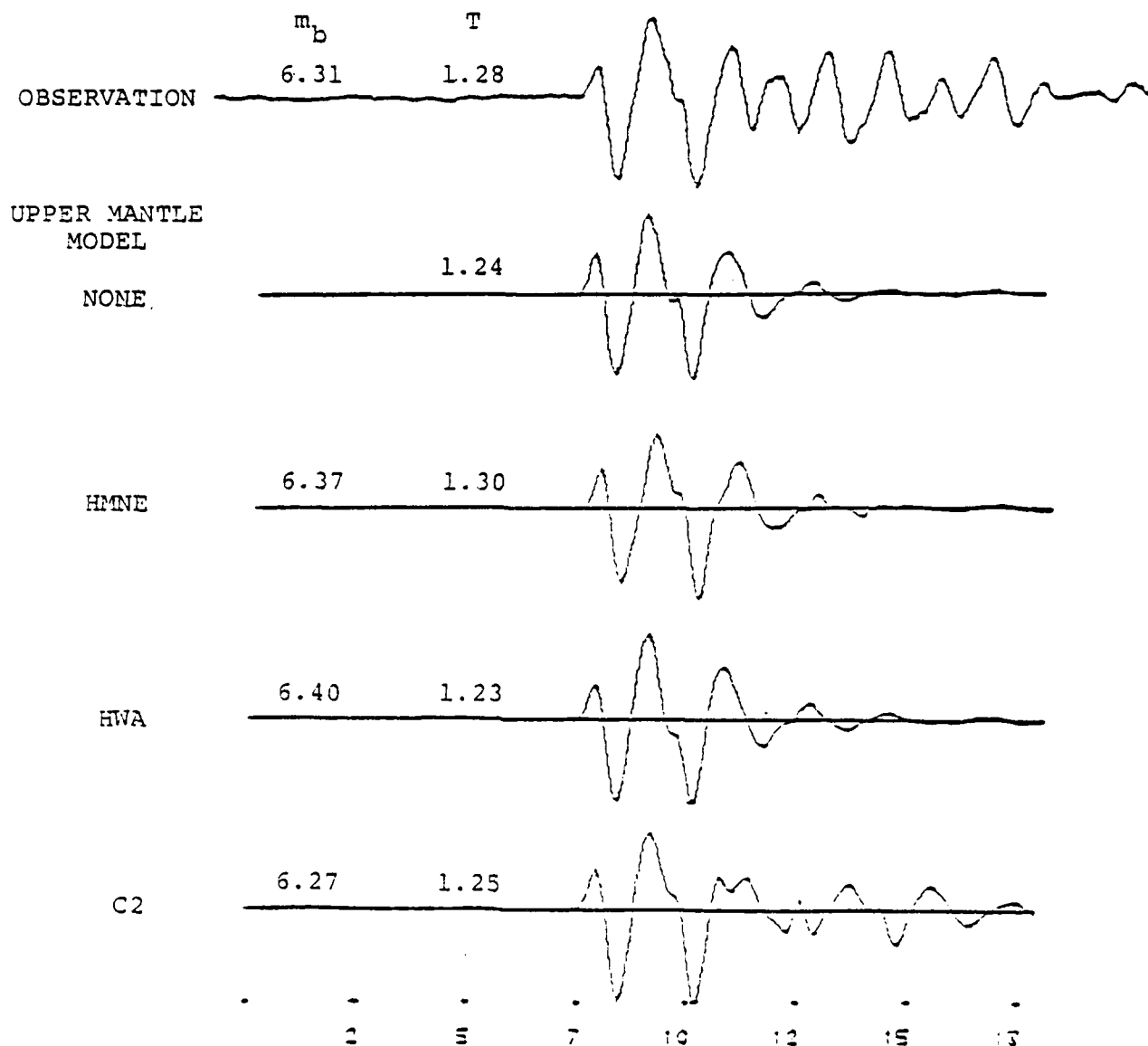


Figure 37. The effects of upper mantle structure are indicated by synthetics for FONTINA.

in the coda. This is scattered energy from deep reflectors and is accompanied by a reduction in the magnitude of this synthetic. However, it is difficult to ascribe too much meaning to this because some of the coda energy is probably associated with the source since it is not a consistent feature of the suite of seismograms plotted in Figure 29. Note that FONTINA has the largest coda of the suite.

Finally, we point out that the t^* values chosen by fitting synthetic and observed seismograms apply to the frequency window of 0.5 to 2.0 Hz. Values controlled by different frequencies, say 3 or 4 Hz, could certainly be different. In fact, observed seismograms often have more high (> 2 Hz) frequency energy than synthetics computed with our t^* values. This may be an indication that t^* is smaller (Q is larger) at these frequencies.

V. SMALL SCALE EXPERIMENTS

5.1 INTRODUCTION

For these experiments, we initiated a small spherical high-explosive (HE) charge located within a block of grout. On the surfaces of the block, measurements were made of the motion due to the stress wave propagated through the grout. Nominally, the known performance of the HE charge and the controlled, uniform properties of the medium would make this configuration amenable to code calculations. Thus the primary objective was to acquire data for comparison with code predictions. A secondary objective was to evaluate changes in the free-surface motion due to changes in the geometry of the charge's confinement.

In a previous report (Coleman, et al., 1979) we described the development of the miniature spherical charges. Here we give details of the experiment design and the results.

5.2 EXPERIMENT DESIGN

Three grout blocks were prepared and tested. Each one was about 610 mm by 610 mm square (in the horizontal direction), 1.22 m high, and contained four charges; see Figure 38. One charge (C#1) in each block was fully tamped and located on the central axis of the block at a height of 305 mm. A second charge was located at an end of a small two-to-one aspect ratio cylindrical cavity aligned with a vertical edge of the block. The cavity was placed so that the charge was on the central axis of the block at a height of 0.92 m; see Figure 39. (Gauge locations are also shown in this figure; the small arrows denote positive signal direction. The PVC cavity had an inner diameter of 10.2 mm, a wall thickness of 0.76 mm and a length of 20.3 mm.) A third charge was like the first charge but at a height of 610 mm. The last charge, fully tamped, was positioned at a height of 610 mm but off axis so that it was 254 mm

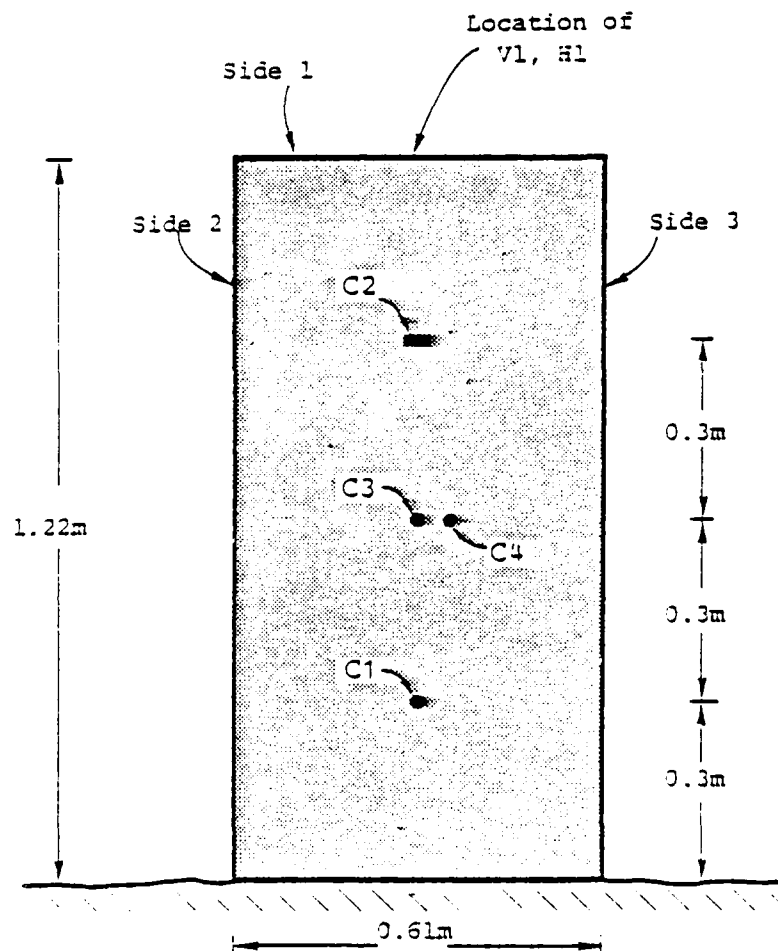


Figure 38. View of side 5 of grout block.
 ('C' is charge number; 'V' is
 "vertical" displacement gauge;
 'H' is "horizontal" displacement
 gauge.)

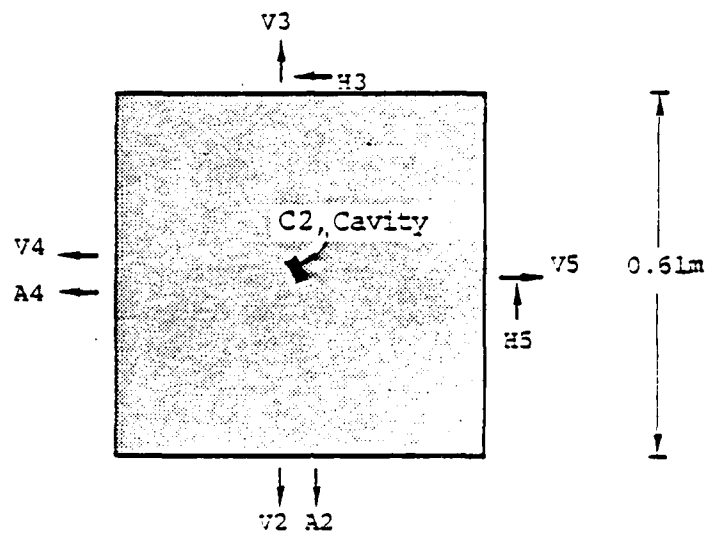


Figure 39. Section view of block at height of 0.9 m.
('A' denotes accelerometer.)

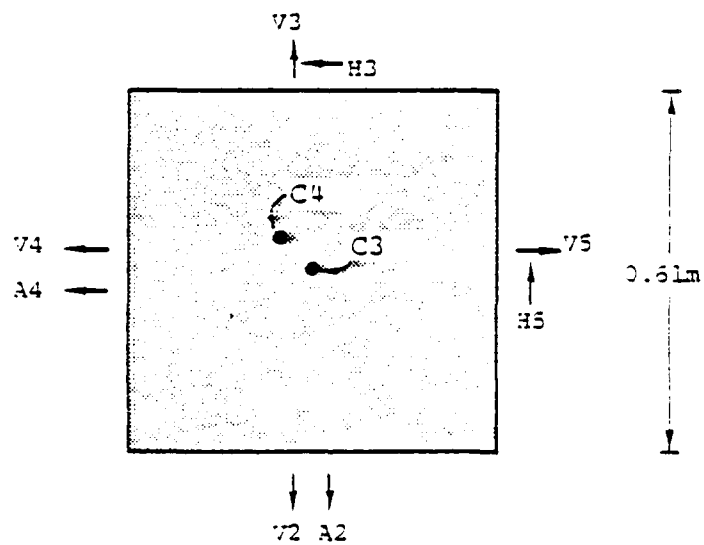


Figure 40. Section view of block at height of 0.6m.

below surfaces 3 and 4 (Figure 40). The purpose of the cavity charge (C#2) was to assess the effects of source asymmetry, and the off axis position of charge #4 was chosen to give some information of the variation of the measured free surface motion with distance from the detonation. The charges were first attached to an array of 0.3 mm diameter wires within the form used to cast the blocks. Then the grout was poured into the form; this ensured intimate coupling of the charges to the grout.

The primary instrumentation consisted of probes* to measure the displacement normal ("vertical") to the top (V1) and side surfaces (V2 through V5). Transverse ("horizontal") displacement was also measured on the top surface (H1) and two of the vertical sides (H3 and H5). See Figure 41 for details on the installation of these sensors. Supplementary motion data were provided by accelerometers (A2 and A4) mounted on sides 2 and 4. All signals were recorded on a FM instrumentation tape machine with response from dc to 80 kHz.

All the charges in each grout block were fired on the same day, typically with an hour between shots. The motion gauges on the sides of the block were relocated between tests so that they were always located at the corresponding height of the charge. On the first block, three of the charges did not detonate, probably due to inadequate waterproofing of the charges. Data for the one good shot were of low quality due to noise from the high voltage detonating unit. For the other two blocks, all charges functioned and we discuss some of the results below.

*These were eddy-current gauges manufactured by Kaman Science Corporation with a full scale range of 500 micrometers and frequency response from DC to 50 kHz (3dB). Sensitivity is 2 millivolt per μm .

-These were piezoresistive bridge type units made by Endevco Corporation, model 2264A, rated to $\pm 50,000$ g's ($\pm 5 \times 10^5$ m/s²) from DC to over 50 kHz. Nominal sensitivity is 1 microvolt per m/s².

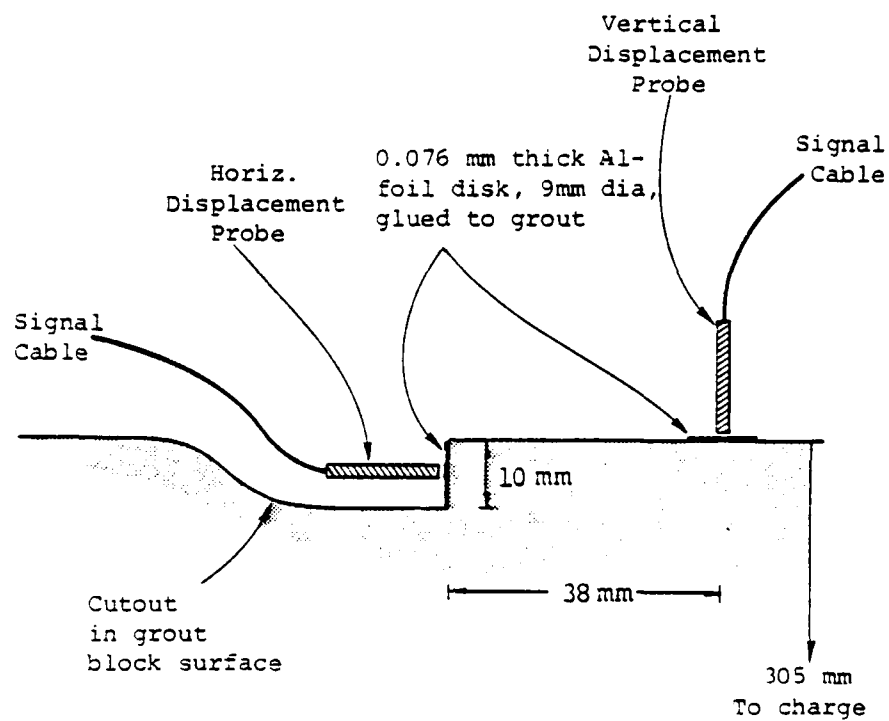


Figure 41. Section view of gauge placement detail. (Probes were mounted on an external support and held at a nominal 0.2 mm from the Al disks.)

5.3 RESULTS FOR THE SMALL SCALE EXPERIMENTS

The grout block was designed with a square cross-section so that the charge could be "viewed" from several equivalent directions, i.e., we wished to confirm the isotropy of the charge and grout. Data for the fully tamped charges (C1 and C3, on the block's centerline) matched to within the $\pm 1 \mu\text{m}$ experimental error*. Figures 42 and 43 demonstrate the similarity in observed waveforms on the four sides. The arrow in each figure denotes the relief wave that reflected off the block walls and arrived about $105 \mu\text{s}$ after the direct P wave signal[†].

The fully tamped shots were also intended to reproduce the results of our previous modelling experiments (Cherry, et al., 1977). The latter showed peak free-surface motions of $5 \mu\text{m}$ and a "static" displacement (after the peak) of about $1 \mu\text{m}$ at a range of 305 mm from 0.25 gram PETN charges. The loading density of the powdered PETN was 1.0 g/cm^3 ; the current charges were loaded at 0.84 g/cm^3 but were larger, 0.4 gram total. The present results are consistent with our previous observations; in particular, the "static" displacement feature is quite evident.

The earlier tests showed an anomalous S wave signal which exceeded $1 \mu\text{m}$ in amplitude. This signal was attributed to asymmetric tamping of the charge. The present data, with an improved charge placement technique, do not show significant S wave anomalies except when there were asymmetries in the charge's vicinity; see the horizontal gauge records shown in Figure 44. The observed P wave arrival (from Figures 42 and 43), the estimated time for arrival of a S wave and the side-wall relief wave arrival are noted in this figure.

*This error is primarily due to the random electronic noise in the displacement gauges' signals.

†The data for all of the shots imply a P wave velocity of $3.5 \times 10^3 \text{ m/s}$ and a S wave velocity of $2.5 \times 10^3 \text{ m/s}$ in this grout.

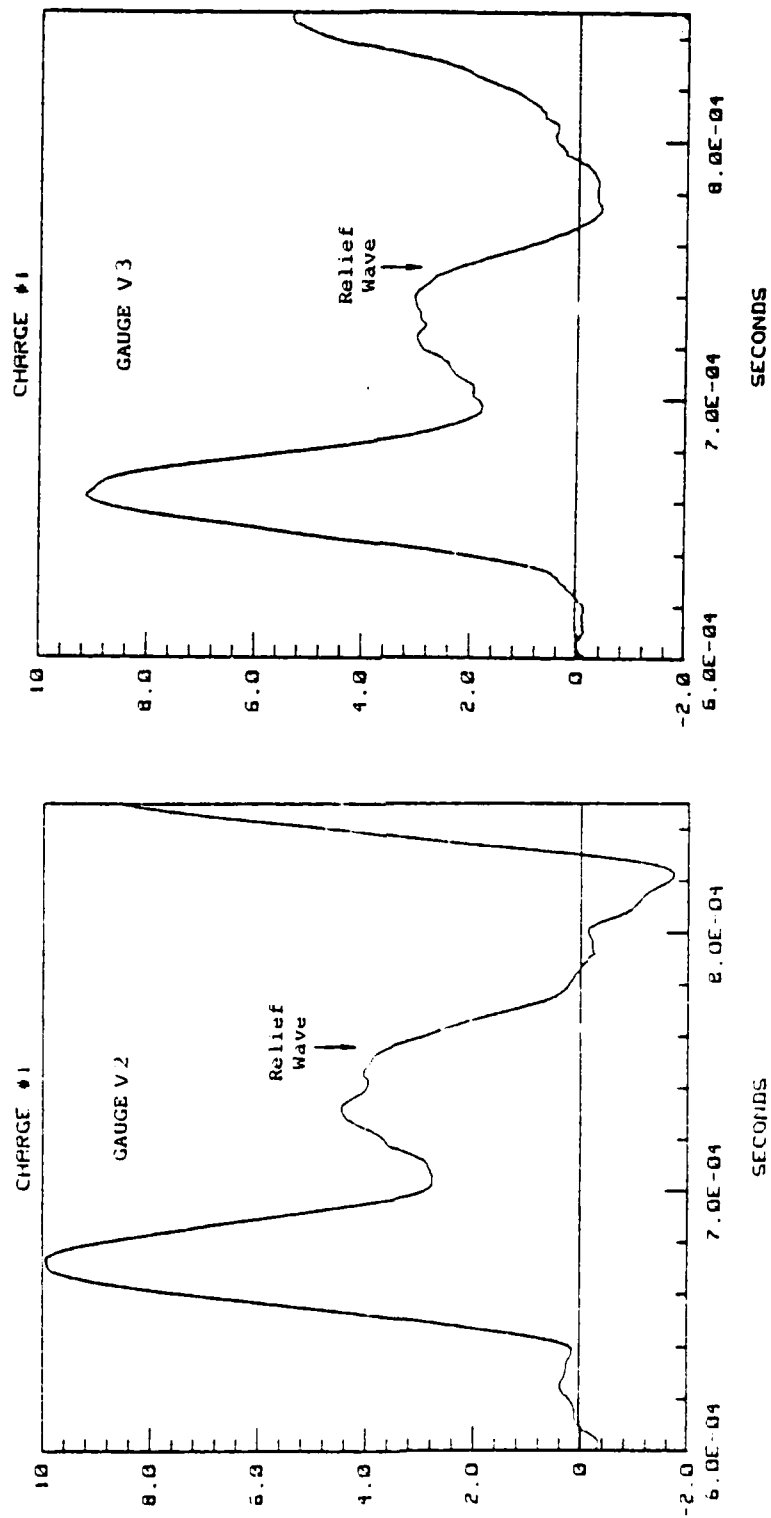


Figure 42. Vertical displacement in micrometers for free surface gauges V2 and V3, fully tamped charge (C1), second grout block.

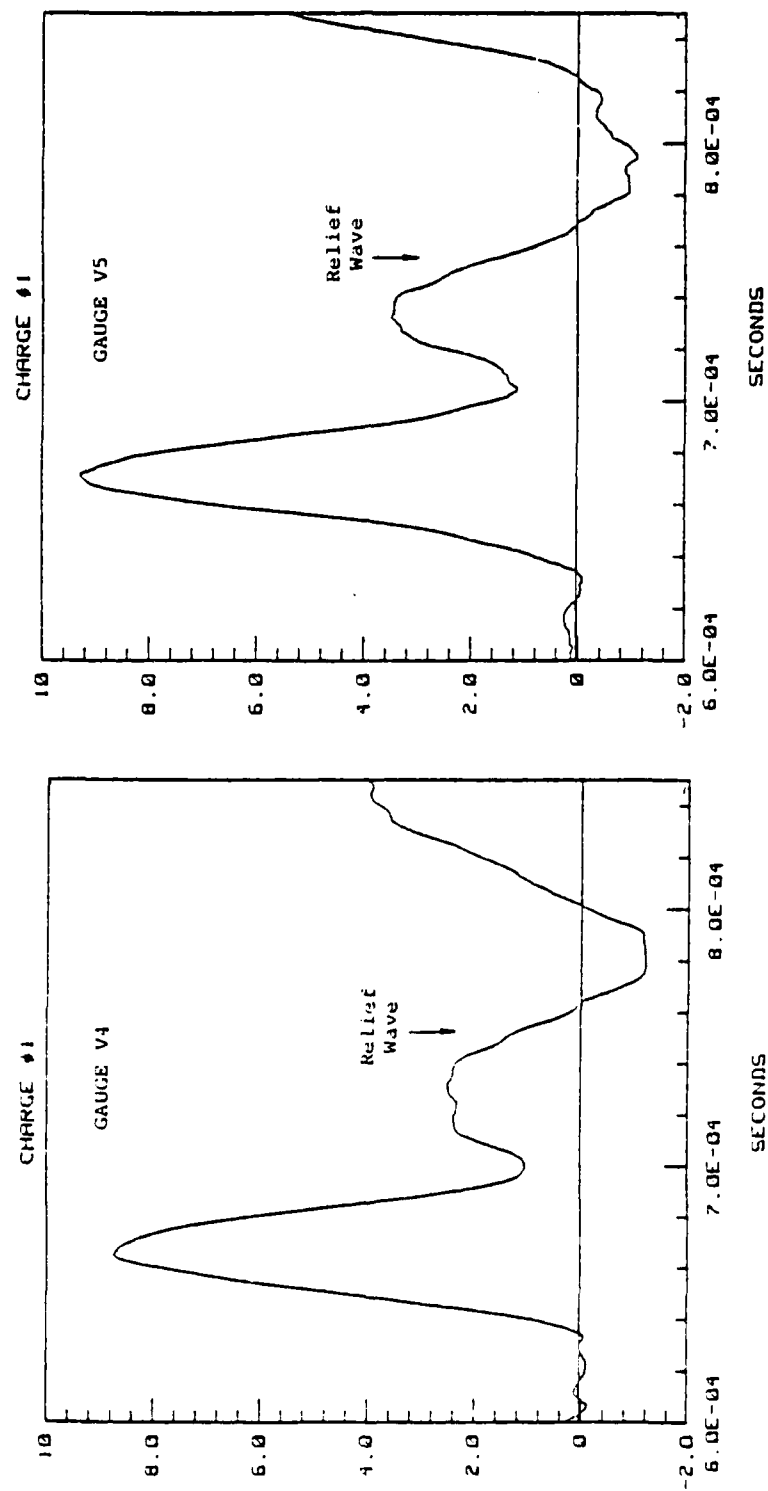


Figure 43. Vertical displacement in micrometers for free surface gauges V4 and V5, fully tamped charge (C1), second grout block.

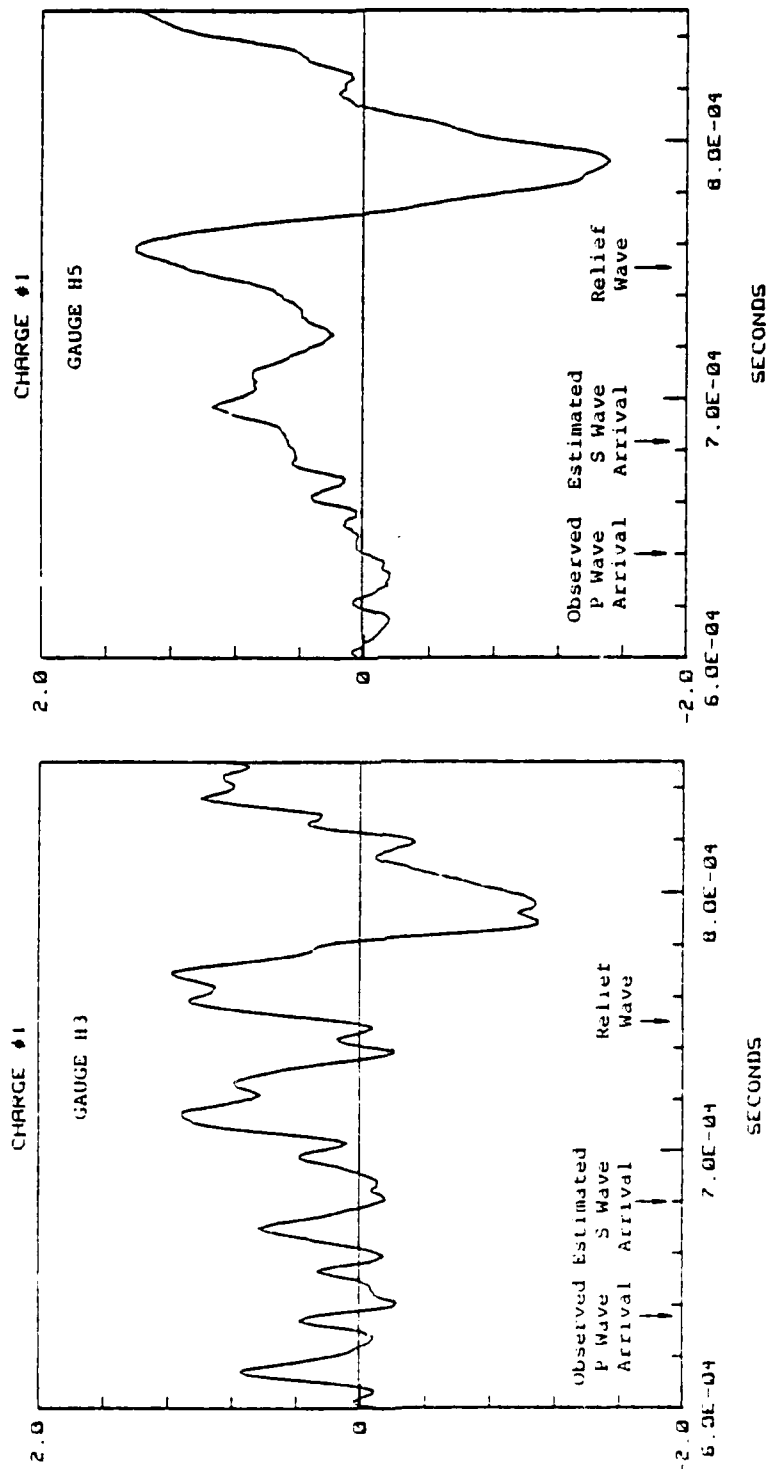


Figure 44. Horizontal displacement in micrometers for free surface gauges H3 and H5, fully tamped charge (C1), second grout block.

The data from the cavity shots (C2) do show very pronounced differences from those for the fully tamped explosions. The vertical motion waveshapes depend strongly on the direction relative to the cylinder's axis; see Figures 45, 46 and 47. Gauges V3 and V4 were closest to the void space in the cavity; their waveforms are roughly similar, remaining high after the initial peak. Gauges V2 and V5 were closest to the charge end of the cavity; their shapes are also comparable, showing a rapid decay after the initial peak. Significant S wave signals are also present; see Figures 48 and 49. Postshot, we removed a core sample containing the HE cavity. The initial dimensions of the cavity, 10 mm diameter by 20 mm length, had increased to about a 15 mm diameter and a 32 mm length. Thus the final volume remained strongly asymmetric, due in part to the relatively low detonation product pressure (estimated at 2 GPa).

Table 3 summarizes peak motions measured by most of the gauges on all eight tests. We note two major features. First, there were systematic differences between the blocks in peak displacements and the shape of the acceleration records; see, for example, Figure 50. While the blocks were intended to be similar to each other, the grouts were in practice different. The most obvious deviation is in the unconfined compressive strength of the core samples taken after the tests. Six samples from the second block showed an average strength of 22 MPa with a standard deviation of ± 2 MPa. For the third block, the strength was 35 ± 5 MPa. A second feature in the data for charges 1, 3 and 4 is the attenuation of the peak normal motion. Compare the peak displacement for V1 with the other vertical component data; for charge 1, V1 was 0.91 m distant; for charges 3 and 4, V1 was 0.60 m from the explosive.

While these results confirmed the principal details of our earlier work and demonstrated the effects of extreme source asymmetry, a significant experimental problem was not solved. For all but charge 2 in the second block, the explosive did

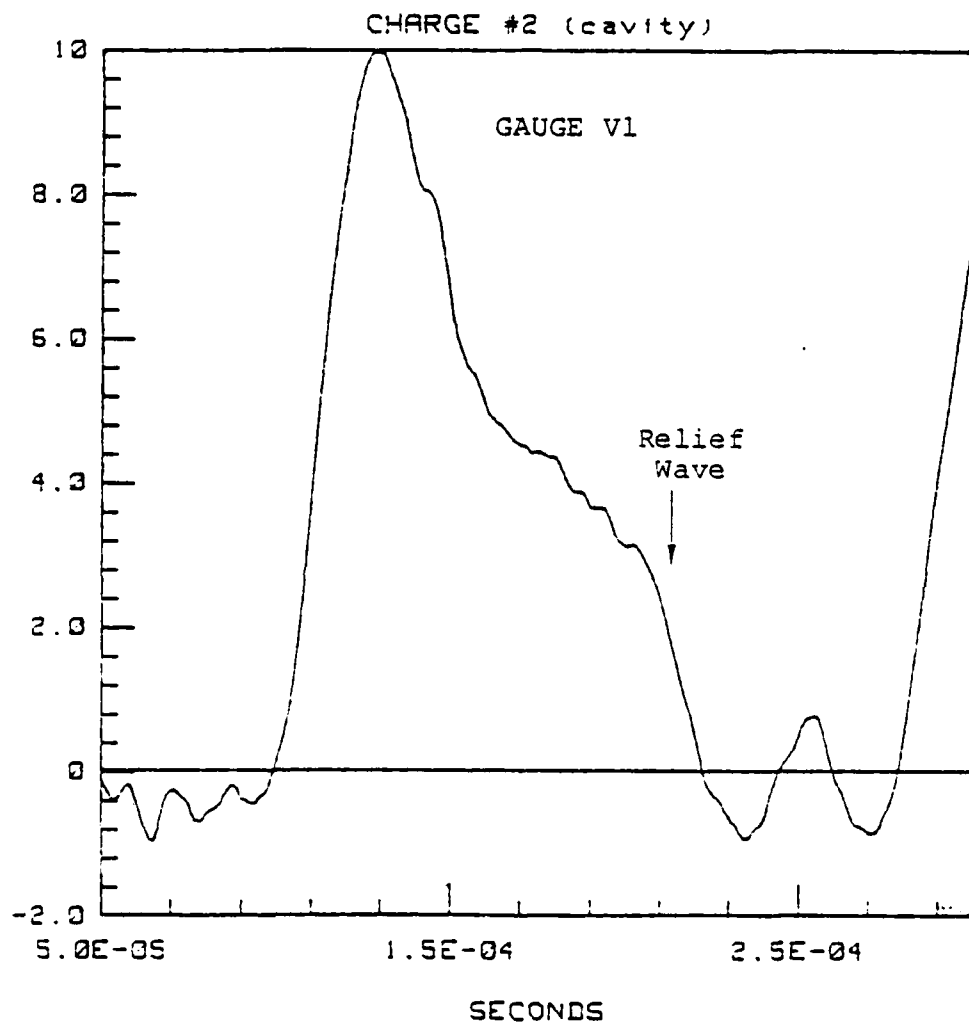


Figure 45. Vertical displacement in micrometers, gauge V1, cavity charge (C2), second grout block.

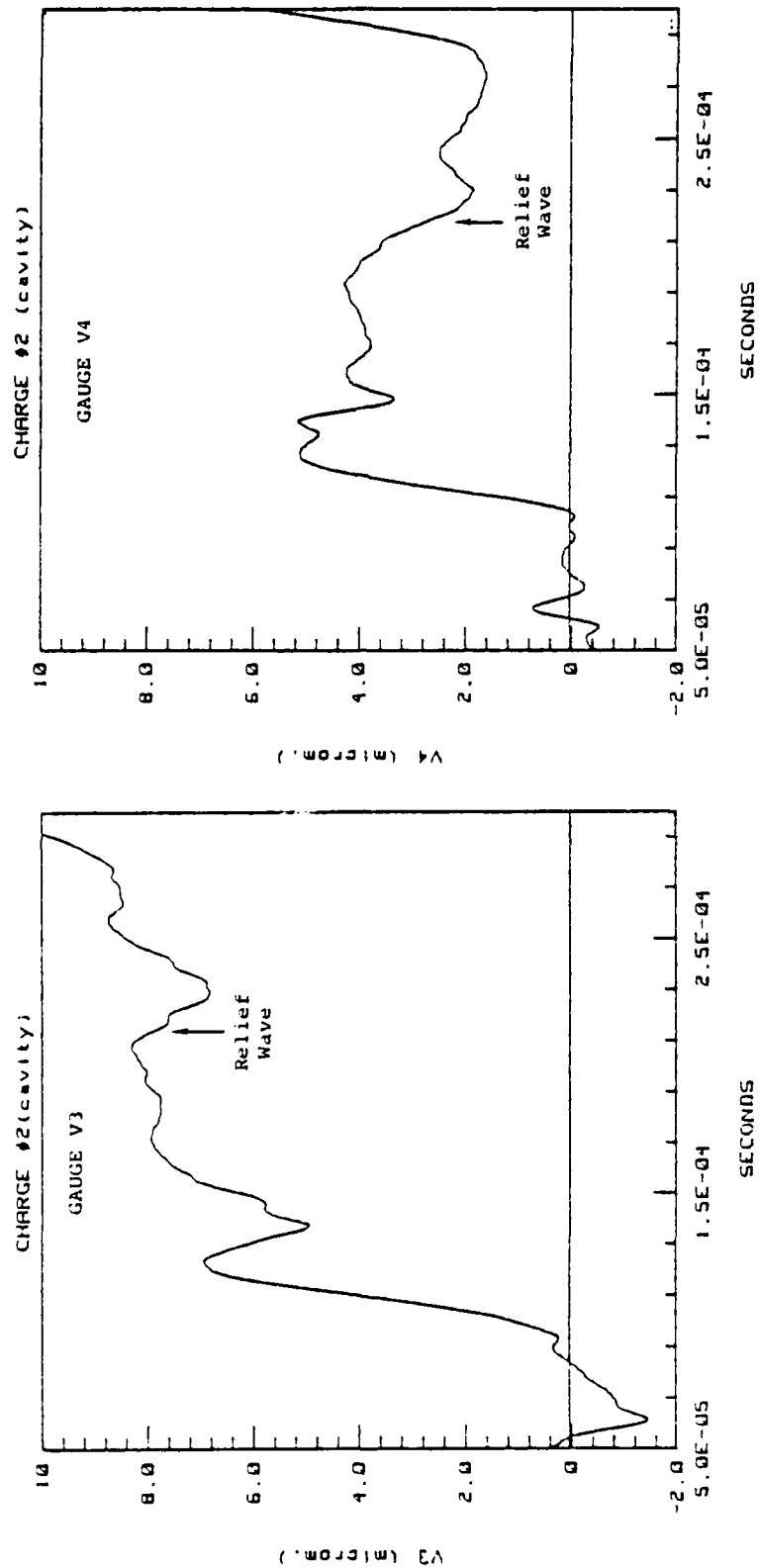


Figure 46. Vertical displacement in micrometers, gauges V3 and V4, cavity charge (C2), second grout block.

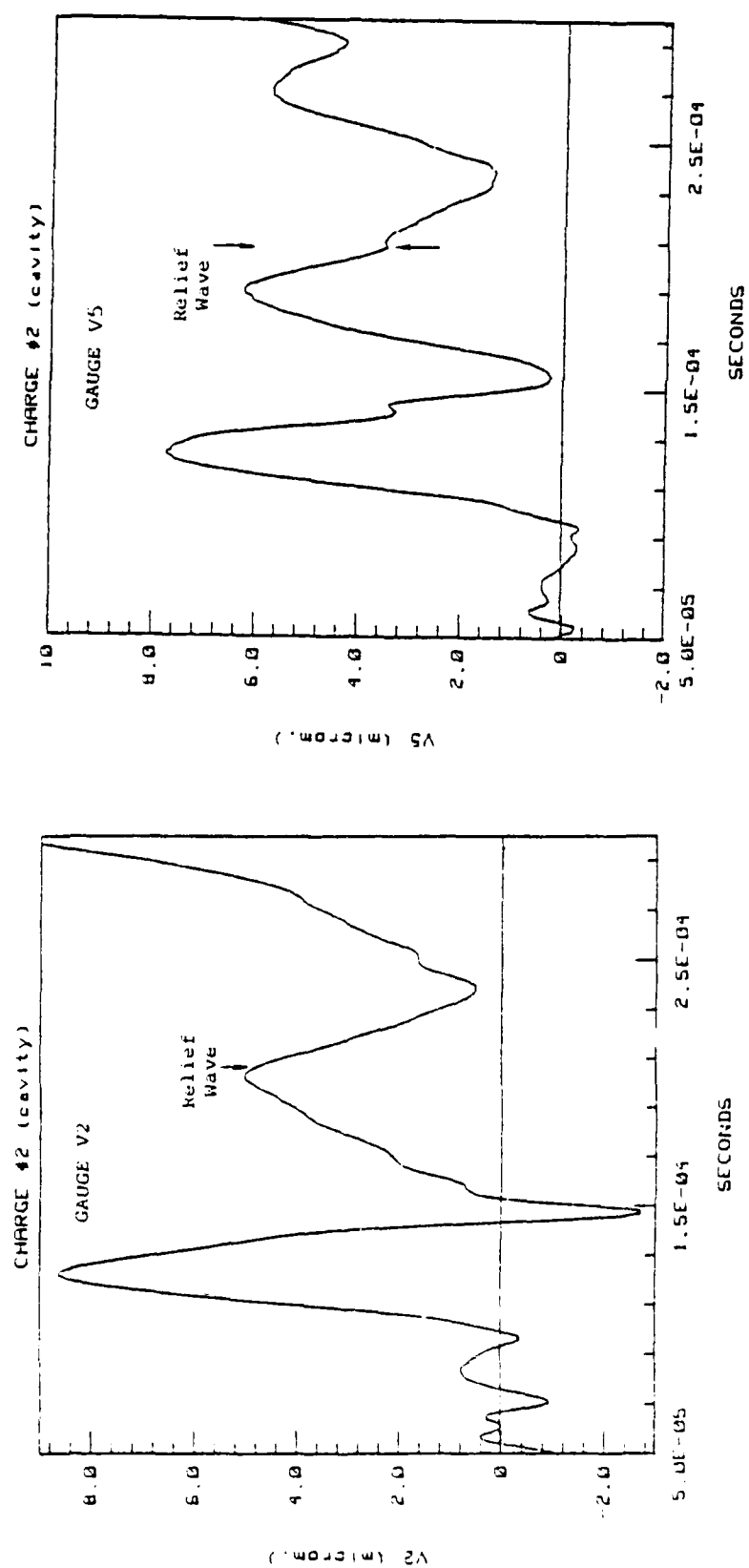


Figure 47. Vertical displacement in micrometers, gauges V2 and V5, cavity charge (C2), second grout block.

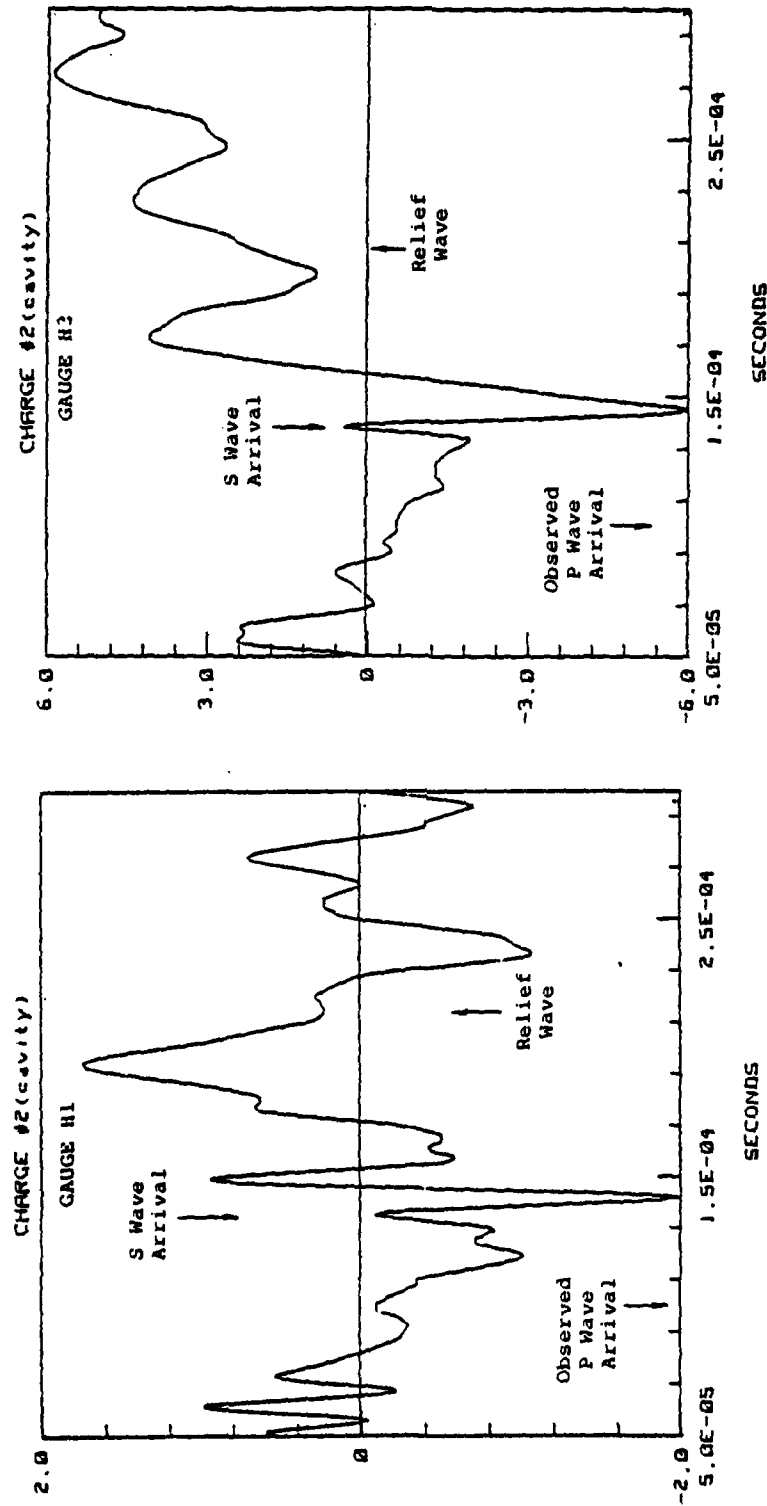


Figure 48. Horizontal displacement in micrometers, gauges H1 and H3, cavity charge (C2), second grout block.

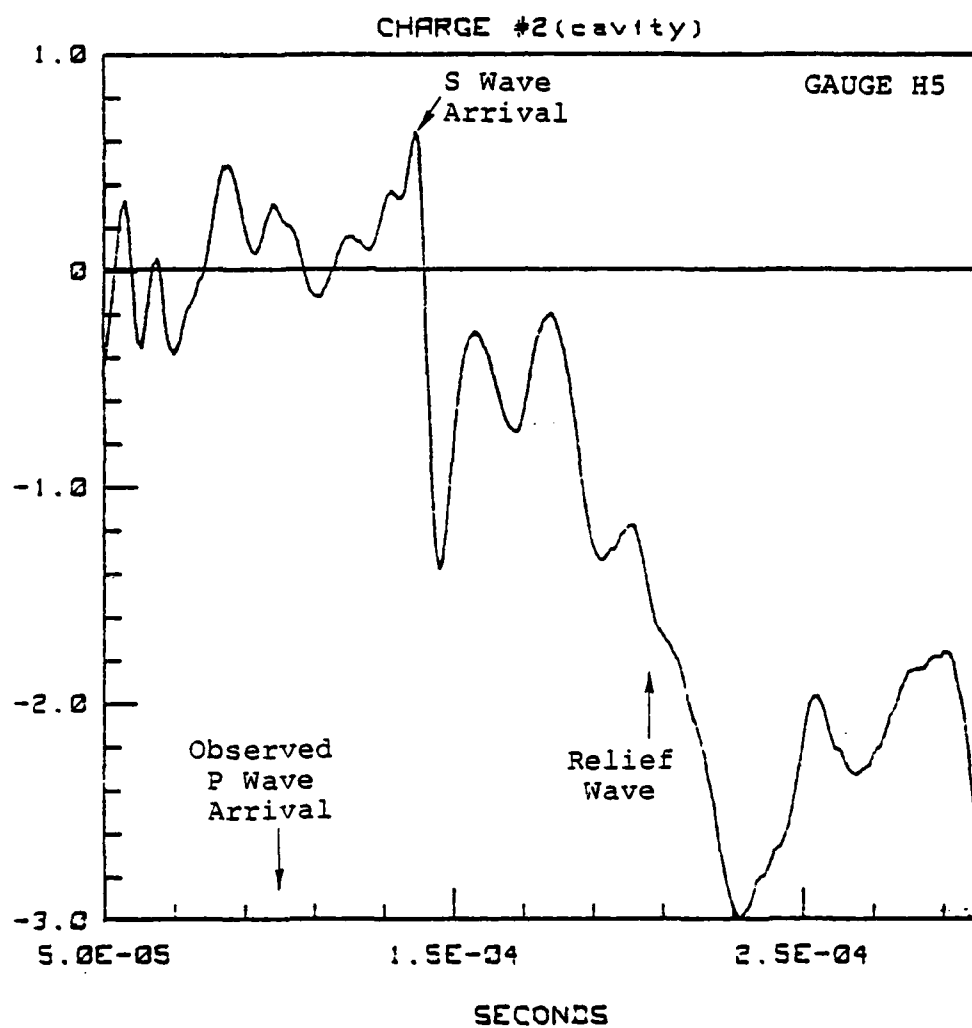


Figure 49. Horizontal displacement in micrometers, gauge H5, cavity charge (C2), second grout block.

TABLE 3

SUMMARY OF PEAK MOTIONS FOR ALL SHOTS

Gauge	Second Block				Third Block			
	C1	C4 ^Δ (Off-Axis)	C2 (Cavity)	C3	C1	C2 (Cavity)	C3	C4 (Off-Axis)
V1	2	3	10	4	~1.4	~3	~1.3	2
V2	10, ~4	7, ~2	9	~12	4, ~1	~2	4, ~1	~4.5
V3	9, ~3	9.5, ~4	6	~11	3.5, ~1	~2	4.5, ~1	~7
V4	8.5, ~2	6, ~1	5	~10	4, ~1	~2	4, ~1	~7
V5	9.5, ~3	9, ~3	8	~11	3, ~1	~2	4, ~1	~3.5
H1	*	*	~1.5	~1	*	*	*	*
H3	*	~3	~6	~3	*	*	*	~1.5
H5	*	~1	~1.5	~5	*	*	*	~4
A2	+9, -5	+2, -2	+8, -7	†	+6, -9	+0.5, -0.5	+5, -8	+7, -8
A4	+8, -6	+3, -3	+7, -8	+8, -4	+6, -10	+0.5, -0.2	+6, -8	+15, -25

V = Vertical (normal) peak displacement in micrometers; "static" displacement also given for some shots.

H = Horizontal (transverse) displacement in micrometers.

A = Vertical (normal) acceleration in units of 10^4 m/s^2 ; plus and minus maxima given.

C = Charge number; listed in order fired.

*denotes no clear, direct P or S wave signal larger than noise level of $0.5 \mu\text{m}$.

†denotes gauge failure.

Athis charge was placed 254 mm below surfaces 3 and 5.

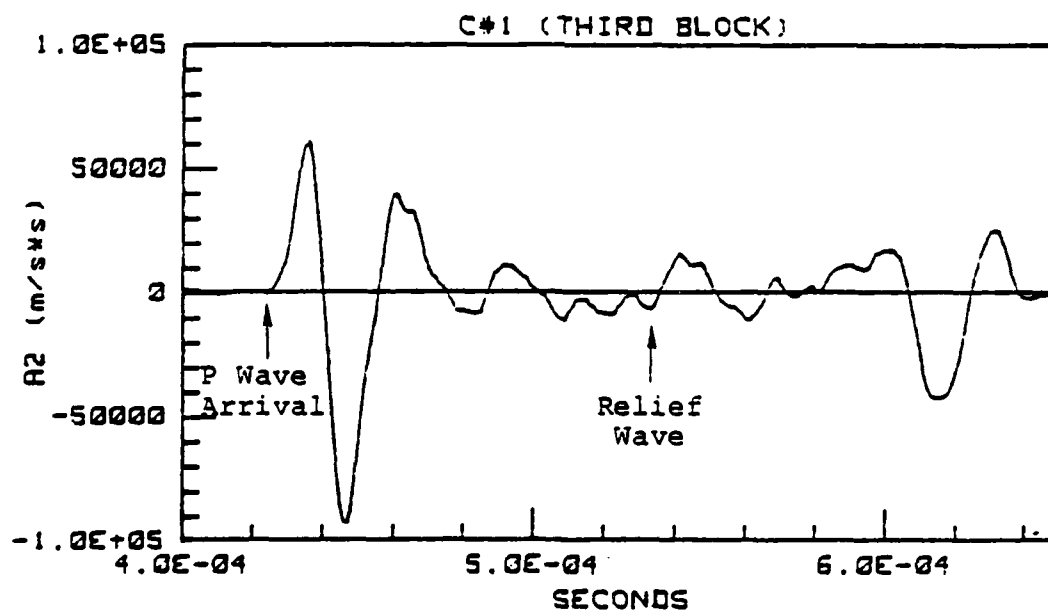
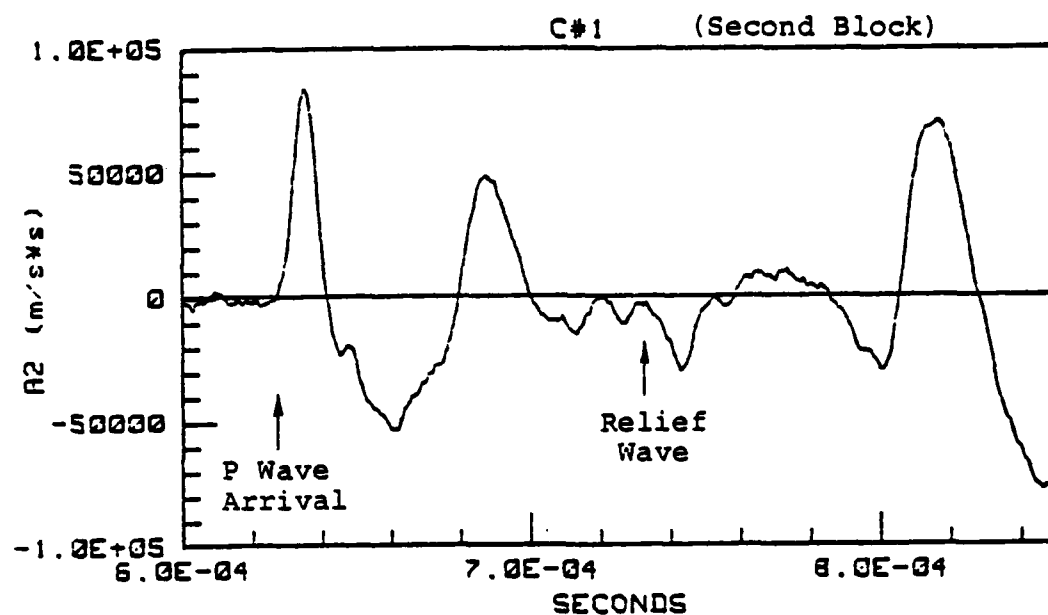


Figure 50. Comparison of vertical accelerations (gauge A2) for fully tamped charges (C1) on second and third grout blocks.

not experience a prompt high order detonation. Typically there was a several hundred microsecond delay between the high voltage firing pulse (i.e., explosion of the bridgewire) and initiation of the PETN explosive. We believe that the heat and vibration* involved in preparing the grout block compromised the contact between the bridgewire and the PETN powder. Some amount of PETN burned first before a full detonation spread to the majority of the explosive. Hence it will be difficult to accurately model the behavior of these charges. We do note that the influence of the delayed detonation is not as striking as the effects of charge asymmetry and grout strength.[†]

*The grout is vibrated after pouring to help release trapped air bubbles.

†Since completing these experiments, we have identified a commercial source of charges that perform without delay. Since these charges use high density PETN (1.7 g/cm^3), the detonation product pressure exceeds 10 GPa.

REFERENCES

- Bache, T. C. (1979), " \hat{m}_b , A Spectral Body Wave Magnitude (U)," Systems, Science and Software Report submitted to the Advanced Research Projects Agency, SSS-CR-79-3901, January, (S).
- Bache, T. C. and T. G. Barker (1978), "The San Fernando Earthquake - A Model Consistent with Near-Field and Far-Field Observations at Long and Short Periods," Systems, Science and Software Report submitted to the U. S. Geological Survey, SSS-R-78-3552, January.
- Bache, T. C., T. C. Barker, N. Rimer, T. R. Blake, D. G. Lambert, J. T. Cherry and J. M. Savino (1975), "An Explanation of the Relative Amplitudes of the Teleseismic Body Waves Generated by Explosions in Different Test Areas at NTS," Systems, Science and Software Report SSS-R-76-2746 submitted to the Defense Nuclear Agency, DNA 3958F, October.
- Bache, T. C., S. M. Day and J. M. Savino (1979), "Automated Magnitude Measures, Earthquake Source Modeling, VFM Discriminant Testing and Summary of Current Research," Systems, Science and Software Quarterly Technical Report submitted to the Advanced Research Projects Agency, SSS-R-79-3933, February.
- Bache, T. C. and D. G. Harkrider (1976), "The Body Waves Due to a General Seismic Source in a Layered Earth Model: 1. Formulation of the Theory," BSSA, 66, pp. 1805-1819.
- Bache, T. C., D. G. Lambert and T. G. Barker (1979), "A Source Model for the March 28, 1975 Pocatello Valley Earthquake from Time Domain Modeling of Teleseismic P Waves," to be submitted to the BSSA.
- Berger, J. (1979), "Design Study for a Seismic Research Center: Hardware Configuration," Systems, Science and Software Topical Report submitted to the Advanced Research Projects Agency, SSS-R-80-4173, September.
- Brune, J. N. and J. Dorman (1963), "Seismic Waves and Earth Structure in the Canadian Shield," BSSA, 53, pp. 167-209.
- Cherry, J. T., C. B. Archambeau, G. A. Frazier, A. J. Good, K. G. Hamilton and D. G. Harkrider (1973), "The Teleseismic Radiation Field from Explosions: The Dependence of Seismic Amplitudes Upon Properties of Materials in the Source Region," Systems, Science and Software Report SSS-R-72-1193 submitted to the Defense Nuclear Agency, DNA 3113Z, August.

REFERENCES (continued)

- Cherry, J. T., T. G. Barker, S. M. Day and P. L. Coleman (1977), "Seismic Ground Motion from Free-Field and Underburied Explosive Sources," Systems, Science and Software Final Report submitted to the Advanced Research Projects Agency, SSS-R-77-3349, July.
- Cherry, J. T., N. Rimer and W. O. Wray (1975), "Seismic Coupling from a Nuclear Explosion: The Dependence of the Reduced Displacement Potential on the Nonlinear Behavior of the Near Source Rock Environment," Systems, Science and Software Report submitted to the Advanced Research Projects Agency, SSS-R-76-2742, September.
- Coleman, P. L., S. M. Day, N. Rimer, J. T. Cherry, J. R. Murphy and T. C. Bache (1979), "Small-Scale Explosion Experiments, Seismic Source Calculations and Summary of Current Research," Systems, Science and Software Quarterly Technical Report submitted to the Advanced Research Projects Agency, SSS-R-79-4023, May.
- Day, S. M., T. C. Bache, T. G. Barker and J. T. Cherry (1978), "A Source Model for the 1975 Pocatello Valley Earthquake," Systems, Science and Software Report to the Air Force Geophysics Laboratory, AFGL-TR-79-0001, December.
- Hartzell, S. H. and J. N. Brune (1979), "The Horse Canyon Earthquake of August 2, 1975 - Two Stage Stress-Release Process in a Strike-Slip Earthquake," BSSA, 69, pp. 1161-1173.
- Masso, J. F., C. B. Archambeau and J. M. Savino (1978), "Implementation, Testing and Specification of a Seismic Event Detection and Discrimination System," Systems, Science and Software Technical Progress Report submitted to the U. S. Arms Control and Disarmament Agency, SSS-R-79-3833, October.
- Mueller, R. A. and J. R. Murphy (1971), "Seismic Characteristics of Underground Nuclear Detonations," BSSA, 61, pp. 1975.
- Murphy, J. R. and T. J. Bennett (1979), "A Review of Available Free-Field Seismic Data from Underground Nuclear Explosions in Alluvium, Tuff, Dolomite, Sandstone-Shale and Interbedded Lava Flows," Systems, Science and Software Topical Report submitted to the Advanced Research Projects Agency, SSS-R-80-4216, September.

REFERENCES (continued)

- Perret, W. R. (1968), "Free Field Particle Motion From a Nuclear Explosion in Salt, Part I," VUF 3012, June.
- Rimer, N., J. T. Cherry, S. M. Day, T. C. Bache, J. R. Murphy and A. Maewal (1979), "Two-Dimensional Calculation of PILEDRIVER, Analytic Continuation of Finite Difference Source Calculations, Analysis of Free Field Data From MERLIN and Summary of Current Research," Systems, Science and Software Report submitted to the Advanced Research Projects Agency, SSS-R-79-4121, August.
- Riney, T. D., G. A. Frazier, S. K. Garg, A. J. Good, R. G. Herrmann, L. W. Morland, J. W. Pritchett, M. H. Rice and J. Sweet (1973), "Constitutive Models and Computer Techniques for Ground Motion Predictions," Systems, Science and Software Report SSS-R-73-1490 submitted to the Defense Nuclear Agency, DNA 3180F, March.
- Rodi, W. L., J. M. Savino, T. G. Barker, S. M. Day and T. C. Bache (1978), "Analysis of Explosion Generated Surface Waves in Africa, Results from the Discrimination Experiment and Summary of Current Research," Systems, Science and Software Quarterly Technical Report submitted to the Advanced Research Projects Agency, SSS-R-78-3653, April.
- Savino, J. M., J. F. Masso and C. B. Archambeau (1979), "Discrimination Results From the Priority 1 Stations (U)," Systems, Science and Software Interim Report submitted to the Advanced Research Projects Agency, SSS-CR-79-4026, May, (S).
- Savino, J. M., N. Rimer, H. J. Swanger and T. C. Bache (1978), "Source Studies, Results From the Discrimination Experiment and Summary of Current Research," Systems, Science and Software Quarterly Technical Report submitted to the Advanced Research Projects Agency, SSS-R-78-3736, August.
- Sobel, P. A. (1978), "The Effects of Spall on m_b and M_s ," Teledyne Geotech Report, SDAC-TR-77-12, April.
- Springer, D. L. and R. L. Kinnamon ([97]), "Seismic Source Summary for U.S. Underground Nuclear Explosions, 1961-1970," BSSA, 61, pp. 1073-1098.

REFERENCES (concluded)

- Thompson, G. A. and D. B. Burke (1974), "Regional Geophysics of the Basin and Range Province," Annual Review of Earth and Planetary Sciences, Vol. 2, pp. 213-238.
- Viecelli, J. A. (1973), "Spallation and the Generation of Surface Waves by an Underground Explosion," JGR, 78, pp. 2475-2487.
- Vinnik, L. and A. Godzikovskaya (1972), "Sounding of the Earth's Mantle by the Method of Seismically Conjugate Points," Izvestiya, Earth Physics, No. 10, pp. 656.

APPENDIX A

ABSTRACTS OF TECHNICAL REPORTS SUBMITTED TO AFTAC/VSC MAY 1975 - DECEMBER 1979

A.1 QUARTERLY REPORTS

- August 1975, "Improved Yield Determination and Event Identification Research," J. T. Cherry, N. Rimer, J. M. Savino and W. O. Wray, SSS-R-75-2696, 28 pages.

A one-dimensional parameter study which identifies the dependence of teleseismic magnitude on near source material properties was carried out. The major results of the material parameter sensitivity study may be summarized as follows: (1) increasing the air-filled porosity greatly reduces seismic coupling; (2) if any parameter describing the yield surface is varied such that the material strength is reduced, seismic coupling may be substantially enhanced; (3) seismic coupling is relatively insensitive to water content; a slight decoupling is observed with increasing water content; (4) increasing the overburden pressure substantially reduces seismic coupling.

The near-field coupling and the equivalent source were computed for the recent underground explosion, MAST, at Pahute Mesa. The next step is to generate synthetic seismograms for this event at recently specified receiver locations. The enhanced computational capabilities for treating realistic earth structures will be exercised in this experiment.

- November 1975, "Improved Yield Determination and Event Identification Research," J. M. Savino, T. C. Bache, T. G. Barker, J. T. Cherry and W. O. Wray, SSS-R-76-2788, 42 pages.

Telesesimic ground motion predictions for the recent Pahute Mesa explosion, MAST, were quite successful in terms

of both amplitude and waveform matching. The predicted short-period body wave amplitudes were within 30 to 50 percent of the observed amplitudes at most of the SDCS stations. In addition, the general character of the first few seconds of the P wavetrains at the various SDCS stations were matched in reasonable detail.

A tension failure model that describes the development of a region of enhanced tension failure (cracking) produced during stress release behind the interacting shock fronts from closely spaced explosions was developed. Calculations for a multiple explosion scenario (three closely spaced explosions detonated simultaneously) were carried out into the elastic region using the two-dimensional CRAM code with the new material failure model included.

- February 1976, "Improved Yield Determination and Event Identification Research," J. M. Savino, SSS-R-76-2870, 64 pages.

Comparison of computed and observed short and long period seismograms for the Pahute Mesa explosion, MAST, were made with respect to amplitude, waveform and travel times. Travel times were closely matched as were the waveforms for surface waves recorded at the SDCS stations. For body waves a number of the SDCS stations are within the triplication range and the waveform match was far from ideal. Still, amplitudes for both body and surface waves were matched to within 50 percent and were much closer in most cases.

- May 1976, "Explosion Source Modeling, Seismic Waveform Prediction and Yield Verification Research," T. C. Bache, T. G. Barker, J. T. Cherry, N. Rimer and J. M. Savino, SSS-R-76-2924, 54 pages.

The theoretically computed and observed amplitudes of both b and d (maximum) body wave phases for KASSERI agree to

well within a factor of two at all of the five SDCS stations. Minor adjustments of the upper mantle model could improve the agreement at all the SDCS sites.

Computations of the effect of material strength on teleseismic body wave amplitudes indicate that the amplitude of the b phase increases with decreasing strength; the rate of increase being more rapid at lower levels of material strength. An additional effect is that the apparent period of the b phase increases rapidly with decreasing strength due to a shift in the corner frequency of the source spectrum.

Further verification of the explosion source modeling code, SKIPPER, was achieved by comparison of free-field ground motion calculations and observations for the PILEDRIIVER and GASBUGGY explosions. In the case of PILEDRIIVER, the exercise of a recently developed elastic wave propagation code verified that the observed PILEDRIIVER RDP was not affected by reflected waves from the free surface or from layer interfaces in the source region.

Excellent free-field ground motion measurements and material properties data are available for the GASBUGGY explosion. The computed RDP, employing these data, agrees quite well with the measured RDP, increasing our confidence in the constitutive modeling of the explosion source and ultimately the teleseismic ground motion predictions based on these source calculations.

- August 1976, "Explosion Yield Verification, Multiple Explosion Scenarios and Three-Dimensional Seismic Modeling Research," D. G. Lambert, C. F. Petersen and J. M. Savino, SSS-R-76-2993, 46 pages.

A procedure for directly inverting teleseismic ground motion data in order to obtain estimates of explosion yields was developed. The particular inversion scheme employs a

a deterministic modeling capability which predicts the teleseismic ground motion from a nuclear explosion. This procedure supplements expected data exchange packages that provide information on the near explosion source environment.

Experiments involving computer simulation and decomposition of multiple explosion scenarios were recently initiated. Application of narrow-band filtering to synthesized multiple event seismograms has yielded accurate determinations of the relative amplitudes and time separations between individual explosions in the multiple explosion event examined.

Preparations are nearing completion for a series of three-dimensional seismic modeling experiments. The intent of these experiments is to measure differences in signals between single and multiple sources and between near surface and deeply buried sources. Theoretical explosion calculations will be compared to the experimental results.

- January 1977, "Seismic Studies for Improved Yield Determination," T. C. Bache, J. M. Savino, M. Baker and P. L. Coleman, SSS-R-77-3108, 80 pages.

The report summarizes the results of the first three months of research on a contract whose main objective is to examine the parameters that affect the seismic signals from underground explosions. Results are presented from research in five areas: (1) theoretical teleseismic magnitudes (M_s and m_b) were determined for a series of nuclear explosion cratering calculations carried out by Applied Theory, Inc.; (2) the relative frequency content of signals from U.S.S.R. and U. S. explosions were studied by comparing the periods of the first few cycles of recordings from several stations at teleseismic ranges; (3) some improved techniques were developed for computing the equivalent point source representation for explosions in highly porous materials; (4) the dependence of body wave magnitude on yield for underground

explosions in salt was studied and compared to that for explosions in granite; (5) small scale experiments were carried out in which underground explosions were modeled by 0.25 gram charges embedded in concrete.

- April 1977, "Seismic Studies for Improved Yield Determination," T. G. Barker, M. Baker, P. Coleman, and D. G. Lambert, SSS-R-77-3191, 48 pages.

The report summarizes the results of the second three months of research on a contract whose main objective is to examine the parameters that effect the seismic signals from underground nuclear explosions. Results were presented on research in five areas: (1) data pertinent to regional bias in m_b and M_s in the United States and central Asia were summarized; (2) signals simulating those from multiple explosions were decomposed and scaled by narrow-band filtering methods; (3) numerical simulations of contained explosions were compared with previous laboratory simulations; (4) laboratory experiments of cratering explosions were completed using 0.25 gram charges embedded in concrete; (5) the primary factors controlling amplitude-yield scaling at regional distances were investigated.

- July 1977, "Seismic Studies for Improved Yield Determination," T. C. Bache, P. L. Goupillaud and B. F. Mason, SSS-R-77-3345, 65 pages.

Results are presented from research conducted during the quarter from April to June 1977. Work in three research areas is discussed:

1. The dependence of observed surface wave amplitudes on explosion yield and the characteristics of the emplacement medium is reviewed. Surface wave data compiled by others are used in conjunction with a new data set consisting of Airy phase amplitudes from the WWSSN stations ALQ and TUC.

2. The theoretical dependence of surface wave amplitude on the important controlling parameters is discussed. Attention is directed to the assumptions of the theoretical models and their consequences.
3. Preliminary results are presented for the development and testing of a deconvolution technique for analyzing short period teleseismic recordings of explosions.

• October 1977, "Seismic Studies of Surface and Body Waves for Improved Yield Determination," T. C. Bache and W. L. Rodi, SSS-R-78-3448, 79 pages.

The majority of the report is devoted to describing the results of two research projects not previously reported. One of these, "Determination of Crustal Structure from Surface Wave Dispersion Data," describes a recently developed method for obtaining crustal structure and gives results from application of this method to two paths in the southwestern United States: Nevada Test Site (NTS) to Albuquerque, New Mexico and NTS to Tucson, Arizona. Phase and group velocities are determined from NTS explosion recordings. These data are used in a formal generalized inversion procedure to determine crustal structures that are also consistent with other available data about the region; e.g., P_n velocities. Theoretical seismograms computed with the new crustal models show remarkable agreement with observations of NTS explosions at the two stations.

The second research study described is entitled, "Small-Scale Laboratory Simulations of Explosion Produced Body Waves - Implications for the teleseismic Signatures of Underground Nuclear Explosions." Small scale laboratory experiments were carried out to measure the ground motions from spherical charges. There were two classes of experiments; one in which the ground motions were free-field and one in which they included a free surface effect. Of the latter, some were quite

shallow and cratered. The most important feature of the experimental data is a large negative pulse that occurs at late-time in the experiments that include free-surface effects. Much of the study is directed toward determining the effect a pulse of this kind would have on the teleseismic body waves from nuclear explosions and m_b -log yield relations. If a late arriving negative pulse like that in the experimental data also occurs in underground nuclear explosions, the effect is to lower the slope of the m_b -log yield relation. This may explain why observed slopes are lower than predicted by theoretical models in which the free surface is represented elastically.

- January 1978, "Station Transfer Functions, Analysis of P-Wave Residuals and Summary of Current Research," J. F. Masso, J. M. Savino and T. C. Bache, SSS-R-78-3559, 80 pages.

Brief summaries of work are given in four topic areas: Source Studies, Data Analysis, Surface Wave Studies and Body Wave Studies.

Also included in the report is a detailed description of a research project not previously reported. This study is entitled, "Worldwide Observations of P-Wave Travel-Time Residuals." A large set of residuals compiled from ISC bulletins by Georges Poupinet of Institute de physique du Globe were compared with other data from the United States. The conclusions are that; (1) large negative residuals correlate with low heat flow and positive magnitude bias, and (2) large positive residuals correlate with high heat flow and negative magnitude bias. The same correlation between heat flow and travel-time residuals holds for stations located on the Russian and Siberian Platforms in the U.S.S.R.

- April 1978, "Analysis of Explosion Generated Surface Waves in Africa, Results from the Discrimination

Experiment and Summary of Current Research," W. L. Rodi, J. M. Savino, T. G. Barker, S. M. Day and T. C. Bache, SSS-R-78-3653, 92 pages.

The majority of the report is devoted to presentation of results not previously reported from four research projects. The first is entitled, "Discrimination Experiment." Digital short- and long-period body and surface wave data for Eurasian events recorded at a global network of stations are being provided for event discrimination. Efforts to date have focused on the application of the VFM (variable frequency magnitude) discriminant to the short period P waves at four stations. Thirteen events have been analyzed and tentative identification has been made.

The second project is entitled, "Analytic Continuation of the Elastic Field from a Complex Source in a Halfspace." We present the mathematical development of a method for linking finite difference numerical source calculations in a halfspace with analytical techniques for propagating elastic waves in layered media.

The third detailed discussion, "Theoretical Computation of Lg," is concerned with the theoretical generation of Lg in a continental earth model. Synthetic seismograms are shown for several ranges and source depths. The fourth topic is, "Analysis of Surface Waves from the French Test Site in the Sahara." For an underground explosion in Algeria surface wave recordings from five stations in or near Africa were analyzed to determine the phase and group dispersion. Using formal linear inversion, these data were inverted to obtain preliminary models for the crust and upper mantle along the five paths. Using these models, synthetic seismograms were computed and were found to be in good agreement with the observations at most of the stations.

• August 1978, "Source Studies, Results from the Discrimination Experiment and Summary of Current Research," J. M. Savino, N. Rimer, H. J. Swanger and T. C. Bache, SSS-R-78-3736, 68 pages.

The majority of the report is devoted to presentation of results not previously reported from three research projects. The first is entitled, "Discrimination Experiment." Digital short and long period body and surface wave data for Eurasian events recorded at a global network of stations are being provided for event discrimination. Efforts to date have focused on the application of the VFM (variable frequency magnitude) discriminant to the short period P waves at eight stations. Twenty-eight events have been analyzed and tentative identification has been made.

The second project is entitled, "Surface Wave Solution for the Elastic Equivalent of a Complex Axisymmetric Source." In our last quarterly report we presented the mathematical development of a method for linking finite difference numerical source calculations with analytical techniques for propagating body waves in layered elastic media. In this report the theory is extended to include the propagation of Rayleigh waves.

The third project is entitled, "Source Calculations." Our one-dimensional constitutive models for the numerical simulation of the explosion source were reviewed to ensure their compatibility with our two-dimensional finite difference programs. Three important improvements to the models were made: (1) the implementation of new equations of state for the cavity gases; (2) an improved treatment of overburden pressure and (3) an improved effective stress model. The new models and their effect on source calculations for PILEDRIVER, SALMON and Rainier Mesa tuff are described.

• February 1979, "Automated Magnitude Measures, Earthquake Source Modeling, VFM Discriminant Testing and Summary of Current Research," T. C. Bache, S. M. Day and J. M. Savino, SSS-R-79-3933, 98 pages.

Brief summaries of work currently underway or completed during the period from 1 October to 31 December 1978 are given in seven sections; Source Calculations, Discrimination, Yield Determination, Small-Scale Experiments, Selected Geological Studies, Magnitude-Yield Improvements and Ground Motion Analysis.

The remainder of the report is devoted to presentation of results not previously reported from three research projects. The first is concerned with the development and testing of an automated spectral body wave magnitude called \hat{m}_b . The \hat{m}_b is based on the spectral amplitude of the recorded signal in a narrow window in both time and frequency. For comparison to the \hat{m}_b , time domain m_b is computed for each recording with a semi-automatic technique in which all records are prefiltered to appear as if recorded by the same instrument. Amplitude and time measurements are made automatically during this process. The \hat{m}_b algorithm is tested by application to synthetic seismograms and to HNME recordings of Pahute Mesa explosions.

The second detailed discussion is entitled, "Three-Dimensional Earthquake Modeling." Results from two finite-difference simulations of earthquake faulting performed on the ILLIAC computer are summarized. In one case the material was elastic and in the second plastic yielding was allowed near the fault plane.

The third detailed discussion is entitled, "Discrimination Experiment." Two modifications to the MARS program used for discrimination are described. One is an algorithm for correcting for the effects of seismic noise. The second is an

algorithm for averaging weighted estimates to obtain the high and low frequency magnitudes used to classify events.

- May 1979, "Small-Scale Explosion Experiments, Seismic Source Calculations and Summary of Current Research," P. L. Coleman, S. M. Day, N. Rimer, J. T. Cherry, J. R. Murphy and T. C. Bache, SSS-R-79-4023, 41 pages.

Brief summaries of work currently underway or completed in the period from 1 January to 31 March 1979 are presented. Technical results not previously reported are given in five sections. One describes the development and testing of small spherical charges which will be emplaced in concrete blocks to simulate large explosions in the laboratory. A second section discussed an analysis of the free-field data from the MERLIN event. The other three sections are concerned with finite difference simulations of explosion and earthquake sources. These include results from calculations of PILEDRIVER and of decoupled explosions in salt. Also described is a fracture criterion for three-dimensional finite difference modeling of earthquake faulting.

- August 1979, "Two-Dimensional Calculation of Piledriver, Analytic Continuation of Finite Difference Source Calculations, Analysis of Free Field Data from MERLIN and Summary of Current Research," N. Rimer, J. T. Cherry, S. M. Day, T. C. Bache, J. R. Murphy and A. Maewal, SSS-R-79-4121, 158 pages.

Brief summaries of work completed during the period 1 April to 30 June are presented in the first section. The remainder of the report is devoted to presentation of technical results from four research projects. The first of these is a two-dimensional finite difference calculation of the PILEDRIVER explosion. Excellent agreement with observed ground motions is obtained for most of the near-field measuring stations at depth and on the surface. The second technical

section describes the implementation and testing of a method for computing far field synthetic seismograms from complex source simulations like that for PILEDRIVER. In the third section we study a large long period arrival at late time on near field recordings of the MERLIN explosion in alluvium. Our study, which includes comparison of synthetic and observed ground motions, indicates that this phase is due to spall closure. Finally, we summarize some results from theoretical seismogram studies of regional ground motions from earthquakes and explosions.

A.2 FINAL CONTRACT REPORTS

- October 1976, "Improved Yield Determination and Event Identification Research," J. M. Savino, T. C. Bache, T. G. Barker, J. T. Cherry, D. G. Lambert, J. F. Masso, N. Rimer and W. O. Wray, SSS-R-77-3038, 61 pages.

Work performed on Contract No. F8606-75-C-0045 has been reported in detail in a series of twelve topical and quarterly technical reports. This final report summarizes the material covered in each of the technical reports and discusses the conclusions obtained. The primary objective of the program is to develop methods for estimating the yield of underground nuclear explosions. The topics addressed include the modeling of both single and multiple explosions, propagation of the resultant stress waves through realistic earth structures, and prediction of short- and long-period explosion seismograms recorded at teleseismically located receivers. The results of these investigations provide a theoretical framework for expressing uncertainties in explosion yield estimates in terms of uncertainties in the near source material properties, local source and receiver crustal structures, and the upper mantle structure of the earth.

- July 1977, "Seismic Ground Motion from Free-Field and Underburied Explosive Sources," J. T. Cherry, T. G. Barker, S. M. Day and P. L. Coleman, SSS-R-77-3349, 44 pages.

Small-scale laboratory experiments were conducted and analyzed to study the effect of the proximity of the free surface on the seismic ground motions. Two classes of experiments were done. In one the charges were far from the free surface and the free-field displacement-time histories were measured. In the second class the charges were near the surface and were either fully contained or formed a crater. The charges were 0.25 g of PETN in concrete cylinders,

120 cm in diameter and 33 to 60 cm thick. In all experiments displacements were measured 30.5 cm directly below the charges. The experiments produced consistent and repeatable data. A striking feature of the ground motions for the near surface experiments is a large long-period negative pulse which is present whether or not cratering occurred.

The results were studied by comparing to numerical simulations of the experiments using a Lagrangian finite difference program and published properties of the concrete and PETN. The calculations are in good agreement with the laboratory data, providing verification of both the constitutive models and the methods.

The large, long-period negative pulse can be explained in the context of linear elasticity. It is due to the near-field interaction of the spherical wave front with the free surface. Therefore, it does not propagate to the far-field and is not important for teleseismic magnitudes.

• November 1978, "Summary of Seismic Discrimination and Explosion Yield Determination Research," T. C. Bache, J. M. Savino, S. M. Day, J. T. Cherry, H. J. Swanger and N. Rimer, SSS-R-79-3847, 127 pages.

This report summarizes the work accomplished in a twenty-four month research program directed toward resolution of technical issues arising in the seismic verification of an underground nuclear test ban treaty. Emphasis is on research conducted during the last year in five subject areas: data analysis, source studies, grout experiments, surface wave studies and body wave studies.

Results are summarized for thirteen research projects.

The report also includes an appendix in which abstracts are listed for seventeen technical reports submitted under this contract. Also included are the abstracts for twelve reports submitted under a preceding fifteen month contract.

A.3 TECHNICAL REPORTS

- September 1975, "Seismic Coupling from a Nuclear Explosion: The Dependence of the Reduced Displacement Potential on the Nonlinear Behavior of the Near Source Rock Environment," J. T. Cherry, N. Rimer and W. O. Wray, SSS-R-76-2742, 68 pages.

The objective of the research presented in this report is to determine the dependence of teleseismic magnitudes on the nonlinear behavior of the near source rock environment. Such information enables one to express uncertainties in explosive yield estimates in terms of uncertainties in the material properties and provides insight concerning the requirements for collection of geophysical data at a specific test site.

A series of spherically symmetric calculations have been performed in which the properties of the near source material were varied systematically. Output from these calculations enables one to determine the relative teleseismic coupling efficiency of a given near source material. Also, since seismic magnitudes are directly related to explosive yield, this parameter study permits an assessment of uncertainties in the estimated yield in terms of uncertainties of the material properties of the test site.

- October 1975, "Constitutive Equations for Fluid-Saturated Porous Media," S. K. Garg, SSS-R-76-2766, 12 pages.

This report develops constitutive relations for fluid-saturated porous media, suitable for inclusion in standard hydrodynamic codes (e.g., CRAM or SKIPPER). The theoretical formulation is based on the models for fluid-saturated rock aggregates previously developed by Garg and Nur (1973) and Garg, et al. (1975).

- February 1976, "Prediction and Matching of Teleseismic Ground Motion (Body and Surface Waves) from the NTS MAST Explosion," T. G. Barker, T. C. Bache, J. T. Cherry, N. Rimer and J. M. Savino, SSS-R-76-2727, 60 pages.

This report presents the results of a theoretical prediction of the teleseismic body and surface wave signatures of the recent underground explosion, MAST, and a detailed comparison of the predicted waveforms with seismograms recorded at stations of the Special Data Collection System (SDCS). This study represents a comprehensive analysis of the MAST event involving computer modeling of the close-in nonlinear ground motion produced by the explosion, propagation of the resultant stress waves through the appropriate earth structures and computation of seismograms recorded at designated teleseismic stations.

- February 1976, "Teleseismic Coupling from the Simultaneous Detonation of an Array of Nuclear Explosions," J. T. Cherry, T. C. Bache, W. O. Wray and J. F. Masso, SSS-R-76-2865, 26 pages.

This report presents the results of a theoretical study undertaken to determine if teleseismic ground motion may be enhanced by the simultaneous detonation of a closely spaced array of nuclear explosions. The specific array analyzed consisted of three 15 kt explosions equally spaced 165 meters apart. The explosive array was assumed contained, i.e., coupling effects due to cratering were not included in the analysis.

- May 1976, "Comparison of Theoretical and Observed Body and Surface Waves for KASSERI, an Explosion at NTS," T. C. Bache, T. G. Barker, N. Rimer and J. M. Savino, SSS-R-76-2937, 44 pages.

This report presents the results of a theoretical calculation of the teleseismic body and surface waves for the NTS

KASSERI explosion, and a detailed comparison of the synthetic seismograms with those recorded at stations of the Special Data Collection System (SDCS). This study is a comprehensive analysis of the KASSERI event including modeling of the close-in nonlinear ground motion produced by the explosion, propagation of the resulting seismic waves through the earth and computation of synthetic seismograms at designated teleseismic stations.

- May 1976, "Teleseismic Verification of Data Exchange Yields," T. C. Bache, T. G. Barker, J. T. Cherry and J. M. Savino, SSS-R-76-2941, 55 pages.

This working paper addressed the possibility of directly inverting teleseismic ground motion in order to obtain explosion yield. We accomplished this inversion via a deterministic model which predicts the teleseismic ground motion for a nuclear explosion. Our intent is to use the data to choose an analog rock whose material properties are consistent with the data furnished in the exchange.

- November 1976, "The Dependence of Body Wave Magnitude on Yield for Underground Explosions in Salt," T. C. Bache, J. T. Cherry and B. F. Mason, SSS-R-77-3057, 36 pages.

In this report we address the dependence of body wave magnitude (m_b) on yield for explosions in salt. Our objective is to compare salt events in Eurasia to similar, though hypothetical, events at NTS and to granite events at NTS. Our study uses deterministic computational methods and our results are based on time domain measurements from synthetic seismograms. The methods have been shown to give theoretical seismograms that agree quite well with observations when appropriate model parameters are included in the calculations.

• January 1977, "Theoretical Body and Surface Wave Magnitudes for Twelve Numerically Simulated Cratering Explosions," T. C. Bache, J. F. Masso and B. F. Mason, SSS-R-77-3119, 142 pages.

The results of the Systems, Science and Software (S³) contribution to a study of cratering explosions are presented. A series of twelve numerical simulations of 150 kt cratering explosions in three materials at several depths were carried out by Applied Theory, Inc. The data from these calculations were processed to compute theoretical far-field body and surface wave seismograms and from these to determine m_b and M_s . The m_b and M_s data are to be analyzed by Pacific Sierra Research.

The theoretical seismogram calculations are done in a two-step process. First, an equivalent elastic source representation of the cratering event is obtained. The wave field is then propagated through realistic layered earth models to teleseismic distances. For this application the procedure is found to be more accurate for the shorter period body waves than for the surface waves. The m_b and M_s values are presented for the twelve 150 kt sources and for these sources scaled to 37.5 and 600 kt. Also given are the values for contained explosions of the same yield in the same emplacement material. The contribution of the ejecta fallback is studied and is found to be insignificant for teleseismic magnitude values.

• February 1977, "Comparison of Theoretical and Observed Short Period Seismograms for Soviet Explosions in Salt," T. C. Bache, SSS-CR-77-3136. (Classified Report, Unclassified Title and Abstract), 44 pages.

In this report we direct our attention to five specific Soviet explosions in salt. These were PNE events and the Soviet estimates for the yield and depth of burial are available. The contracting officer has also provided us with estimates of the near-source crustal layering for these events.

The question to be addressed in our report is then, with all this information, how well can we match the recorded waveforms and amplitudes of these events?

- March 1977, "A Review of the Nature and Variability of the Anelastic Properties of the Upper Mantle Beneath North America and Eurasia," B. J. Mitchell and T. C. Bache, SSS-R-77-3164, 25 pages.

All reasonable mechanisms for producing low-velocity zones in the upper mantle should also produce zones of low Q. The available studies of upper mantle Q and the velocity for the same regions suggest that a coincidence of low velocity and low Q zones does indeed occur.

Seismic body- and surface-wave data indicate a substantial low velocity, low Q zone in the upper mantle beneath western North America. The zone appears to be 150 km thick or more, the velocities for both P and S waves being lower than typical upper mantle velocities for stable regions.

The available evidence for eastern North America indicates that a low velocity zone is either absent for that region or more poorly developed than it is in western North America. Most interpretations for P waves in eastern North America include no low velocity zone. Surface wave studies of the shear wave velocity structure beneath eastern North America indicate the possibility of a low velocity zone for S waves, at least in some regions.

The available data for northern Europe and Asia indicate that it is a stable region with velocity and attenuative properties much like those of eastern North America. The difference in attenuative properties of the upper mantle between the western United States and northern Asia might lead to higher m_p values for the Asian nuclear events than for equivalent NTS events, if the low velocity, low Q zone beneath the

western United States is sufficiently thick and has low enough values. Thickness and Q values suggested by most published research can easily cause m_p values for events in the Basin and Range province to be a few tenths of a magnitude unit lower than events in shield regions.

- June 1977, "Simulation and Decomposition of Multiple Explosions," D. G. Lambert, T. C. Bache and J. M. Savino, SSS-R-77-3194, 66 pages.

The purpose of the study is to develop procedures for using seismic measurements to verify the number and yields of individual explosions making up a multiple event. Multiple explosion seismograms are simulated by straightforward summations of single explosion records. Several types of multiple explosions are simulated. These include closely spaced equal yield explosions (no consideration given to propagation path effects between explosions and receiver) and relatively more widely spaced explosions (propagation path effects included) of varying yields. The data employed are principally close-in seismic recordings of the Nevada Test Site explosions obtained from Sandia Laboratories in Albuquerque, New Mexico. Decomposition of the simulated multiple explosion records is accomplished using a series of narrow-band filters with center frequencies ranging from 3 to 100 Hz. In general, our results show that the narrow-band filter technique is able to achieve accurate time separation and amplitude scaling. The limitation on the technique is essentially the requirement for the presence of sufficient signal energy at frequencies greater than about 3.5 times the inverse of the lag time between arriving signals.

- October 1977, "Identification of Individual Events in a Multiple Explosion from Teleseismic Short Period Body Wave Recordings," D. G. Lambert and T. C. Bache, SSS-R-78-3421, 40 pages.

The objective of this study is to detect and identify the individual events in a hypothetical multiple explosion. The data analyzed are simulated short period body wave recordings of that event. These were, presumably, constructed by lagging, scaling and summing a single event record according to some formula unknown to the analysts. Data for two stations, including both the single event and multiple event records, were provided to Systems, Science and Software by the VELA Seismological Center.

The data were analyzed by the MARS (Multiple Arrival Recognition System) program which uses a series of narrow-band filters to identify phase arrivals. Their amplitude and arrival time are accurately preserved. The variable frequency magnitude (VFM) discriminant is also computed and the multiple explosion records are clearly identified as being from an explosion.

For decomposition of the multiple event the MARS output for the single and multiple event records were cross-correlated. Two main groups of events separated by 6.7 to 7.8 seconds, depending on azimuth, were identified. Each of these groups appeared to include two or more explosions.

Subsequent comparison with the actual array configuration showed that the two main groups of events had been correctly identified. There were two events in each group and their lag times were correctly identified within 0.1 second. For these four events the relative amplitude estimates were correct within 10 to 20 percent. The actual array also included two other smaller and later events that were not identified by our analysis.

• April 1978, "Analysis of Two Decoupled Explosion Simulations," T. C. Bache and J. F. Masso, SSS-R-78-3627, 44 pages.

Two axisymmetric ground motion calculations were carried out by Applied Theory, Inc. to simulate 25 kt decoupled nuclear explosions in mined cavities in salt. One cavity was spherical with a radius of 66 meters while the other was a 3/1 aspect ratio ellipsoid of revolution. Both had the same volume. Results of the two calculations were analyzed to determine the character of the teleseismic body and surface waves.

The spherically symmetric portion of the field is slightly (20 to 25 percent) smaller for the spherical cavity. Comparing to results of tamped explosions, the decoupling factor for this case is about 140 at 1 Hz. The radiation from the ellipsoidal cavity is substantially perturbed from spherical symmetry; the maximum S wave amplitudes are nearly three times as large as maximum P wave amplitudes at 1.0 Hz. However, theoretical body and surface wave seismograms indicate that the m_b and M_s values are not substantially different for the two cavities.

- June 1978, "Source Amplitudes of NTS Explosions Inferred from Rayleigh Waves at Albuquerque and Tucson," T. C. Bache, W. L. Rodi and B. F. Mason, SSS-R-78-3690, 91 pages.

Comparing observed and synthetic seismograms, source amplitudes of NTS explosions are inferred from Rayleigh wave recordings from the WWSSN stations at Albuquerque, New Mexico (ALQ) and Tucson, Arizona (TUC). The potential influence of source complexities, particularly surface spallation and related phenomena, is studied in detail.

As described in earlier work by Bache, Rodi and Harkrider, the earth model for the synthetic were converted from observations at ALQ and TUC. The agreement of observed and synthetic seismograms is quite good and is sensitive to important features of the source.

The events studied are in three distinct areas, Yucca Flat, Pahute Mesa and PILEDRIVER in climax granite. All events were below the water table and the yields varied from 40 to 200 KT. Within each group the mean static value of the reduced displacement potential (Ψ_0) was determined at a fixed scaled yield, assuming a spherically symmetric point source. The source is then modified to study the effect of: (1) the addition of a double-couple component; (2) the addition of a surface impulse associated with impact of the material spalled from the surface; (3) loss of energy from the free surface reflected waves due to spallation. Comparing observed and synthetic seismograms, the extent of the effect of these secondary phenomena is outlined.

For Yucca Flat and Pahute Mesa events the inferred source amplitudes are in general agreement with values obtained by other methods. The spall impulse is too small to be of much importance. More likely to be important, especially for the Pahute Mesa events, is the loss of energy from the up-going waves. For PILEDRIVER the double-couple and attenuation of up-going waves dominate the source determination. Correcting for these phenomena, the explosion source level (Ψ_0) is considerably smaller than has usually been supposed.

• August 1978, "A Detailed Listing of the Data and Results for the Unclassified Report: Source Amplitudes of NTS Explosions Inferred from Rayleigh Waves at Albuquerque and Tucson," T. C. Bache, W. L. Rodi and B. F. Mason, SSS-CR-78-3745, 17 pages.

An analysis of Rayleigh waves at the indicated stations is presented. The objective was to infer the amplitude and character of the source function. This report is intended to serve as an Appendix to the earlier report. Detailed listings of the data and the results of the analysis are given.

• January 1979, " \hat{m}_b , A Spectral Body Wave Magnitude(U)," T. C. Bache, SSS-CR-79-3901, 99 pages.

An automated spectral magnitude called m_b is described and tested by application to recordings of eleven Pahute Mesa explosions from six widely distributed stations. The m_b is based on spectral amplitude of the recorded signal in a narrow window in both time and frequency. It is computed by first processing the data with a frequency dependent series of narrow band filters. Selected peak filter amplitudes are then averaged over an automatically selected band to obtain the spectral amplitude used to compute \hat{m}_b .

For subsequent comparison to \hat{m}_b , time domain m_b is computed for each recording with a semi-automatic technique in which all records are prefiltered to appear as if recorded by the same instrument. The peak amplitude and time measurements are then made automatically during computer processing of the data. Instrument response variations are found to introduce m_b differences of as much as 0.2 units.

Based on a comparison of the statistics of mean network magnitudes for each event and for magnitude versus log yield, the \hat{m}_b is at least as good a measure as the time domain \hat{m}_b . In addition, the m_b can be implemented as part of an automated data processing system.

• May 1979, "Discrimination Results from the Priority 1 Stations," J. M. Savino, J. F. Masso and C. B. Archambeau, SSS-CR-79-4026, 323 pages.

Our objective in the discrimination experiment is to analyze seismic waveforms from a large population of Eurasian events in order to identify these events as either earthquakes or underground explosions. The waveforms that we are concentrating on are short-period P waves recorded at a global network of seismograph stations.

In this report we describe the details of the variable frequency magnitude (VFM) discrimination method that is used in this experiment. Briefly, the central feature of the VFM method is the use of a set or "comb" of Gaussian shaped ultra narrow band filters to decompose a digital time series, consisting of signal plus noise, into a set of quasi-harmonic modulated signals. The filter center frequencies are selected to span the frequency range of the expected signal spectra. For each filter a time domain envelope function is constructed from the filtered and quadrature signals. The time of the maximum of a particular envelope function is the group or energy arrival time, t_g , of "signal" with a frequency near the filter center frequency. The amplitude of the envelope function at time, t_g , is the spectral amplitude, $A_g(f)$, of the signal energy arrival at the filter center frequency.

For identification of a signal as to the originating event type, the procedure is simply to compute the magnitude $m_b(f) \propto \log A_g(f)$ and construct $m_b(f)$ planes wherein event $m_b(f)$ values at a high frequency (i.e., > 2.0 Hz) are plotted versus $m_b(f)$ values at a lower frequency (i.e., 0.5 Hz). Observed signals can then be characterized by the location of their $m_b(f)$ values in these planes. It is predicted theoretically (Archambeau, et al., 1974) that ordinary earthquake signals fall in one particular area within such planes and that explosions (of all types) fall within a distinctly separate area. While the observational results obtained to date from this experiment tend to support these theoretical predictions, the degree of separation of the earthquake and explosion populations in the $m_b(f)$ plane representation is also found to depend on the geologic setting of a particular recording station, the spectrum of background earth noise at a station, and the epicentral distance range of events.

- September 1979, "Design Study for a Seismic Research Center: Hardware Configuration," J. Berger, SSS-R-80-4173, 53 pages.

The design of a seismic research center is considered. This system is to perform the tasks of the present SDAC and to meet the requirements of a seismic data center which can record and process the data from up to 50 NSS Mod II type seismic stations.

A design is developed consisting of four modules: a multi-microcomputer front end for communications and detection of seismic signals in the data stream; a recording mini-computer to archive the data and write the detections to disk; a network analysis computer to perform associations of events with detections; and a research computer to perform general scientific computing in a multi-user, multi-task environment. Specific hardware is recommended for each module and for a local network which will connect the machines to each other.

- September 1979, "A Review of Available Free-Field Seismic Data From Underground Nuclear Explosions in Alluvium, Tuff, Dolomite, Sandstone-Shale and Interbedded Lava Flows," J. R. Murphy and T. J. Bennett, SSS-R-80-4216, 143 pages.

This report summarizes the results of efforts to collect and organize the available free-field ground motion data from underground nuclear tests in alluvium, tuff, dolomite, sandstone-shale and interbedded lava flows. The primary objective of this effort has been to reformat the published data into a homogeneous form which will serve as a useful reference for researchers who are attempting to define theoretical seismic source functions for contained explosions in these media.